The dynamics of plastid membrane systems

Kumulative Inaugural-Dissertation

zur

Erlangung des Doktorgrades der

Mathematisch-Naturwissenschaftlichen Fakultät

der Heinrich-Heine-Universität Düsseldorf

vorgelegt von

Frederique Hans Marco Karl Heinz Breuers

aus Erkelenz

Düsseldorf,

April 2013

aus dem Institut für Biochemie der Pflanzen

der Heinrich-Heine Universität Düsseldorf

Gedruckt mit der Genehmigung der

Mathematisch-Naturwissenschaftlichen Fakultät

der Heinrich-Heine-Universität

Düsseldorf

Referent: Prof. Dr. Andreas P. M. Weber

Korreferent: Prof. Dr. Michael Feldbrügge

Tag der Mündlichen Prüfung:

12. Juni 2013

gewidmet

all jenen, die mich begleitet haben

all jenes,

das vorstellbar ist,

ist prinzipiell zu erreichen möglich

Danksagung/Acknowledgment

Unglaublich viele Menschen haben Anteil an meinem ‚Schaffen und Wirken' in meiner Doktorandenzeit gehabt. Ein guter Teil aktiv, weit mehr in passiver Weise. Diese Menschen sollen daher, hier die volle Wucht meines Dankes spüren.

Besonderer Dank gilt natürlich zuvorderst dem Mann, der diese Dissertation in erster Line möglich gemacht hat. **Andreas Weber**, Themengeber, Chef und Doktorvater, dessen Fähigkeiten und insbesondere dessen Hilfsbewusstsein ich im Nachhinein betrachtet, viel zu selten ausgeschöpft und auch lange Zeit verkannt habe. Danke für mindestens drei großartige Möglichkeiten und viele, viele kleinere! **Andrea Bräutigam** war mir post-doktorale Betreuerin, Zugang zur Forschung, unbeeindruckbare Reibungsfläche und in einigem Verhalten Vorbild. Aufrichtigster Dank!

Vielen Dank an **Michael Feldbrügge** für die Übernahme des Koreferats, besonders aber für harte Direktheit, überzeugenden Humor und klaren Input. Und vielen Dank dem Dritten des Komitees, **Jürgen Zeier**, für Bereitschaft zur Teilnahme..

I want to thank **Federica Brandizzi, Gianni and Luciana** and the Brandizzi Lab for an incredible opportunity, support and help! I learned a lot about plants and lab work and far more about myself! I bet your pardon for being incurable. Also thanks to **Sabrina and Payam**, **Yani, Kyaw and the Kids** for friendship, support and interaction inside and outside the lab.

Ich kenne **Nicole Linka** seit einem Praktikum 2008 und habe sie seit dem jeden Tag ein wenig mehr schätzen gelernt! Danke für Möglichkeiten, die ich zum Teil zu dumm war, anzunehmen. Danke für Freundschaft, Verständnis und Unterstützung! Corresponding, I would like to thank two formative personalities – **David Gagneul** and **Marc Linka** – for being friends and hard to reach paragons.

Alisandra Denton – The first document I forwarded you for corrections was red. Fortunately, every further one lost color. Thanks for reading and correcting everything I gave to you, but also for communications, support, friendship and fun. Dank auch alle den anderen **Weber Labriden** für Kollegialität, Kooperation und Reibungsfläche, wenn es nötig war. Besonders aber: **Katja und Kristin** – Für anfänglich gemeinsame Bürozeit und das abarbeiten großen Kommunikationsbedarfes! **Sarah und Christian** – Für herausstechende Kollegialität und Freundschaft. Besonders das letzte Jahr wird mir in Erinnerung bleiben. **Thea,**

Manuel und Dominik, deren positive Lebenseinstellung ein Quelle der Inspiration war. **Kirsten, Lisa und Sam –** Für Unterstützung und Spaß. **Simon** – Humor und oftamal verquere Anschauungen. **Katrin, Elisabeth und Maria** – Den ersteren insbesondere für die intensive GC/MS Hilfe in der Endphase, der letzten für einige hilfreiche Erkenntnisse und Gespräche im Mittelteil meiner Arbeit. **Daria, Max, Lion, Dan, Yann** und einigen anderen Studenten und Kollegen, die bereitwillig meine Hilfe angenommen haben und mir damit einen weisenden Finger für meine Zukunft gaben. **Fabio**, der viel zu spät ins Weber Lab gekommen ist und den ich als Tischnachbarn (und in einigen anderen Situationen) zu schätzen lernen durfte. Speziell möchte ich natürlich auch **Anja Nöcker** herzlichst danken – Der Sekretärin der Herzen! Thanks also to the illustrious group of **iGRAD*plant*;** exceptional good team and worth to be remembered – Fellows as well as Faculties. Besonders zu nennen: **Peter Jahns, Peter Westhoff, Rüdiger Simon, Laura Rose**; **Thorsten, Julia und Steffi**, und **Fred**.

Ganz besonders, und das an sich zu aller erst, möchte ich aber **Sigrun Wegener-Feldbrügge** herzlichst danken; für großartige Gespräche, Wegweisung und Unterstützung in erschöpfenden Situationen! And also Thanks to **Barb Sears**, for the real 'Green and White' and the 'Skat' experience!

Allerbester Dank gilt einer meiner Triebfedern, die „Gesäß-Tritt-Erprobteste" Ex-Kommilitonin und liebe Freundin – **Britta** – für eben erwähntes und noch viel mehr! Auch lieben Dank an den verständnisvollen Ehemann **Chrickel**. Thanks to **Vivi, Nadine, Rike, and Hanicka**, close friends and supportive forces in a long and energy consuming time! Concluded in one sentence, but you really should already know, how much you all four mean to me. Tiefer Dank gilt **Silke**, für die unerwartet geöffnete Tür, den Glauben an mich und das rigorose Unterminieren meiner Selbstzweifel. Und **Jessy, Katja, Thomas, Mareike, Mareike, Uli** und den vielen anderen für den Spaß am Sport und die ausgleichende Zeit neben der Wissenschaft.

Natürlich gilt mein Dank auch **meinen Eltern, Ursula und Karl-Heinz**, die beide, auf ihre ganz eigene Art, ihren großen Beitrag zu dieser Arbeit geleistet haben, sowie **Brigitte**, einer Großmutter, wie sie im Buche steht. Der abschließende und weitreichendste Dank gilt meinem Bruder **Sebastian**, der das getan hat, was Brüder tun sollten und das in der bestmöglichen Weise. Danke für Zugkraft, Druck und Ableitung.

Zusammenfassung

Das definierende Organell der photosynthetisch aktiven Eukaryoten ist der Chloroplast und seine „nicht-grünen“ Abarten. Neben der Photosynthese sind Plastiden auch Standort diverser, essenzieller, metabolischer Produktionswege, wie Fettsäuresynthese und Aminosäure-Biosynthese. Diese plastidären Produktionswege sind weitreichend mit denen der umgebenden Zelle verflochten. Aus diesem Grund ist ein massiver Austausch von metabolischen Vorstufen, Intermediaten und Endprodukten zwischen den beiden Reaktionsräumen Plastid und Zytosol unumgänglich. Diesem Austausch entgegen, stehen zwei, den Plastiden umgebende Hüllmembranen, die ‚Innere Hülle‘ (inner envelope; IE) und die ‚Äußere Hülle‘ (outer envelope; OE). Diese Hüllen zeichnen sich neben besonderen physikalischen und biochemischen Eigenschaften auch durch eine enge physikalische Nähe aus, welche zu analytischen Problemstellungen führt.

Der Standort eines Proteins besitzt besondere Bedeutung für die Funktion desselben und des Organismus. Die Analyse von Proteomen basiert meist auf der biochemischen Trennung der Proteinstandorte (Membranen oder lösliche Fraktionen) und der subsequenten Analyse der Proteine. Die Trennung von eng beieinander liegenden Kompartimenten, wie den Plastiden Hüllmembranen, gestaltet sich jedoch schwierig. Daraus resultierende Kontaminationen durch das jeweils andere Kompartiment führen zur Verfälschung von erzielten Daten. Es hat sich jedoch gezeigt, dass die beiden Hüllmembranen sich in ihren Dynamiken deutlich unterscheiden – insbesondere wenn ihr Proteingehalt unnatürlich verändert wird. Diese Arbeit stellt diese dynamische Manipulation der Hüllmembranen als Methode zur einwandfreien Lokalisation von Proteinen mit Hilfe konfokaler Mikroskopie und fluoreszierender Proteine vor. Auch versucht sie, die Identität dieser Dynamik auf molekularer Ebene zu ergründen.

Die Hüllmembranen unterscheiden sich jedoch nicht nur durch ihre Dynamik sondern auch in ihre Bedeutung für die Zelle. Beide Hüllen besitzen profund differente Transporteigenschaften und sind Standorte verschiedener lebensnotwendiger und wichtiger stressregulatorischer Faktoren. Während die innere Hülle von einer Vielzahl hochspezifischer Transportproteine durchsetzt ist, wird die äußere Hülle durch verhältnismäßig wenige, jedoch auch weniger spezifische Transportporen dem Transportgut geöffnet. Besondere Bedeutung kommt der äußeren Hülle jedoch auch während Frostsituationen, Phosphatmangel und mechanischer Stresseinwirkung zu. Es kann davon ausgegangen werden, dass neben den bekannten Transportporen und den stressregulatorischen Proteinen der äußeren Hülle, weitere Faktoren in dieser Membran vorkommen.

Diese Arbeit beschäftigt sich daher auch mit der Analyse des hochabundanten Hüllmembranproteins SoOMP24 aus Spinat Chloroplasten und dessen Homolog in *Arabidopsis*, AtOMP24. Die angeführten Analysen dieser Arbeit zeichnen das Bild zweier α-helikaler Proteine der äußeren Hüllmembran und liefern erste Einblicke in die Funktion dieser Proteine.

Summary

The defining organelle of photosynthetic eukaryotes is the chloroplast and its "non-green" varieties. In addition to photosynthesis, plastids are the location of essential metabolic pathways, such as fatty acid synthesis and amino acid biosynthesis. These plastidic pathways are extensively intertwined with those of the surrounding cell. For this reason a massive exchange of metabolic precursors, intermediates, and final products between plastid and cytosol is unavoidable. Counter to this exchange, there are two plastid-surrounding membranes – the plastid inner envelope (IE) and the outer envelope (OE). Besides their unique physical and biochemical properties, the envelopes are also characterized by close physical proximity, which leads to analytical problems.

The location of a protein has special meaning for the function of the protein and the viability of the organism. The analysis of proteomes is based on the biochemical separation of the protein locations (membrane or soluble fractions) and the subsequent analysis of the proteins. The separation of closely spaced compartments, such as the plastid envelope membranes appears to be difficult. This results in contamination of each other's fraction and leads to false localization results. However, it has been shown that the two envelope membranes are very different in their dynamics - especially if their protein content is altered unnaturally. This work presents the dynamic manipulation of the envelope membranes as a method for proper localization of proteins using confocal microscopy and fluorescent proteins.

The envelope membranes differ not only in their dynamics but also in their impact on the viability of the plant. Both membranes differ in their transport abilities and are location of vital and crucial stress regulatory factors. While the IE is interspersed by a large number of highly specific transport proteins, the OE is opened by a relatively small number of less specific transport pores. However, particular importance is

given to the outer envelope during freezing stress, phosphate starvation and exposure to mechanical stress. It can be expected that besides the known transport pores and stress regulators, additional factors reside in the outer envelope.

This work is concerned with the analysis of a highly abundant OE protein from spinach SoOMP24 and its homolog in Arabidopsis, AtOMP24. The analyses demonstrated in this work paint a picture of two α-helical proteins of the outer membrane and provide initial insights into these proteins' potential function in the OE.

Table of contents

I. Preface

Aims and Intentions of the PhD thesis

The aim of this cumulative PhD thesis is to deepen the knowledge of the outer envelope membrane of the primary plastids of land plants and to paint a picture of this vital and highly dynamic interface.

i) As the first barrier between the organelle and the surrounding cell, this envelope presents a crucial factor in the flow of transport between the both compartments. While transport is the most obvious role of the outer envelope, it also provides mechanisms against stress situations like insect attacks, freezing, and starvation. All these abilities are mediated by a large set of rather unique proteins, residing in the outer envelope membrane. The summary of the knowledge on the outer envelope proteome and a parts list is provided in the introduction part of this thesis (**Publication 1: Breuers et al., 2011**).

The investigations on the outer envelope proteome have closely followed gradient of protein abundance. Nowadays highly abundant proteins are largely investigated or at least are under investigation. However, the less abundant proteins often slip through the cracks. Even though, isolation methods have become more accurate and proteome analysis techniques are in a constant process of developing, low abundance results in imponderables. Especially in compartments like the outer and inner envelope of the plastid, isolation protocols have to deal with contaminations caused by the close proximity of the membranes. The misinterpretation of localization data disturbs research flow and can lead to wrong conclusions.

ii) To prevent such misinterpretations, a medium throughput and highly efficient method was invented, to solve this problem. A live cell imaging approach was designed, using the dynamic response of the plastid envelopes to high protein amounts for the verification of localizations. When supplying the membranes with unnaturally high amounts of resident proteins, inner and outer envelopes respond in

prominent different ways. While the inner envelope proliferates in several folded layers, as a reaction to excess resident protein amounts, the outer envelope proteins force a co-proliferation of outer and inner envelope in thin stroma-filled tubule-like structures (stromules). These differences can be used for the high confidence localization of envelope proteins (**Publication 2: Breuers et al., 2012**).

iii) The modality of this proliferation process is of high interest, especially in relation to naturally existing proliferation processes like stromule formation. Since proliferation is an expansion process, it logically requires more membrane material. The major membrane components are membrane lipids and proteins. Discovering which of these is involved in the proliferation process under artificial laboratory conditions might allow inference about the natural processes. Therefore, fatty acid analyses were performed, to investigate the impact of membrane lipids on the artificial induced proliferation processes. (**Addendum 1: Breuers et al., unpublished**).

iv) After painting the big picture of the outer envelope as the dynamic interface and its useful applicability, the last part of this thesis is an analysis of a specific outer envelope residing protein. When started, this part aimed to provide another piece to the puzzle or in this case rather "another hole in the barrier outer envelope". Constructed on the hypothesis, that OMP24 proteins are novel transport pores, the final part of the thesis provides new insights into the structure of OMP24 proteins and finally questions and compares the pore hypothesis to a novel protector hypothesis (**Addendum 2: Breuers et al., unpublished**).

II. Introduction

Publication 1 (Review): The plastid outer envelope – a highly dynamic interface between plastid and cytosol

Status: **published** (December 2011)

Authors: **Frederique K. H. Breuers, Andrea Bräutigam, and Andreas P. M. Weber**

Journal: "**Frontiers in plant science**"

Impact factor: **not yet available**

1. Author

Own contribution: 90%

- Literature search
- Graphic design
- Writing the manuscript
- Follow-up

frontiers in
PLANT SCIENCE

REVIEW ARTICLE
published: 14 December 2011
doi: 10.3389/fpls.2011.00097

The plastid outer envelope – a highly dynamic interface between plastid and cytoplasm

Frederique K. H. Breuers, Andrea Bräutigam and Andreas P. M. Weber*

Institut für Biochemie der Pflanzen, Heinrich-Heine Universität Düsseldorf, Düsseldorf, Germany

Edited by:
Alisdair Fernie, Max Planck Institute for Plant Physiology, Germany

Reviewed by:
Alisdair Fernie, Max Planck Institute for Plant Physiology, Germany
Shan Lu, Nanjing University, China

****Correspondence:***
Andreas P. M. Weber, Institut für Biochemie der Pflanzen, Heinrich-Heine Universität Düsseldorf, Universitätstrasse 1, D-40225 Düsseldorf, Germany.
e-mail: andreas.weber@uni-duesseldorf.de

Plastids are the defining organelles of all photosynthetic eukaryotes. They are the site of photosynthesis and of a large number of other essential metabolic pathways, such as fatty acid and amino acid biosyntheses, sulfur and nitrogen assimilation, and aromatic and terpenoid compound production, to mention only a few examples. The metabolism of plastids is heavily intertwined and connected with that of the surrounding cytosol, thus causing massive traffic of metabolic precursors, intermediates, and products. Two layers of biological membranes that are called the inner (IE) and the outer (OE) plastid envelope membranes bound the plastids of Archaeplastida. While the IE is generally accepted as the osmo-regulatory barrier between cytosol and stroma, the OE was considered to represent an unspecific molecular sieve, permeable for molecules of up to 10 kDa. However, after the discovery of small substrate specific pores in the OE, this view has come under scrutiny. In addition to controlling metabolic fluxes between plastid and cytosol, the OE is also crucial for protein import into the chloroplast. It contains the receptors and translocation channel of the TOC complex that is required for the canonical post-translational import of nuclear-encoded, plastid-targeted proteins. Further, the OE is a metabolically active compartment of the chloroplast, being involved in, e.g., fatty acid metabolism and membrane lipid production. Also, recent findings hint on the OE as a defense platform against several biotic and abiotic stress conditions, such as cold acclimation, freezing tolerance, and phosphate deprivation. Moreover, dynamic non-covalent interactions between the OE and the endomembrane system are thought to play important roles in lipid and non-canonical protein trafficking between plastid and endoplasmic reticulum. While proteomics and bioinformatics has provided us with comprehensive but still incomplete information on proteins localized in the plastid IE, the stroma, and the thylakoids, our knowledge of the protein composition of the plastid OE is far from complete. In this article, we report on the recent progress in discovering novel OE proteins to draw a conclusive picture of the OE. A "parts list" of the plastid OE will be presented, using data generated by proteomics of plastids isolated from various plant sources.

Keywords: plastid outer envelope, endoplasmic reticulum, plastid associated membranes, stromules

INTRODUCTION

Plastids are the eponymous cellular organelles of the Archaeplastida (i.e., photosynthetic eukaryotes that contain plastids of primary endosymbiotic origin, also known as the Plantae) and they host the majority of anabolic pathways. Archaeplastida that have lost the ability to photosynthesize, such as parasitic plants, still contain plastids. *De novo* fatty acid synthesis is exclusively localized in plastids. Fatty acid synthesis is based on the production of acetyl-Coenzyme A (acetyl-CoA) by the pyruvate dehydrogenase complex in the plastids (Johnston et al., 1997). The plastidic acetyl-CoA carboxylase drives the first reaction in the fatty acid biosynthesis resulting in malonyl-CoA (Konishi et al., 1996). These fatty acids are used for lipid biosynthesis in the plastid envelopes and in the endoplasmic reticulum (ER).

Of the 20 proteinogenic amino acids, nine are synthesized exclusively in plastids: the aspartate derived amino acids methionine, threonine, and lysine (Mills and Wilson, 1978; Mills, 1980; Wallsgrove and Mazelis, 1980; Curien et al., 2005, 2009), the aromatic amino acids phenylalanine, tryptophan, and tyrosine (Bickel et al., 1978), and the threonine and pyruvate derived branched-chain amino acids leucine, valine, and isoleucine (Singh and Shaner, 1995; Binder et al., 2007).

Purines, the building blocks of RNA and DNA bases and of ATP are also synthesized in plastids, as is the pyrimidine backbone. All 10 enzymatic steps of inosine monophosphate biosynthesis occur in the plastids (Zrenner et al., 2006). Furthermore, five of the six steps of pyrimidine synthesis are catalyzed by the plastidic enzymes carbamoylphosphate synthase (Giermann et al., 2002), aspartate transcarbamoylase, dihydroorotase, and uracil monophosphate synthase (Doremus and Jagendorf, 1985).

The reduction of sulfate to sulfide is also confined to the plastid (summarized in Takahashi et al., 2011) as well as the production of sulfolipids (compare Okanenko, 2002). Chloroplasts fix inorganic carbon in the form of CO_2 in the Calvin–Benson cycle

and incorporate nitrogen in the form of ammonia into glutamate and glutamine. The chloroplasts provide energy in the form of reducing equivalents through photosynthesis. Further chloroplast products, such as triose phosphates (TP), carbohydrates, and amino acids are exported from the chloroplasts to feed processes in the cell (Weber, 2004; Weber et al., 2004, 2006; Linka and Weber, 2009; Weber and Linka, 2011).

The anabolic versatility of chloroplasts traces back to their prokaryotic ancestor. An ancestral cyanobacterium was engulfed and stably integrated into the eukaryotic host during primary endosymbiosis (for a recent review, see Weber and Osteryoung, 2010). Approximately 1, 6 billion years of co-evolution irreversibly integrated the photoautotrophic prokaryote into the host cell, creating the plant cell as we know it (**Figure 1**; Yoon et al., 2004; Reyes-Prieto et al., 2007; Tyra et al., 2007).

Plastids derived from this initial event, primary plastids, are bound by two surrounding envelope membranes, the inner (IE) and the outer (OE) envelope membrane. It is believed that both envelope membranes are derived from cyanobacterial membranes (Gould et al., 2008). The IE traces back to the plasma membrane (PM) of the ancestral cyanobacteria. The OE traces to the bacterial outer membrane since (i) it contains galactolipids (Jarvis et al., 2000), (ii) β-barrel forming proteins are in both envelope membranes and the bacterial outer envelope (Schleiff et al., 2003a), and (iii) traces of peptidoglucan biosynthesis are present in plastids of glaucophytes (Steiner et al., 2005).

Although the plastid harbors the majority of anabolic pathways and is well separated from the cytosol by two membranes, the extant plastid is only semiautonomous (Gould et al., 2008). During domestication, the organelle lost almost its complete genome to the nucleus. Only approximately 2% of the plastid proteome are encoded on the plastom (Abdallah et al., 2000), and almost all of the proteins the plastid needs to function are imported from the cytosol (Schnell et al., 1994; Hinnah et al., 1997). It also lost the ability to freely replicate, because the complete protein set for division is encoded in the nucleus (Hashimoto and Possingham, 1989; Kuroiwa et al., 1998). Furthermore, cell- and plastid-divisions are synchronized (El-Shami et al., 2002; Raynaud et al., 2005), although it can be uncoupled to a certain degree, as demonstrated by several mutant lines defective in plastid division (Pyke and Leech, 1992; Osteryoung et al., 1998; Asano et al., 2004; Raynaud et al., 2004).

Extant plastids are well integrated into their host cells, exchanging metabolites, proteins, membrane lipids, and information. The ultimate barriers between these compartments are the plastid envelope membranes. For the IE the reader is directed to several recent reviews about the function of the inner envelope membrane (Linka and Weber, 2009; Kovacs-Bogdan et al., 2010; Facchinelli and Weber, 2011; Fischer, 2011; Weber and Linka, 2011). In this

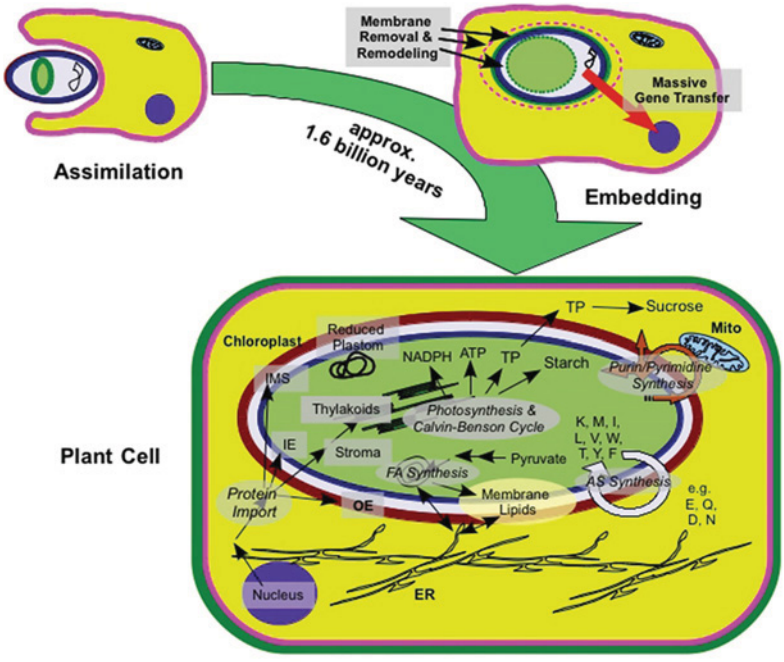

FIGURE 1 | From endosymbiont to plastid. Schematic representation of plastid origin and extant anabolic pathways in plastids; ER, endoplasmic reticulum; Mito, mitochondrion; IE, inner envelope; IMS, intermembrane space; OE, outer envelope; FA, fatty acid; AS, amino acid (specific amino acids are denoted in one letter code); TP, triosephosphate

review, we will focus on the role of the outer envelope and we provide a parts list of the OE proteome (**Tables 1** and **2**).

SOLUTE TRANSPORT ACROSS THE OUTER ENVELOPE

Since the plastid is the anabolic factory of the cell, substrates that cannot be produced from intermediates of the Calvin–Benson cycle need to be imported while many products need to be exported. All substrates and products cross two envelope membranes, the IE and the OE. The IE contains a diverse set of substrate specific proteins processing and possibly controlling export and import to the organelle (Linka and Weber, 2009; Bräutigam and Weber, 2011; Facchinelli and Weber, 2011; Weber and Linka, 2011). Pores with broad substrate specificity have not yet been described in the inner envelope. For a long time the OE was considered as a molecular sieve for molecules larger than 10 kDa not contributing to the barrier between stroma and cytosol. This view has been disputed (Pohlmeyer et al., 1997; Flügge, 2000; Soll et al., 2000). In the past 15 years, four pore forming proteins of different selectivity have been characterized and were named by their apparent molecular masses as OEP16 (Pohlmeyer et al., 1997), OEP21, OEP24 (Pohlmeyer et al., 1998), and OEP37 (Schleiff et al., 2003a; **Table 1**). They were initially identified in *Pisum sativum* (pea) and later pursued in *Arabidopsis*.

OEP24

OEP24 is a member of β-barrel forming proteins and is proposed to consist of seven β-strands spanning through the membrane (Pohlmeyer et al., 1998). OEP24 shows no similarity in its primary structure to mitochondrial and bacterial porins, and does not show sensitivity to bacterial porin inhibitors (Pohlmeyer et al., 1998). However, the high amounts of hydrophilic amino acids (49%) reflect the properties of other pore forming proteins in bacteria and mitochondria (Röhl et al., 1999).

When reconstituted in proteoliposomes *in vitro*, the channel is slightly selective for cations and it is highly conductive. The 2.5- to 3-nm wide pore is created by at least two OEP24 proteins. This homodimer facilitates the transport of triose phosphates (TP), hexose-phosphates, sugars, ATP, phosphates (P_i), dicarboxylates like 2-oxoglutarate, and charged amino acids (**Table 1**; Pohlmeyer et al., 1998). Hence, OEP24 carries the major fluxes across the envelope membrane in the shape of TP, the product of photosynthesis as well as dicarboxylates and amino acids needed for nitrogen assimilation. The importance of OEP24 is underlined by its expression pattern. OEP24 pores exhibit equal distribution in plastids of all kind and each tissue. Moreover, paralogs can be found in monocotyledons and in dicotyledons (Pohlmeyer et al., 1998).

The pea protein PsOEP24 can functionally complement a yeast mutant that lacks the mitochondrial voltage-dependent anion channel (VDAC). Also, like VDAC proteins, PsOEP24 can induce apoptosis in cancer cells (Liguori et al., 2010) indicating a role in programmed cell death for PsOEP24. In both heterologous systems PsOEP24 is targeted to the mitochondrial outer membrane (Röhl et al., 1999).

Most information on OEP24 is currently based on PsOEP24. Two homologs of OEP24 are found in *Arabidopsis* (Duy et al., 2007) and proteomic databases suggest that at least three homologs exist (Sun et al., 2009; Ferro et al., 2010). The AtOEP24 encoded by At1g45170 was predicted *in silico* to contain 12 β-strands (Schleiff et al., 2003a), which may indicate functionality as monomer. Unpublished data of Timper et al. mentioned in Duy et al. (2007) describe defects during pollen germination in a so called AtOEP24.1 mutant. It is hypothesized that this defect is due to a lipid and energy deprivation during early pollen development

Table 1 | The known solute transport proteins of the outer envelope.

Name (structure)	Transport	Homologs (mentioned in this review)	Publications
PLASTID OUTER ENVELOPE SOLUTE TRANSPORTER			
OEP16 (α-helix)	Export of amino acids and amines	PsOEP16.1, PsOEP16.2 AtOEP16.1 (At2g28900) AtOEP16.2 (At4g16160) AtOEP16.4 (At3g62880) HvOEP16 (COR TMC-AP3) ZmOEP16	Pohlmeyer et al. (1997), Baldi et al. (1999), Rassow et al. (1999), Steinkamp et al. (2000), Linke et al. (2004), Reinbothe et al. (2004), Drea et al. (2006), Duy et al. (2007), Murcha et al. (2007), Philippar et al. (2007), Bräutigam and Weber (2009), Pudelski et al. (2010)
OEP21 (β-barrel)	Phosphorylated carboxylates, Pi Anion Rectifying	PsOEP21 AtOEP21.1 (At1g20816) AtOEP21.2 (At1g76405) ZmOEP21	Bolter et al. (1999), Hemmler et al. (2006), Bräutigam et al. (2008)
OEP24 (β-barrel)	TP, hexose-phosphates, sugar, ATP, Pi, dicarboxylates, charged amino acids	PsOEP24 Putative AtOEP24 (At3g52230, At5g42960, At1g45170) ZmOEP24	Pohlmeyer et al. (1998), Schleiff et al. (2003a), Duy et al. (2007), Sun et al. (2009), Ferro et al. (2010)
OEP37 (β-barrel)	Peptides Cations Rectifying	PsOEP37 AtOEP37 ZmOEP37	Schleiff et al. (2003a), Goetze et al. (2006), Bräutigam et al. (2008)

Table 2 | Parts list of the proteome of the OE.

Name	Function	Isoforms and homologs (locus on *Arabidopsis* genome)	Publication
PROTEIN TRANSLOCON COMPLEX			
Toc34 family	GTPase, protein import receptor	AtToc33/PPI1 (At1g02280), AtToc34/PPI2 (At5g05000), PsToc34	Jarvis et al. (1998), Chen et al. (2000), Gutensohn et al. (2000), Schleiff et al. (2003b), Ivanova et al. (2004), Andres et al. (2010), Dhanoa et al. (2010), Huang et al. (2011)
Toc64	Protein import co-receptor/co-chaperone	AtToc64-III (At3g17970), AtToc64-I/Ami1 (At1g08980), AtToc64-like/OEP61 (At5g21990)	Becker et al. (2004), Aronsson et al. (2007), Qbadou et al. (2007), Bae et al. (2008), Barsan et al. (2010), Von Loeffelholz et al. (2011)
Toc75	Protein import translocator pore	AtToc75-III/Mar1 (At3g46740), AtToc75-IV (At4g09080), AtToc75-V/AtOEP80 (At5g19620), PsOEP75	Perry and Keegstra (1994), Schnell et al. (1994), Tranel et al. (1995), Hinnah et al. (1997), Sveshnikova et al. (2000), Jackson-Constan and Keegstra (2001), Hinnah et al. (2002), Schleiff et al. (2003a), Wallas et al. (2003), Gentle et al. (2004), Baldwin et al. (2005), Patel et al. (2008)
Toc159 family (Toc86)	GTPase, protein import receptor	AtToc159 (At4g02510), AtToc132/Mar2 (At2g16640), AtToc120 (At3g16620), AtToc90 (At5g20300)	Bauer et al. (2000), Jackson-Constan and Keegstra (2001), Schleiff et al. (2003b), Hiltbrunner et al. (2004), Ivanova et al. (2004), Kubis et al. (2004), Stanga et al. (2009), Andres et al. (2010), Huang et al. (2011), Infanger et al. (2011)
LIPID METABOLISM			
LACS9	Long-chain acyl-CoA synthase	AtLacs9 (At1g77590)	Schnurr et al. (2002), Zhao et al. (2010)
DGD	Digalactosyldiacylglycerol (DGDG) synthase	AtDGD1 (At3g11670), AtDGD2 (At4g00550)	Dörmann et al. (1995), Dörmann et al. (1999), Härtel et al. (2000), Froehlich et al. (2001a), Kelly and Dörmann (2002), Xu et al. (2003)
MGD	Monogalactosyldiacyl glycerol (MGDG) synthase	AtMGD2 (At5g20410), AtMGD3 (At2g11810)	Miege et al. (1999), Härtel et al. (2000), Awai et al. (2001)
GGGT/SFR2	Galactolipid:galactolipid galactosyltransferase	AtGGGT/AtSFR2 (At3g06510)	Heemskerk et al. (1983), Heemskerk et al. (1986), Kelly and Dörmann (2002), Xu et al. (2003), Thorlby et al. (2004), Fourrier et al. (2008), Moellering et al. (2010)
PLASTID MOVEMENT AND DIVISION			
CHUP1	Anchor protein for plastid movement	AtCHUP1 (At3g25690)	Oikawa et al. (2003), Oikawa et al. (2008), Von Braun and Schleiff (2008), Kadota et al. (2009), Suetsugu et al. (2010), Whippo et al. (2011)
PDV	Plastid division	AtPDV1 (At5g53280), AtPDV2 (At2g16070)	Gao et al. (2003), Miyagishima et al. (2006), Glynn et al. (2008), Glynn et al. (2009)
CRL1	Unknown; mutant effect on plastid number and size	AtCRL1 (At5g51020)	Asano et al. (2004), Chen et al. (2009)
MOLECULAR AND BIOCHEMICAL TOOLS OF UNKNOWN FUNCTION			
OEP7	Unknown	AtOEP7 (At3g52420), PsOEP14, SoOEP7 (E6.7)	Salomon et al. (1990), Li et al. (1991), Tu and Li (2000), Lee et al. (2001), Dyall et al. (2004), Bae et al. (2008), Oikawa et al. (2008), Kim et al. (2011)
OEP9	Unknown	OEP9.1 (At1g16000), Putative homolog OEP9.2 (At1g80890)	Dhanoa et al. (2010)
OTHERS			
PTM	Plant homeodomain transcription factor with transmembrane domains	PTM (At5g35210)	Sun et al. (2011)
HPL	Hydroxide lyase	AtHPL/AtCYP74B (At4g15440), LeHPL, StHPL	Blee and Joyard (1996), Froehlich et al. (2001b), Vancanneyt et al. (2001), Shiojiri et al. (2006), Kishimoto et al. (2008)
KO	*ent*-kaurene oxidase/ gibberellin synthesis	AtKO1/GA3 (At5g25900)	Helliwell et al. (2001)

(Continued)

Table 2 | Continued

Name	Function	Isoforms and homologs (locus on *Arabidopsis* genome)	Publication
OMP24	Unknown; outer membrane protein of spinach chloroplasts	SoOMP24	Fischer et al. (1994)
WBC7	Unknown; transport of hydrophobic compounds	AtWBC7 (At2g01320)	Schleiff et al. (2003a), Zybailov et al. (2008)
OEP6	Unknown	AtOEP6 (At3g3160)	Ferro et al. (2010)
Putative OE proteins in PPDB database	Unknown	OMP85-family proteins of 35 kDA (At3g48620) and 39 kDa (At3g44160) Putative GTPase of 15kDa (At4g02482) Putative p-loop containing nucleoside triphosphate hydrolase 100 kDa (At4g15810)	Sun et al. (2009)

This list contains the proteins discussed in this review with residence in the outer plastid envelope except proteins already listed in ***Table 1****.*

(Duy et al., 2007). In contrast, the expression of another homolog (AtOEP24.2) is upregulated during late seed development (Duy et al., 2007). At least the findings for AtOEP24.1 indicate that the more selective transport pores of the OE (see below) cannot compensate for the loss of OEP24. The question remains whether, and if so how, OEP24 controls the metabolic flux. Proteomics data indicates that protein abundance in different plastids subtypes does reflect flux (Bräutigam et al., 2008; Bräutigam and Weber, 2009; Bräutigam and Weber, 2011). For example, OEP24 is more abundant in maize mesophyll chloroplasts compared to pea chloroplasts. Since the required flux of TP is at least three times higher in maize mesophyll chloroplasts compared to pea chloroplasts (Bräutigam et al., 2008; Weber and Von Caemmerer, 2010; Bräutigam and Weber, 2011), the increased abundance of OEP24 in maize indicates that an outer envelope porin might be limiting metabolite flux (Bräutigam et al., 2008). Studies with altered levels of AtOEP24 either by knockouts or knock-downs may shed light on the flux control by OEP24.

OEP16

The first described and best-investigated outer envelope solute channel is OEP16. Like OEP24, OEP16 lacks sequence and structural homology to known porins, which classifies it as a non-classical porin (Pohlmeyer et al., 1997). The OEP16 channel is slightly cation selective and is a high-conductance solute channel (Pohlmeyer et al., 1997) that selectively transports amino acids and amines. Although the pore is principally large enough, OEP16 excludes carbonates such as TP or sugars (**Table 1**; Pohlmeyer et al., 1997).

The structure of OEP16 was controversially discussed. It was assumed to consist of four β-sheets and three alpha-helices (Pohlmeyer et al., 1997). Based on other porin structures and the transport properties of the channel, it was concluded, that the protein is a β-barrel forming pore (Steinkamp et al., 2000). However, structural analysis and enhanced prediction algorithms later revealed a purely alpha-helical structure (Linke et al., 2004). These findings were supported by the sequence similarity of OEP16 to other alpha-helical transport proteins. The similarity to members of the mitochondrial protein translocon family of the inner membrane (TIM proteins), and to the bacterial amino acid permease LivH led to the classification of OEP16 as preprotein and amino acid transporter (PRAT) relatives (Rassow et al., 1999; Murcha et al., 2007; Pudelski et al., 2010). The similarity to preprotein transporters was also the cause for one group claiming OEP16 to be a protein importer. This claim was recently conclusively disproved (summarized in Pudelski et al., 2010).

The high selectivity for amino acids is achieved via a loop between the pore forming helix1 and helix2 (Linke et al., 2004). Whether this loop is facing the intermembrane space (IMS) or the cytosol is not known (Linke et al., 2004). The model described by Pudelski et al. (2010) puts the loop into the IMS (Pudelski et al., 2010). The location of the regulatory element to the IMS points to a function of OEP16 as amino acid exporter. In addition to this transport regulation, the channel is also redox-regulated by cysteine residues in the first helix (Steinkamp et al., 2000)

Recently a second homolog of PsOEP16 was found and named PsOEP16.2 (Pudelski et al., 2010). Yet, *Arabidopsis* contains three homologs of OEP16 (Philippar et al., 2007). The protein most similar to PsOEP16.1 is AtOEP16.1 (63%), also called AtOEP16-L (Drea et al., 2006), due to its highest expression levels in leaves. AtOEP16.2/AtOEP16-S is exclusively expressed in mature seeds, cotyledons, and early pollen stages (Drea et al., 2006; Philippar et al., 2007). It contains additional amino acids in the loop responsible for substrate selectivity of the channel (Drea et al., 2006; Philippar et al., 2007). AtOEP16.2 is hypothesized to be involved in seed development, dormancy, and/or desiccation tolerance. Binding elements of the phytohormone abcisic acid in

the promoter region of AtOEP16.2 support this hypothesis (Drea et al., 2006).

A third homolog, AtOEP16.4, with a similarity of 20% to PsOEP16 is expressed at low levels throughout all stages of development. It shows higher expression during seed maturation and in pollen, indicating a function as backup for AtOEP16.2 (Pudelski et al., 2010). PsOEP16 also shares slight similarity (comparable with the similarity to AtOEP16.4) to another PRAT protein earlier described as the third homolog of AtOEP16, AtOEP16.3 (Reinbothe et al., 2004; Drea et al., 2006). This protein is localized to the mitochondrial outer membrane and is now labeled PRAT3 (Murcha et al., 2007; Philippar et al., 2007).

A cold regulated protein (COR) TMC-AP3 in barley (*Hordeum vulgaris*) is also a paralog of OEP16. It was investigated due to its upregulation during cold stress (Baldi et al., 1999). The role in cold acclimation of OEP16 is supported by a recent study on *Arabidopsis* (Kaplan et al., 2007). Here, increased levels of amino acids were found during cold stress. This indicates that the amino acids are needed as signal substance in cold acclimation and points on OEP16 as necessary transporter in this process. Proteomics also indicates that the OEP16 content is dynamically adjusted between plastid types. Proplastids contain large amounts of OEP16 reflecting the active amino acid synthesis during differentiation (Bräutigam and Weber, 2009).

OEP37

The most recently described member of the transmembrane channels for solutes in the OE is PsOEP37 and its *Arabidopsis* paralog AtOEP37. It was found in a combined *in silico* and proteomics study on β-barrel proteins in the OE of pea and *Arabidopsis* (Schleiff et al., 2003a). Its functional characterization revealed a rectifying, cation selective, high-conductance channel, selective for peptides. It is hypothesized to form a β-barrel with 12 β-strands (Schleiff et al., 2003a). It forms an hourglass shaped pore with a size of 3 nm narrowing to 1.5 nm in the restriction zone (Goetze et al., 2006). A long negatively charged loop responsible for the selectivity is facing the IMS and is regulated by the pH values of the surrounding area (Schleiff et al., 2003a; Goetze et al., 2006). OEP37 is likely regulated by the redox state of the environment due to the oxidation of two neighboring cysteine residues similar to OEP16.

Its expression levels are fairly low but it is ubiquitously distributed in all developmental stages and organs in *Arabidopsis*. It was observed that during germination the mRNA levels increased indicating a role during early plant development (Goetze et al., 2006).

OEP37 displays binding affinity to the precursor of the inner envelope translocon compound 32 (Tic32), which is imported non-canonically (Nada and Soll, 2004). Consequently, it was assumed to be transported by OEP37 (Goetze et al., 2006). However, reverse genetic analysis of AtOEP37 disproved this hypothesis, since AtOEP37 knock out plants were not lethal while Tic32 mutants are. In addition, the transport of Tic32 into the IE was not impaired in the *oep*37-1 knock out plants (Goetze et al., 2006).

The *in vivo* role of OEP37 in plants is unknown. The *Arabidopsis oep*37-1 mutant has no obvious phenotype although *OEP*37 is a single copy gene albeit expressed at low levels. OEP37 function may overlap with or is partially redundant in function with OEP16 and/or OEP24. High expression levels during early seedling germination and late embryogenesis indicate a function in early development of the plant (Goetze et al., 2006). It may also become important during stress conditions where higher metabolite fluxes are needed. Similar to OEP24, chloroplast envelopes of the C_4 plant maize contain a higher amount of OEP37, which might reflect the higher metabolite flux across this membrane (Bräutigam et al., 2008).

OEP21

The fourth solute pore protein of the OE is OEP21 (Pohlmeyer et al., 1998). Like for the other three OEPs, OEP21 is distributed through all plastid types in varying abundance (Bräutigam et al., 2008). Also, OEP21 is present in both mono- and dicotyledons (Pohlmeyer et al., 1998). It is a rectifying, anion selective channel for phosphorylated carbohydrates and TP (**Table 1**; Bolter et al., 1999). Like OEP24 and OEP37, OEP21 is a β-barrel forming protein. Its secondary structure displays eight β-strands but just seven are hypothesized to be pore forming. Since this seven β-strands are not enough to form a fully hourglass shaped 2.4 nm pore, OEP21 was proposed to acts at least as dimer. The N- and C-terminus of the protein face the cytosol (Hemmler et al., 2006). The transport through OEP21 is regulated by a substrate gradient and most likely exports TP and phosphorylated carbohydrates during light periods in green tissue. In contrast, import of these compounds would occur during darkness and in non-green tissue (Bolter et al., 1999). Additional regulation OEP21 obtains by two highly affine ATP binding sites (Bolter et al., 1999). The internal ATP binding site is proposed to provide major regulation by blocking the channel. The IMS orientated FX_4K motive only provides regulatory function in transport processes, and is 100-fold less affine to ATP. The competitive binding of substrates like TP is initiating the release of ATP from the internal ATP binding side. This leads to the opening of the pore and to reduction of the anion selectivity (Bolter et al., 1999; Hemmler et al., 2006). One of the two *Arabidopsis* OEP21 homologs, AtOEP21.1, lacks the FX_4K motive and has a 50% reduced ability for modulating the ion selectivity of the channel (Hemmler et al., 2006).

In summary, the import and export of cations (e.g., potassium, calcium, iron), anions (e.g., nitrite, sulfate, phosphate), and metabolites across the OE is driven by the set of known solute channels OEP16, OEP21, OEP24, and OEP37. Their ability to shuttle photosynthetic products, amino acids, and nitrogen assimilates likely accounts for the bulk of the metabolic exchange between plastid and cytosol. However, the high and low specificity channel proteins are most likely not the only metabolic shuttling systems of the OE.

PUTATIVE METABOLITE SHUTTLES AND OE PROTEINS OF UNKNOWN FUNCTION

THE ABC TRANSPORTER OF UNKNOWN TRANSPORT FUNCTION WBC7

An ABC transporter of unknown function, white–brown-complex protein 7 (WBC7), was localized to the outer envelope of pea chloroplasts (Schleiff et al., 2003a) and to *Arabidopsis* chloroplast envelope fractions (Zybailov et al., 2008; Ferro et al., 2010; Joyard et al., 2010) by proteomics. AtWBC7 is a member of the G family

of ABC transporters with a single ABC cassette and six transmembrane domains (TMD). The G family contains half size ABC transporters, which form homo- or heterodimers (Kusuhara and Sugiyama, 2007). Two proteins of this family have been investigated in *Arabidopsis*. AtWBC11 and AtWBC12 reside in the PM and are involved in the export of cuticular lipids in epidermal cells (Mcfarlane et al., 2010). No experimental evidence is available on the function of AtWBC7 although it is tempting to speculate about a role in transport of hydrophobic or partially hydrophobic substances (**Figure 2J**).

THE PUTATIVE PORPHYRIN SCAVENGER OR TRANSPORTER TSPO

TSPO is at most a temporary resident in the OE of plastids (Balsemao-Pires et al., 2011). Expression in *Arabidopsis thaliana* is induced by salt stress (Balsemao-Pires et al., 2011) or ABA treatment (Vanhee et al., 2011). A *Physcomitrella TSPO* mutant is hypersensitive to oxidative stress (Frank et al., 2007). The protein is conserved throughout eukaryotes including yeast (Vanhee et al., 2011) in which it is degraded by autophagy upon heme binding. AtTSPO co-localizes with autophagy markers (Vanhee et al., 2011). AtTSPO is a membrane protein, which has been localized to the ER and Golgi (Balsemao-Pires et al., 2011; Vanhee et al., 2011) and to the outer envelope of plastids (Balsemao-Pires et al., 2011) where it only appears after salt treatment. The precise function of TSPO is unknown but it is targeted for autophagy after treatments which presumably increase free porphyrins (Guillaumot et al., 2009; Vanhee et al., 2011). TSPO is hypothesized to protect plant cells against oxidative stress by binding and thus detoxifying free porphyrins (**Figure 2F**; Vanhee et al., 2011).

TRANSPORT OF GIBBERELLIN PRECURSORS FROM THE PLASTID

Gibberellins are produced from geranyl–geranyl-diphosphate generated by the isoprenoid pathway in plastids. The first two biosynthetic enzymes, copalyl diphosphate synthase and *ent*-kaurene synthase, are soluble stromal proteins (Helliwell et al., 2001). They produce a lipophilic intermediate, *ent*-kaurene, which likely partitions to the membranes (Helliwell et al., 2001). The next step, the production of the less lipophilic intermediate *ent*-kaurenoic acid, occurs at the outer envelope of the plastid since *ent*-kaurene oxidase localizes to the OE of the plastids judged by GFP fusion proteins and *in vitro* import assays (Helliwell et al., 2001). Whether passage through the IMS requires a dedicated transporter or occurs in conjunction with lipid transfer or spontaneously has not been addressed. Further oxidation of *ent*-kaurenoic acid occurs in the ER (**Figure 2G**).

The transfer of the gibberellin precursor presents a model by which lipophilic plastid produced precursors may cross the envelope membranes to their destination in the cytosol without the need of dedicated transporters.

UNUSUAL PROTEIN OF UNKNOWN FUNCTION

In 1994 a small OE protein from spinach chloroplasts was cloned and biochemically investigated (Fischer et al., 1994). While its calculated weight is approximately 16 kDa, its abnormal amino acid composition led to an apparent molecular weight of approximately 24 kDa on SDS gel for which the protein was named OMP24. The insertion of OMP24 into the membrane is independent of surface receptors and target peptides. ATP has been shown to stimulate the insertion of the protein into the membrane (Fischer et al., 1994). The function of this integral protein is unknown.

THE ROLE OF THE OUTER ENVELOPE IN LIPID SYNTHESIS

Unlike small hydrophilic compounds, fatty acids or lipids cannot easily be transported through the aqueous phase. Yet the interplay between the plastid and the cytosol, especially the ER is extensive.

TRANSPORT OF FATTY ACIDS

Fatty acids are amphipatic: a small hydrophilic head group caps a highly hydrophobic long hydrocarbon tail. Several studies revealed that from 62% (*Arabidopsis* green tissue, represents "16:3"-plants) up to 90% (non-green tissue and green tissue of "18:3"-plants, see below) of fatty acids are exported from the plastid and transferred to the ER. The major and likely only transport direction is from plastids to the remainder of the cell (Browse et al., 1986, 1993; Somerville and Browse, 1991). The transport of these metabolites across two envelopes has not yet been resolved. However, long-chain-fatty-acid-Coenzyme-A synthetases (LACSs) are expected to play a prominent role in this process since they can catalyze a vectorial reaction in bacteria (Benning, 2009). Nine isoforms of this protein family are distributed to all sub cellular compartments of in *Arabidopsis* and can be found in peroxisomes, mitochondria, and the plastid (Schnurr et al., 2002; Shockey et al., 2002). Already in the late 1970s LACS activity in spinach chloroplast was shown to localize to the outer envelope membrane (Roughan and Slack, 1977). More than 20 years later, AtLACS9 was located to the envelope membranes by proteomics (Sun et al., 2009; Ferro et al., 2010; Joyard et al., 2010) and is most likely located to the OE (compare Koo et al., 2004; Sun et al., 2009). AtLACS9 is the only known exclusively plastid localized LACS and catalyzes 90% of the acetylation reactions. Its V_{max} is higher than needed for complete fatty acid export. However, a knockout mutant shows no apparent phenotype (Schnurr et al., 2002). Possibly, the ER localized AtLACS1 can take over at least part of its function at least in triacylglycerol (TAG) biosynthesis (Zhao et al., 2010), which would require very close contact between the OE and the ER. Proteomics studies suggest three additional proteins with LACS activity in the plastid envelopes, AAE15 and AAE15-like as well as AtLACS8 of which the majority is localized to the ER or peroxisomes (Koo et al., 2004; Ferro et al., 2010; Joyard et al., 2010).

Fatty acid transport via LACS through the OE still leaves the inner envelope to be crossed. Extrapolating from the function of a known fatty acid transporter, peroxisome ABC transporter 1 (PXA1), which is localized to the peroxisomal membrane, the following model is proposed: The inner envelope contains an ABC transporter of the same class as PXA1, transporter associated with antigen processing protein 1 (TAP1), which has been consistently detected in all envelope proteome projects to date (Koo and Ohlrogge, 2002; Garcia et al., 2004; Sugiyama et al., 2006; Bräutigam et al., 2008; Bräutigam and Weber, 2009; Kunz et al., 2009; Ferro et al., 2010; Joyard et al., 2010) and whose function is unknown.

TAP1 or possibly another ABC transporter transports esterified fatty acids across the inner envelope where they are taken over by LACS9 and de-esterified in the process of transport out of

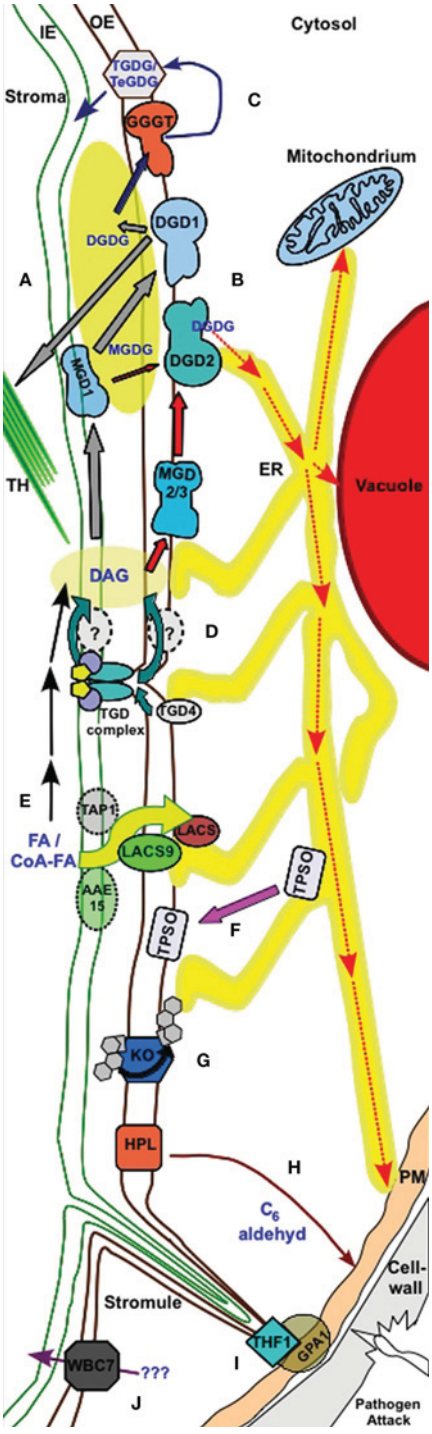

FIGURE 2 | Continued

FIGURE 2 | Continued

Processes in the outer plastid envelope. (A) Galactosyl diacylglycerol biosynthesis under normal growth conditions. MGD1 produces MGDG from DAG. MGDG is either used in plastid membranes or is further processed by the OE resident DGD1 to produce DGDG for plastidic membrane use. Gray arrows label transport processes. **(B)** DGDG production under phosphate deprivation occurs via the OE resident MGD2/3 and DGD2. DGDG is transported to non-plastidic membranes, such as the tonoplast, mitochondrial membranes, and plasma membrane, possibly via the ER. Red arrows label transport processes. **(C)** GGGT produces TGDG and TeGDG during freezing stress to provide dehydration by thickening hydrophilic parts of the membrane. This process is labeled by blue arrows. **(D)** TGD1–3 complex disrupts the OE to mediate lipid exchange from ER to the IE. ER resident TGD4 may provide membrane lipid precursors directly to the OE. This process most likely involves further proteins in the OE and/or IE. **(E)** Free fatty acids are processed by LACS proteins resident in the OE and may IE. An ABC transporter Tap1 putatively involved in esterified fatty acids (CoA-FA) mediates the transport through the IE. At the OE LACS9 takes over the CoA-FA and de-esterifies these during transport across the OE. ER resident LACS further process FA. An alternative pathway involves putative IE resident proteins with LACS activity (AAE15). **(F)** Transfer of TPSO during salt and osmotic stress from ER to OE. **(G)** Transfer of *ent*-kauren across the OE during oxidation to *ent*-kaurenoic acid by OE resident *ent*-kauren oxidase. **(H)** OE resident HPL is integrated into pathogen defense via C_6 aldehyde production when wounding occurs. **(I)** OE resident THF1 interacts with plasma membrane (PM) resident GPA1 in sugar signaling. Stromule bridge the process. **(J)** The G family ABC transporter WBC7 mediate transport of unknown compounds through the OE.

the plastid. The free fatty acid is immediately bound by different LACS localized to one of the extraplastidial compartments and esterified again. This *modus operandi* would limit the exposure of the plastid to free fatty acids, which can act as detergents (Shine et al., 1976; Koo and Ohlrogge, 2002; Koo et al., 2004). However, it requires physically close association of the plastid to the ER to prevent the escape of free fatty acids. ^{18}O labeling indeed showed that the transport involves a free fatty acid stage (Pollard and Ohlrogge, 1999). The reverse pathway of transport is impossible in this model since the ABC transporter is not reversible (Higgins, 1992). Alternatively, if an IE transporter transports free fatty acids, AtLACS9 could transfer the fatty acid by esterification thus leading to the release of CoA-fatty acid esters to the cytosol. Fatty acids are incorporated into lipids in chloroplasts and the ER (**Figure 2E**; compare Koo et al., 2004).

OXYLIPIN SYNTHESIS AT THE OE

Oxylipins have prominent roles in plant development and pathogen defense. They are produced from alpha linoleic acid liberated from lipids of the chloroplast. At least one branch of oxylipin synthesis can involve the OE, since the OE localized hydroperoxide lyase (HPL) catalyzes the first step toward C_{12} omega-keto-fatty acid and C_6 aldehydes (Blee and Joyard, 1996; Froehlich et al., 2001b). The C_{12} omega-keto-fatty acid is the precursor for traumatin while the C_6 aldehydes are directly involved in pathogen defense (summarized in Howe and Schilmiller, 2002; Arimura et al., 2009). It has been shown, that during fungal attack AtHPL expression is upregulated and leads to an increase of C_6 aldehyde concentration at wound sites (Shiojiri et al., 2006). Defense against the pathogen is directly provided by the toxicity of the

HPL metabolized compound (**Figure 2H**; Kishimoto et al., 2008). Studies on potato HPL also suggest a role for HPL in defense against sucking insects. However, the potato isoforms of the HPL are not localized to the OE (Vancanneyt et al., 2001).

GALACTOGLYCEROLIPID SYNTHESIS IN PLANTS

Galactoglycerolipids (GGL) are essential to photosynthetic function (Reifarth et al., 1997; Guo et al., 2005; Hölzl et al., 2006) but can be found throughout the cell depending on the environmental conditions (Härtel et al., 2000; Kelly and Dörmann, 2002). They represent the main membrane lipids in green tissue of land plants and are in majority localized to the thylakoids. Each GGL carries two fatty acids in the sn-1 and sn-2 position which show where the precursor came from before the head groups were attached at the envelopes. Lipid backbones produced by the eukaryotic pathway carry 18:3 fatty acids at positions sn-1 and sn-2 (Browse et al., 1986). In contrast, lipid backbones produced in the plastid carry a 16:3 fatty acid at position sn-2 (Browse et al., 1986).

In the green algae *Chlamydomonas reinhardtii* the precursors of GGL biosynthesis are exclusively provided by the chloroplast itself since only the sn-2 position carries a 16:3 fatty acid (Giroud et al., 1988). Plants like spinach and *Arabidopsis* belong to the group of "16:3"-plants. In 16:3 plants the use of ER derived and plastid-derived precursors in GGL biosynthesis is about equal (Browse et al., 1986). Plants like pea use only ER derived precursors for GGL production (Heemskerk et al., 1990) and are called 18:3 plants. It has been shown that "16:3"-plants can be forced to use only ER derived precursors. The knock out of the major enzyme in the prokaryotic diacylglycerol (DAG) production, the plastidic glycerol-3-phosphate acyltransferase (ACT1) leads to a complete shift to ER derived precursor use in *Arabidopsis* (Kunst et al., 1988). In summary, in all land plants, a high volume of traffic is necessary to supply between 50 and 100% of lipid precursors for GGL synthesis, which is envelope bound, from the ER. The major GGLs are monogalactosyldiacylglycerol (MGDG), synthesized at the IE in *Arabidopsis* and digalactosyldiacylglycerol (DGDG), synthesized at the OE. MGDG and DGDG represent approximately 50 and 20% of the plastidic membrane lipids, respectively (Block et al., 1983).

The production of MGDG in *Arabidopsis* is mainly processed by the inner membrane bound protein MGDG synthase 1 (AtMGD1; **Figure 2A**; Marechal et al., 1994; Jarvis et al., 2000). In pea, the MGD activity is divided equally between the IE and the OE (Cline and Keegstra, 1983; Tietje and Heinz, 1998). This distribution possibly reflects the precursor supply by only the eukaryotic pathway in the ER. Consistent with these findings, OE membranes do contain additional enzymes with MGD activity in *Arabidopsis* and also soybean and corn. They are classified as type B MGDs, whereas the major MGDs like AtMGD1 and its paralogs are classified as type A proteins (Miege et al., 1999). *Arabidopsis* contains two type B MGDs, AtMGD2 and AtMGD3 (**Figures 2A,B**). Compared to MGD1, these enzymes show higher selectivity for eukaryotic pathway derived DAG. In photosynthetic active tissue they are underrepresented compared to AtMGD1, while non-green tissues display equal expression patterns for all three MGDs (Awai et al., 2001). These findings are consistent with the importance of type A MGDs for thylakoid lipid assembly. Knock down mutants of AtMGD1 show that the type B MGDs cannot compensate the complete loss of the type A enzyme (Jarvis et al., 2000).

In contrast to MGDG, DGDG is exclusively synthesized at the OE. The predominant enzyme in DGDG biosynthesis is the OE bound DGDG synthase 1 (AtDGD1; **Figure 2A**; Froehlich et al., 2001a). This enzyme drives the UDP-galactose dependent glycosylation of MGDG and produces αβDGDG. Knock out mutant analysis in *Arabidopsis* revealed that AtDGD1 catalyzes 90% of DGDG biosynthesis (Dörmann et al., 1999). The massive decrease in DGDG in mutant plants lead to a strong morphological and developmental defect, which reflects the deficiency in the photosynthetic apparatus (Dörmann et al., 1995). DGD activity in *Arabidopsis* is also not limited to one enzyme. AtDGD2 is an UDP-galactose dependent galactosyl transferase. It localizes to the OE and similar to alternative MGDs, AtDGD2 also shows far less activity and also lower expression levels than the major enzyme (**Figure 2B**; Dörmann et al., 1995; Härtel et al., 2000; Kelly and Dörmann, 2002). AtDGD2 can produce trigalactosyldiacylglycerol (TGDG) *in vitro* (Kelly and Dörmann, 2002), but there is no evidence for the production of TGDG by AtDGD2 *in vivo*.

An additional enzyme involved in GGL biosynthesis and localized to the OE is the galactolipid:galactolipid galactosyltransferase (GGGT) which uses MGDG as the galactosyl donor (Heemskerk et al., 1983, 1986). Its activity was already described in the 1970s when galactosyltransferase activity was analyzed in spinach (Van Besouw and Wintermans, 1978). GGGT catalyzes the synthesis of TGDG or even tetragalactosyldiacylglycerols (TeGDG), while DAG is released (Benning and Ohta, 2005). All galactosyl groups in GGGT produced GGLs are in β-configuration, while DGDs produce DGDGs with alpha-configuration in the second position (Kelly and Dörmann, 2002; Xu et al., 2003). GGGT is equivalent to sensitive to freezing 2 (SFR2; Moellering et al., 2010), a mutant identified earlier as freezing sensitive (Thorlby et al., 2004; Fourrier et al., 2008). Freezing damage is represented by rupture and fusion of membrane bilayers and non-bilayer structures can provide stability to lamellar membrane structures. The change in the membrane lipid composition affected by oligo GGLs leads to the formation of hexagonal-II-type structures at least in the OE, creating a non-bilayer shape of the membrane. Oligo GGLs mediate protection against the dehydration effect by providing a higher thickness of the hydrophilic part of the OE (**Figure 2C**; Moellering et al., 2010).

TRANSPORT OF LIPID PRECURSORS FROM THE ER TO THE PLASTID

Massive lipid traffic occurs between the chloroplast and the ER. Precursors for the galactolipid biosynthesis have to be transported from the ER to the plastid and therefore through the envelopes. The magnitude of lipid flux is increased in "18:3"-plants. While lipid transfer is only partially understood, some proteins involved in ER to plastid transfer have been investigated in detail (summarized in Benning, 2009).

At least four proteins are involved in the transfer of lipids between ER and chloroplast. They are named after the unusual abundance of TGDG in mutant lines, and are called TGD1, 2, 3, and 4 (Xu et al., 2003). TGD1–3 likely form a high molecular weight complex and reside in the IE. While TGD1 is assumed to

channel the lipid, TGD3 was demonstrated to be the ATP hydrolyzing component in the super complex, providing the energy for this process (Lu et al., 2007). TGD2 is hypothesized to be anchored in the IE and interact via its C-terminus with the OE. TGD2 is postulated to disrupt or destabilize the OE to form a conduit for lipid transport from the outer envelope across the IMS (Roston et al., 2011). TGD2's binding affinity to phosphatidic acid (PA) lead to the assumption, that the TGD1–2–3-complex drives the transport of PA from the OE to the IE where it is dephosphorylated to DAG (**Figure 2D**; Awai et al., 2006; Benning, 2009; Lu and Benning, 2009).

A fourth protein in the lipid shuffling process is TGD4. TGD4 is located to the ER and/or the OE and is assumed to transfer eukaryotic lipid precursors to the plastid together with the TGD1–3 machinery (Xu et al., 2008; Benning, 2009). TGD mutants show that TGD proteins are exclusively involved in the lipid transport to the chloroplast (Xu et al., 2010). It is currently not known which, if any, proteins act between the TDG1–3 complex and TGD4 (Benning, 2009). However, the TGD mutant screens include two more complementation groups with the potential to fill the remaining gaps (**Figure 2D**; Xu et al., 2003).

TRANSPORT OF LIPIDS FROM THE PLASTID TO THE ER

During phosphate deprivation plant cells reclaim phosphate from phospholipids. Phospholipids in the PM (Andersson et al., 2003, 2005), mitochondrial membranes (Jouhet et al., 2004), and the tonoplast (Andersson et al., 2005) are replaced by GGLs. Under such stress conditions the underrepresented isoforms AtMGD2, AtMGD3, and AtDGD2, all localized to the outer envelope, are highly expressed. The main surrogate for phospholipids during phosphate deprivation is DGDG that can represent more than 30% of extraplastidial membrane lipids in *Arabidopsis*. The DGDG produced during phosphate limitation is independent of DGD1 since *DGD*1 knock out plants increase their DGDG content under phosphate starvation (Härtel et al., 2000). These enzymes preferably use precursors of the eukaryotic pathway to provide extraplastidic DGDG. It is currently not known how GGLs produced in the outer envelope reach their destination membranes during phosphate starvation. Although the envelopes can form vesicles toward the stroma (Hatta et al., 1973) as well as to the IMS (Park et al., 1999), no vesicular transfer directed from the plastid to the cytosol has been demonstrated. Possibly, the transport is driven by extensive formation of contact sides by the plastid and the ER (**Figure 2B**).

PROTEIN TURNOVER ACROSS AND INTO THE OUTER ENVELOPE

PROTEIN IMPORT THROUGH THE ENVELOPES

The massive gene transfer from the cyanobacterial endosymbiont to the host nucleus necessitated a protein distribution system for the chloroplast. Most chloroplast-bound preproteins in the cytosol contain an N-terminal amino acid sequence, a transit peptide, to address it for import into the chloroplast through the TIC/TOC Complex (Bionda et al., 2010). This complex is abundant in chloroplasts as well as in non-green plastids, such as proplastids (Bräutigam and Weber, 2009) and etioplasts (Von Zychlinski et al., 2005; Reiland et al., 2011). We briefly summarize the knowledge about import with special focus on the outer envelope. The reader is referred to several excellent recent reviews for more details (Soll and Schleiff, 2004; Inaba and Schnell, 2008; Andres et al., 2010; Schwenkert et al., 2010)

The first recognition of the preprotein occurs by cytosolic chaperones HSP90 and HSP70 as well as by 14-3-3-proteins (Schwenkert et al., 2010). These proteins facilitate the transfer of the preproteins to the different receptors in the OE, proteins of the Toc159- and Toc34-family (Gutensohn et al., 2000; Ivanova et al., 2004). In *Arabidopsis* the Toc159 family (earlier known as Toc86-family) consists of four known members in *Arabidopsis*, AtToc90, AtToc120, AtToc132, and AtToc159, named by their different molecular weight. This difference is due to variation in the length of the acidic domain, while they share high sequence similarity in the GTPase-domain and the membrane binding domain (Bauer et al., 2000; Jackson-Constan and Keegstra, 2001; Hiltbrunner et al., 2004; Agne et al., 2010). Since Toc90 can only partially restore the *Arabidopsis* mutant *ppi*2, a plant deficient in AtToc159, it can be assumed that the different acidic domains of the proteins lead to specialization of the receptors (Bauer et al., 2000; Hiltbrunner et al., 2004; Ivanova et al., 2004; Kubis et al., 2004; Agne et al., 2010; Infanger et al., 2011).

The smaller GTPases AtToc33 and AtToc34 represent the Toc34-family in *Arabidopsis* (Jarvis et al., 1998; Chen et al., 2000; Gutensohn et al., 2000). The receptors also partially provide the energy for the protein translocation process by GTP hydrolysis (**Figure 3B**; Schleiff et al., 2003b; Andres et al., 2010). AtToc159 and AtToc33 facilitate the transport of proteins involved in photosynthesis related processes while AtToc120 and AtToc132 are

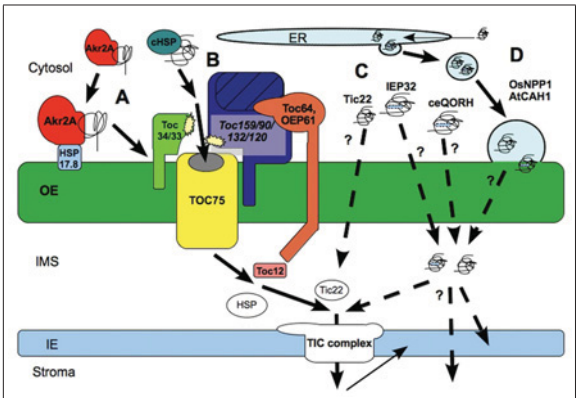

FIGURE 3 | Protein transfer through and into the outer envelope (OE). **(A)** Akr2a pathway for the insertion of OE proteins into the membrane, enhanced by HSP17.8; **(B)** Toc Complex mediated protein translocation via Toc75 and GTPase receptor proteins of the Toc159- and Toc34- family. Translocation is supported by cytosolic HSPs and transmembrane co-chaperones and co-receptors Toc64/OEP61; **(C)** Non-canonical protein translocation through the OE. Pathways are unclear and diverse. Protein internal signals might support the translocation; **(D)** Transfer of proteins through the OE via vesicle fusion. Complete proteins are synthesized in the cytosol, transferred to the ER and transported to the OE via vesicle transport; The transport from the inter membrane space (IMS) into the inner Envelope (IE) or stroma is mainly processed by the translocon complex of the IE (TIC) but other mechanisms have been postulated, too.

more associated to Toc34 and seem to process house-keeping proteins (Ivanova et al., 2004; Huang et al., 2011). These roles are supported by proteomic comparisons between proplastids and chloroplasts, since AtToc120 and AtToc132 can be identified from proplastids but not chloroplasts (Bräutigam and Weber, 2009). AtToc159 can be identified from plastids, etioplasts, and chloroplasts (Von Zychlinski et al., 2005; Bräutigam and Weber, 2009; Reiland et al., 2011). Receptors of the TOC complex have not been identified from chromoplasts (Siddique et al., 2006; Barsan et al., 2010), which may either reflect their absence or technical limitations.

In addition to their function in protein translocation, some Toc components display also other less investigated features. For example, AtToc159 has binding affinity to actin filaments *in vitro* (Jouhet and Gray, 2009). The import receptor for house-keeping proteins, AtToc132, and the pore AtToc75-III are involved in root gravitropism (Stanga et al., 2009). Mutations in AtToc132 or in AtToc75-III, called *mar*2 (*modifier of arg*1 2) and *mar*1, modulate the gravitropism defects in *altered response to gravity* 1 (*arg*1) mutants. The modulation is not dependent on defects in starch orientation. Since the mutants do not show defects in gravitropism on their own, the molecular connection between the import complex components and gravitropism remains unresolved.

The channel protein AtToc75-III facilitates actual transport of the preprotein across the membrane (Perry and Keegstra, 1994; Schnell et al., 1994; Tranel et al., 1995; Hinnah et al., 1997, 2002; Sveshnikova et al., 2000; Jackson-Constan and Keegstra, 2001). As a member of the Omp85-family it contains a N-terminal POTRA (polypeptide-transport-associated) domain. The 16–18 *in silico* predicted β-strands at the C-terminus form the β-barrel domain, the pore (Sveshnikova et al., 2000; Hinnah et al., 2002; Schleiff et al., 2003a; Gentle et al., 2004; Baldwin et al., 2005). It has been shown, that AtToc75-III is not selective for a specific form of protein precursors (Baldwin et al., 2005) and this protein can be found in all plastid types investigated by proteomics (e.g., Bräutigam and Weber, 2009; Barsan et al., 2010; Reiland et al., 2011). A protein similar to AtToc75-III, AtToc75-V/OEP80, is required for accumulation of AtToc75-III in the membrane (Wallas et al., 2003). AtToc75-III in turn is required for the TOC-receptor compounds (Wallas et al., 2003).

Several proteins are reportedly associated with the import complex, however their precise function remains elusive. Toc64 and AtOEP61 likely interact with cytosolic chaperones and function as co-chaperone and co-receptor for the TOC complex (Qbadou et al., 2007; Von Loeffelholz et al., 2011). Another protein is the IMS localized Toc12, which interacts with Toc64 (Becker et al., 2004) and the inner membrane space proteins Tic22 and a chaperone (**Figure 3B**; Becker et al., 2004).

Virtually all known inner envelope, stromal, and thylakoid proteins are imported through the import complex. However, a subset of proteins identified during proteomic analysis of chloroplasts lacks a recognizable transit peptide (Baginsky and Gruissem, 2004). These proteins may either be contaminations or they may enter the plastid through a different pathway. The majority of outer envelope proteins also lacks a recognizable target peptide and enters the outer envelope without the benefit of the TOC Complex.

TOC COMPLEX INDEPENDENT PROTEIN IMPORT

One possible alternative route for proteins into the chloroplast has been shown for the a-type family carbonic anhydrase CAH1 in *A. thaliana* (Villarejo et al., 2005) and ADP-glucose hydrolytic nucleotide pyrophosphatase/phosphodiesterase (NPP) 1 in rice (Nanjo et al., 2006). CAH1 as well as NPP1 have an N-terminal signal peptide for the secretory pathway, which targets the proteins to the ER. *In vivo* localization studies with GFP fusion revealed CAH1 and NPP1 localization in the stroma. The localization in both studies was altered by the Golgi vesicle transport inhibitor brefeldin A, and CAH1–GFP as well as NPP1–GFP accumulated in ER and golgi (Villarejo et al., 2005; Nanjo et al., 2006). Based on these results CAH1 and NPP1 are transported from the cytosol into the ER and on to the chloroplast by Golgi-mediated vesicle transport. At the OE it is assumed that Golgi vesicles fuse with the envelope and release the fully folded protein into the IMS between IE and OE (**Figure 3D**; Villarejo et al., 2005; Nanjo et al., 2006). How the transport from the IMS into the stroma is accomplished is speculative.

An internal signal sequence is important for the transfer of NPP1 to the chloroplast (Kaneko et al., 2010). The requirement of an internal signal sequence was also shown for the TOC-independent insertion of the IE proteins chloroplast envelope quinone oxidoreductase (ceQORH; Miras et al., 2002, 2007), and the inner envelope protein (IEP) 32 (**Figure 3C**; Nada and Soll, 2004). While the presence of internal sequence motives important for transport appears to be a general theme, ceQORH, IEP32, and the protein Tic22 (Kouranov et al., 1998, 1999) were shown to be transferred to their destinations by different pathways (**Figure 3C**; Kouranov et al., 1999; Nada and Soll, 2004; Miras et al., 2007).

The study of early branching Archaeplastida provides further insights into the transport independent of the TOC complex. Recent studies on the amoeboid *Paulinella chromatophora* and its photosynthetic endosymbiont revealed an involvement of the ER in protein sorting to the plastid in earlier evolutionary stages (Mackiewicz and Bodyl, 2010).

PROTEIN INSERTION INTO THE OE

Unlike TOC based transport, the insertion of OE proteins into the membrane is mostly independent of energy equivalents. Many proteins can insert in thermolysin-treated plastids. This was taken as evidence for protein independent insertion, however, since OEP7 (called OEP14 in pea) insertion is inhibited by trypsin and *N*-ethylmaleimide but not thermolysin, it is more likely that the proteins involved are not affected by thermolysin treatment. Protein insertion has been studied with several model proteins: OEP7 (*Arabidopsis*), OEP14 (pea), and E6.7 (spinach) although their function is still not determined, Toc64, (Salomon et al., 1990; Li et al., 1991; Tu and Li, 2000; Lee et al., 2001; Dyall et al., 2004; Nada and Soll, 2004; Bae et al., 2008; Oikawa et al., 2008), the tail-anchored proteins OEP9 and Toc33 and Toc34 (Dhanoa et al., 2010) and the major import pore Toc75-III.

The ankyrin repeat proteins 2A and 2B (Akr2A and Akr2B) are involved in protein trafficking to the OE based on OEP7 and cOEP64/AtToc64 import experiments. The recognition and insertion of OEPs into the membrane requires a single C-terminal TMD and an upstream target signal. This signal is part of the functional

protein and not cleaved off after translocation into the membrane (Tu and Li, 2000; Lee et al., 2001; Tu et al., 2004; Bae et al., 2008). The Akr2A protein mediates recognition of the preprotein. Akr2A binds with its N-terminal region to the target signals of the OE protein while the C-terminal region is required for binding to the OE. Akr2A also provides chaperone activity to OEPs (**Figure 3A**; Bae et al., 2008). Akr2B functions similarly to Akr2A (Bae et al., 2008)

Akr2a mediated import is also required to target tail-anchored proteins to the chloroplast (Dhanoa et al., 2010). Tail-anchored protein import can be divided into delivery of the protein to the appropriate organelle and insertion into the target membrane. While Akr2A mediates targeting to the appropriate organelle, insertion pathways diverge. The insertion of newly synthesized Toc33/34 depends on the presence of Toc33 in the membrane and is thus dependent on proteins and not or not only on the composition of the lipid bilayer. While insertion of OEP9 is also protein dependent, it does not require Toc33 or Toc34 for insertion and may be dependent on Toc75 (Dhanoa et al., 2010).

A second cytosolic factor is required for at least OEP7 insertion. A small cytosolic class 1 heat shock protein, Hsp17.8 which can dimerize or assemble into a temperature induced oligomeric complex, interacts with the C-terminal ankyrin repeat domain of Akr2A and, as a dimer, binds with high affinity to the OE. This mediates an enhanced binding affinity of Akr2A to the OE. Knock down lines of class1 HSPs including HSP17.8 exhibit reduced targeting efficiency for OEP7 and overexpression lines enhance OE targeting (**Figure 3A**; Kim et al., 2011). At least four other small cytosolic heat shock proteins can also interact with AKR2A to varying degrees (Kim et al., 2011).

Targeting of one of the major outer envelope proteins, AtToc75-III, remains enigmatic. Unlike all other outer envelope proteins tested, AtToc75-III carries a bipartite targeting signal, which consists of a cleavable targeting signal to the chloroplast stroma and a polyglycine stretch required for insertion into the outer envelope (Tranel et al., 1995; Tranel and Keegstra, 1996; Inoue and Keegstra, 2003). The exact mechanism for Toc75 insertion is currently unknown but other OMP85 related proteins like AtTOC75-V/OEP80 (Patel et al., 2008; Huang et al., 2011) and the N-terminal truncated Toc75 homolog, AtToc75-IV, which is inserted into the membrane without any cleavable target peptide (Baldwin et al., 2005), may help to understand the insertion process of AtToc75-III.

The rapid progress in dissecting the import pathways into the outer envelope in recent years (Bae et al., 2008; Dhanoa et al., 2010; Kim et al., 2011) since the focus was shifted from the well understood TIC–TOC Pathway (Soll and Schleiff, 2004; Inaba and Schnell, 2008; Andres et al., 2010; Schwenkert et al., 2010) to other import pathways may indicate that a systematic picture of targeting machinery and signals may soon arise from additional studies.

PROTEIN REPAIR AND DEGRADATION

The interior of the chloroplast is a hazardously oxidizing environment with multiple protection systems (Baier and Dietz, 2005; Oelze et al., 2008). Yet, no protein repair or turnover mechanism is known in addition to those of cyanobacterial origin affecting the thylakoid membranes themselves (Nixon et al., 2010). Mitochondria can be turned over entirely by autophagy. The complete organelle is engulfed, digested, and its parts recycled (Mijaljica et al., 2007). However, plastids are too big to fit into the autophagy machinery (Ishida and Yoshimoto, 2008; Izumi et al., 2010). There are organisms containing only a single plastid such as *C. reinhardtii*. Turning over the complete plastid is not a viable route in these organisms. Cytosolic proteins can also be recycled by autophagy or they are targeted for degradation through the proteasome by ubiquitination (Van Doorn and Woltering, 2005; Reape et al., 2008; Uchiyama et al., 2008). Unlike the IE and the proteins within the plastids, the OE is exposed to the cytosol and hence to the protein degradation machinery. However, ubiquitination of any plastid protein has not yet been reported from any of the proteome studies, likely because these studies were not designed to identify such post-translational modifications (e.g., Rolland et al., 2003; Bräutigam et al., 2008; Bräutigam and Weber, 2009; Ferro et al., 2010). Since it is highly unlikely that all plastid proteins survive intact for the duration of plant life (some plants can reach several thousand years in age), one or several methods for protein turnover at the plastid must exist. During plastid differentiation from proplastids to chloroplasts, the protein complement of the stroma (compare Sun et al., 2009; Ferro et al., 2010), the IE, and the OE (e.g., Bräutigam and Weber, 2009) is changed in quality and quantity again necessitating protein degradation. Although it is tempting to speculate about vesicular transport out of the plastids of envelope proteins especially in light of the unresolved lipid transfer from plastids to the remainder of the cell, the question of protein turnover in the plastids envelopes remains completely unresolved.

INTERACTION OF THE OUTER ENVELOPE WITH THE CYTOSOL

SITES MEDIATING THE CONTACT BETWEEN THE PLASTID AND THE ER

Fatty acid and lipid metabolism require close physical contact of the ER and the plastids. Yet, the structural components mediating the interaction have not been identified to date. Plastid associated membranes (PLAMs) are a vesicular structure attached to the plastids from the cytosolic side (Andersson et al., 2007a,b). They were identified by GFP labeling the ER and isolating plastids, which were then decorated with fluorescing vesicles. Optical tweezers needed a force of 400 pN to overcome the attachment, which is a force equivalent to that of a protein–protein interactions (Florin et al., 1994). The vesicles can also be removed by a low pH/low salt wash in MES buffer (pH 6.0) supplemented with sucrose (details in Andersson et al., 2007a,b). Their lipid composition is intermediate between the composition of the outer envelope and the ER.

A second structure has been implicated in mediating interaction between the plastid and the cytosol, especially the ER: the stromules (Köhler and Hanson, 2000). Stromules are defined as stroma-filled tubules jutting out from plastids. They were observed in many tissues and different species, so they are likely a general feature of at least moss and higher plant plastids (Gray et al., 2001; Pyke and Howells, 2002; Waters et al., 2004; Gunning, 2005; Hanson and Sattarzadeh, 2008; Holzinger et al., 2008; Reski, 2009; Shaw and Gray, 2011). Stromules are hypothesized to be built by the joint action of internal pressure and external draw. Filament forming proteins, such as the plastid division protein FtsZ are under debate to be involved in the formation of stromules since they are abundant in tomato chromoplasts where

plastid division is unlikely to occur (Reski, 2009; Barsan et al., 2010; Hanson and Sattarzadeh, 2011). The cytosolic compounds in the stromule formation process are most probably the actin cytoskeleton (Kwok and Hanson, 2004) in combination with specific myosin proteins. Stromule formation is decreased by actin inhibitors and by gene silencing of myosin class XI motor proteins (Kwok and Hanson, 2003; Sattarzadeh et al., 2009). Actin inhibitors lead to collapse of existing stromules, which remain tubular but collapse onto the plastid surface (Kwok and Hanson, 2003). Since the material does not spontaneously reinsert, the formation and reinsertion of stromules is probably an active process. In addition to the involvement of actin in stromule movement, motor proteins like myosin XI of the F-class are assumed to drive the chloroplast dynamics (Sattarzadeh et al., 2009). The best evidence for a direct interaction of myosin with the stromule and plastidic OE was described for a myosinXI-2 relative of *Arabidopsis* in *N. benthamiana*. This has been shown to interact with its cargo-binding domain at the C-terminus directly with the OE (Natesan et al., 2009). Therefore, one or more myosins of the XI-F-family are proposed to be anchors in the OE, building connection between actin skeleton and stromules (Sattarzadeh et al., 2009).

Similar to PLAMs the functional significance of stromules has not been experimentally tested. Direct substance transport between connected plastids is possible, yet likely slow since dense stroma fills the connecting tubules (Köhler et al., 2000; Hanson and Sattarzadeh, 2011). Plastids have almost perfect lens-shape, which limits the surface to volume ratio. Stromules massively increase the surface area (compare Hanson and Sattarzadeh, 2011) and provide space for proteins such as transporters. If this hypothesis was true, stromules should be present in cells and tissues with increased import or export requirements for metabolites across the envelope membranes. Remarkably, stromules are barely detectable in mature leaf chloroplasts, which actively photosynthesize but frequently observed in other tissues, which rather have sink characteristics (Köhler and Hanson, 2000; Pyke and Howells, 2002; Waters et al., 2004). Apparently, the high flux of photosynthates in leaf chloroplasts does not require surface area increases as is also evident by the absence of stromules in algal chloroplasts. Stromules may also bridge the distance between plastids and other organelles or maintain connections while allowing movement of chloroplasts. Plastids can "hug" or surround completely other organelles via stromules (e.g., Sage and Sage, 2009). Dynamics of stromules and of the cortical ER correlate with each other, mediated either by shared cytoskeletal interaction or by direct interaction (Schattat et al., 2011) possibly through PLAMs. The ER and the plastids use different myosins but a common actin backbone to mediate their individual movements (Sattarzadeh et al., 2009; Ueda et al., 2010). Stromules may mediate signaling between plastids and the PM. The protein thylakoid formation 1 (THF1) is localized to the stroma and to the OE of plastids (Wang et al., 2004; Huang et al., 2006; Joyard et al., 2010). It is also distributed to stromules. While deletion of the THF1 gene leads to defects in thylakoid formation (Wang et al., 2004), it is detectable in chromoplasts (Siddique et al., 2006), a plastid type with frequent stromule sightings (Pyke and Howells, 2002; Waters et al., 2004) but without photosynthesis. Recent findings revealed, that THF1 physically interacts with the plasma membrane G-protein GPA1 (Huang et al., 2006). This interaction requires proximity of the plastid or its stromule with the plasma membrane. Stromules may also play a role in stress response (Holzinger et al., 2007; Gray et al., 2011)

The evidence for stromules interacting with other cellular compartments is circumstantial hence the function of stromules remains as unknown as the mechanism that builds them.

MOVEMENT OF CHLOROPLAST

One of the adaptations of the plant to different light dosage is the dynamic positioning of the chloroplasts inside the cell (Trojan and Gabrys, 1996). On the one hand, the position change increases the light-use-efficiency during low light conditions. On the other hand, it reduces photo-damage during high light conditions. The OE is the interface for the moving devices of the cell. Mutants deficient in chloroplast unusual positioning 1 (CHUP1) display defects in the distribution and positioning of chloroplasts in the cell. CHUP1 is N-terminal anchored in the OE membrane by a single TMD representing also the targeting signal for its insertion. Its C-terminus is facing the cytosol and contains an actin binding motif. CHUP1 directly interacts with the PM via a C-terminal coiled coil domain (Oikawa et al., 2003, 2008; Von Braun and Schleiff, 2008). Two kinesin-like proteins (KAC1 and KAC2) are CHUP1 interaction partners at the PM (Suetsugu et al., 2010). The interaction between CHUP1 and KAC1/2 is mediated by a specific type of chloroplast associated actin filaments (cp-actin). The accumulation of cp-actin at the actin binding domain of CHUP 1 and their connection to the PM are regulated by two blue light receptor phototropins, Phot1 and Phot2 (Kadota et al., 2009). The PM protein THRUMIN1 has also been postulated to be a link for plastidial movement. The study suggests F-actin as the moving devise for plastid movement (Whippo et al., 2011) as described earlier (Oikawa et al., 2003).

While several extra plastidic factors are involved in the chloroplast movement, CHUP1 is the only detected plastidic factor involved in this process so far (Kadota et al., 2009; Whippo et al., 2011).

THE ROLE OF OE IN PLASTID–NUCLEUS INTERACTION

Retrograde signaling from the plastid to the nucleus is a necessity. However, retrograde signals remain unknown. A recent study describes a protein possibly involved in the retrograde signaling from the plastid outer envelope to the nucleus (Sun et al., 2011). The protein contains a plant homeodomain (PHD) and is bona fide a transcription factor since it can activate transcription. It is bound to the OE via TMDs, hence its name PTM (PHD type transcription factor with TMDs). Immunoblot analysis revealed re-localization of the soluble N-terminal part of PTM to the nucleus upon signal dependent cleavage (Sun et al., 2011). PTM was shown to be involved in the expression of ABI4, which in turn regulates light harvesting complex associated chlorophyll binding proteins (Sun et al., 2011). *Ptm* knock out plants did not show any phenotype, indicating compensation of the loss of function by other factors. How signals are related from the inside of the plastid to the outer envelope remains unknown. The identification of a chloroplast derived transmitter, the cleavable PTM, holds promise for identification of additional parts in the signaling cascade.

DIVISION OF THE CHLOROPLAST

Two systems in concerted action, one on the stromal side of the envelopes and a second one on the cytosolic side of the OE accomplish plastid division. The stromal machinery originated from cyanobacteria (summarized in Yang et al., 2008) while the OE machinery was evolved from host proteins (summarized in Miyagishima, 2005) Both machineries are coordinated through ARC6 (accumulation and replication of chloroplast; Glynn et al., 2008) and PARC6 (paralog of ARC; Glynn et al., 2009) two IEPs that connect the inner machinery to the outer envelope through recruiting PDV1 (plastid division) and PDV2 (Miyagishima et al., 2006; Glynn et al., 2008, 2009). PDV1 and PDV2 in turn recruit ARC5, a dynamin-like protein (Gao et al., 2003), which forms a constriction force on the outside. They can mediate interactions between the plastid and the cytosol since their C-terminus faces the IMS where it can interact with IEPs. Their N-terminus faces the cytosolic site where it can interact with host proteins (Miyagishima et al., 2006). However, PDVs do not control plastid volume per cell; chloroplast number correlates negatively with chloroplast volume, the smaller they are, the more of them are present (Okazaki et al., 2009). The intriguing double mutant in IE mechano-sensitive (MS) ion channels also changes the plastid number per cell but not plastid volume (Haswell and Meyerowitz, 2006; Wilson et al., 2011) as do all known division machinery mutants (summarized in Yang et al., 2008). Pleiotropic effects of the MSL (MS-like) mutant include fewer cells, thicker leaves, and empty leaves. The CRL1 (crumbled leaf) mutants defective in an OE protein of unknown function as well as ARC6 mutants also show developmental abnormalities (Asano et al., 2004; Chen et al., 2009).

All mutants in the division machinery affect the plastid number and size, which are inversely correlated. If the number of plastids is reduced the remaining plastids increase in size and vice versa. Hence it is unlikely that the division machinery, which is localized to the envelopes controls plastid volume. The mechanism by which the cell determines how much of its volume it devotes to plastids is unknown but clearly, different cell types in plants devote different amounts of volume to plastids indicating that plastid volume is developmentally controlled. Recently it was discovered that ER tubules mark the site of mitochondrial division in yeast (Friedman et al., 2011). It is thus tempting to speculate that interactions between chloroplast and ER, such as PLAMs, might be involved in governing or coordinating plastid division.

CONCLUSION

In this review we described the multitude of functions associated with the outer plastid envelope. The opinions about its relevance for the function of the plant cell have changed over the past decades. Study of the plastids has mostly focused on protein rich, abundant subcompartments, such as the thylakoids. However, a detailed understanding of how the plastids integrate into the cytosol can only be achieved through understanding of the barrier between the compartments, the outer envelope. Metabolite transfer through the outer envelope is reasonably well understood, as are lipid synthesis and the division machinery. Progress has been made in studying ER to chloroplast transfer of lipids and protein targeting. However, transfer of lipids out of the plastids, protein turnover, and signal transduction remain mostly unknown.

ACKNOWLEDGMENTS

This work was supported by a grant of the Deutsche Forschungsgemeinschaft (WE2231/4-1 to APMW) in the framework of the *Arabidopsis* Functional Genomics Network (AFGN).

REFERENCES

Abdallah, F., Salamini, F., and Leister, D. (2000). A prediction of the size and evolutionary origin of the proteome of chloroplasts of *Arabidopsis*. *Trends Plant Sci.* 5, 141–142.

Agne, B., Andres, C., Montandon, C., Christ, B., Ertan, A., Jung, F., Infanger, S., Bischof, S., Baginsky, S., and Kessler, F. (2010). The acidic A-domain of *Arabidopsis* TOC159 occurs as a hyperphosphorylated protein. *Plant Physiol.* 153, 1016–1030.

Andersson, M. X., Goksor, M., and Sandelius, A. S. (2007a). Membrane contact sites: physical attachment between chloroplasts and endoplasmic reticulum revealed by optical manipulation. *Plant Signal. Behav.* 2, 185–187.

Andersson, M. X., Goksor, M., and Sandelius, A. S. (2007b). Optical manipulation reveals strong attracting forces at membrane contact sites between endoplasmic reticulum and chloroplasts. *J. Biol. Chem.* 282, 1170–1174.

Andersson, M. X., Larsson, K. E., Tjellstrom, H., Liljenberg, C., and Sandelius, A. S. (2005). Phosphate-limited oat. The plasma membrane and the tonoplast as major targets for phospholipid-to-glycolipid replacement and stimulation of phospholipases in the plasma membrane. *J. Biol. Chem.* 280, 27578–27586.

Andersson, M. X., Stridh, M. H., Larsson, K. E., Liljenberg, C., and Sandelius, A. S. (2003). Phosphate-deficient oat replaces a major portion of the plasma membrane phospholipids with the galactolipid digalactosyldiacylglycerol. *FEBS Lett.* 537, 128–132.

Andres, C., Agne, B., and Kessler, F. (2010). The TOC complex: preprotein gateway to the chloroplast. *Biochim. Biophys. Acta* 1803, 715–723.

Arimura, G.-I., Matsui, K., and Takabayashi, J. (2009). Chemical and molecular ecology of herbivore-induced plant volatiles: proximate factors and their ultimate functions. *Plant Cell Physiol.* 50, 911–923.

Aronsson, H., Boij, P., Patel, R., Wardle, A., Topel, M., and Jarvis, P. (2007). Toc64/OEP64 is not essential for the efficient import of proteins into chloroplasts in *Arabidopsis thaliana*. *Plant J.* 52, 53–68.

Asano, T., Yoshioka, Y., Kurei, S., Sakamoto, W., and Machida, Y. (2004). A mutation of the CRUMPLED LEAF gene that encodes a protein localized in the outer envelope membrane of plastids affects the pattern of cell division, cell differentiation, and plastid division in *Arabidopsis*. *Plant J.* 38, 448–459.

Awai, K., Marechal, E., Block, M. A., Brun, D., Masuda, T., Shimada, H., Takamiya, K., Ohta, H., and Joyard, J. (2001). Two types of MGDG synthase genes, found widely in both 16:3 and 18:3 plants, differentially mediate galactolipid syntheses in photosynthetic and nonphotosynthetic tissues in *Arabidopsis thaliana*. *Proc. Natl. Acad. Sci. U.S.A.* 98, 10960–10965.

Awai, K., Xu, C. C., Tamot, B., and Benning, C. (2006). A phosphatidic acid-binding protein of the chloroplast inner envelope membrane involved in lipid trafficking. *Proc. Natl. Acad. Sci. U.S.A.* 103, 10817–10822.

Bae, W., Lee, Y. J., Kim, D. H., Lee, J., Kim, S., Sohn, E. J., and Hwang, I. (2008). AKr2A-mediated import of chloroplast outer membrane proteins is essential for chloroplast biogenesis. *Nat. Cell Biol.* 10, 220–227.

Baginsky, S., and Gruissem, W. (2004). Chloroplast proteomics: potentials and challenges. *J. Exp. Bot.* 55, 1213–1220.

Baier, M., and Dietz, K. J. (2005). Chloroplasts as source and target of cellular redox regulation: a discussion on chloroplast redox signals in the context of plant physiology. *J. Exp. Bot.* 56, 1449–1462.

Baldi, P., Grossi, M., Pecchioni, N., Vale, G., and Cattivelli, L. (1999). High expression level of a gene coding for a chloroplastic amino acid selective channel protein is correlated to cold acclimation in cereals. *Plant Mol. Biol.* 41, 233–243.

Baldwin, A., Wardle, A., Patel, R., Dudley, P., Park, S. K., Twell, D., Inoue, K., and Jarvis, P. (2005). A molecular-genetic study of the *Arabidopsis* Toc75 gene family. *Plant Physiol.* 138, 715–733.

Balsemao-Pires, E., Jaillais, Y., Olson, B. J., Andrade, L. R., Umen, J. G., Chory, J., and Sachetto-Martins, G. (2011). The *Arabidopsis* translocator protein (AtTSPO) is regulated at multiple levels in response to salt stress and perturbations in tetrapyrrole metabolism. *BMC Plant Biol.* 11, 108. doi:10.1186/1471-2229-11-108

Barsan, C., Sanchez-Bel, P., Rombaldi, C., Egea, I., Rossignol, M., Kuntz, M., Zouine, M., Latche, A., Bouzayen, M., and Pech, J. C. (2010). Characteristics of the tomato chromoplast revealed by proteomic analysis. *J. Exp. Bot.* 61, 2413–2431.

Bauer, J., Chen, K. H., Hiltbunner, A., Wehrli, E., Eugster, M., Schnell, D., and Kessler, F. (2000). The major protein import receptor of plastids is essential for chloroplast biogenesis. *Nature* 403, 203–207.

Becker, T., Hritz, J., Vogel, M., Caliebe, A., Bukau, B., Soll, J., and Schleiff, E. (2004). Toc12, a novel subunit of the intermembrane space preprotein translocon of chloroplasts. *Mol. Biol. Cell* 15, 5130–5144.

Benning, C. (2009). Mechanisms of lipid transport involved in organelle biogenesis in plant cells. *Annu. Rev. Cell Dev. Biol.* 25, 71–91.

Benning, C., and Ohta, H. (2005). Three enzyme systems for galactoglycerolipid biosynthesis are coordinately regulated in plants. *J. Biol. Chem.* 280, 2397–2400.

Bickel, H., Palme, L., and Schultz, G. (1978). Incorporation of shikimate and other precursors into aromatic amino acids and prenylquinones of isolated spinach chloroplasts. *Phytochemistry* 17, 119–124.

Binder, S., Knill, T., and Schuster, J. (2007). Branched-chain amino acid metabolism in higher plants. *Physiol. Plant* 129, 68–78.

Bionda, T., Tillmann, B., Simm, S., Beilstein, K., Ruprecht, M., and Schleiff, E. (2010). Chloroplast import signals: the length requirement for translocation in vitro and in vivo. *J. Mol. Biol.* 402, 510–523.

Blee, E., and Joyard, J. (1996). Envelope membranes from spinach chloroplasts are a site of metabolism of fatty acid hydroperoxides. *Plant Physiol.* 110, 445–454.

Block, M. A., Dorne, A. J., Joyard, J., and Douce, R. (1983). Preparation and characterization of membrane fractions enriched in outer and inner envelope membranes from spinach chloroplasts. II. Biochemical characterization. *J. Biol. Chem.* 258, 13281–13286.

Bolter, B., Soll, J., Hill, K., Hemmler, R., and Wagner, R. (1999). A rectifying ATP-regulated solute channel in the chloroplastic outer envelope from pea. *EMBO J.* 18, 5505–5516.

Bräutigam, A., Hofmann-Benning, S., and Weber, A. P. M. (2008). Comparative proteomics of chloroplast envelopes from C3 and C4 plants reveals specific adaptations of the plastid envelope to C4 photosynthesis and candidate proteins required for maintaining C4 metabolite fluxes. *Plant Physiol.* 148, 568–579.

Bräutigam, A., and Weber, A. P. M. (2009). Proteomic analysis of the proplastid envelope membrane provides novel insights into small molecule and protein transport across proplastid membranes. *Mol. Plant* 2, 1247–1261.

Bräutigam, A., and Weber, A. P. M. (2011). Do metabolite transport processes limit photosynthesis? *Plant Physiol.* 155, 43–48.

Browse, J., Mcconn, M., James, D. Jr., and Miquel, M. (1993). Mutants of *Arabidopsis* deficient in the synthesis of alpha-linoleate. Biochemical and genetic characterization of the endoplasmic reticulum linoleoyl desaturase. *J. Biol. Chem.* 268, 16345–16351.

Browse, J., Warwick, N., Somerville, C. R., and Slack, C. R. (1986). Fluxes through the prokaryotic and eukaryotic pathways of lipid synthesis in the "16:3" plant *Arabidopsis thaliana*. *Biochem. J.* 235, 25–31.

Chen, K. H., Chen, X. J., and Schnell, D. J. (2000). Initial binding of preproteins involving the Toc159 receptor can be bypassed during protein import into chloroplasts. *Plant Physiol.* 122, 813–822.

Chen, Y. L., Asano, T., Fujiwara, M. T., Yoshida, S., Machida, Y., and Yoshioka, Y. (2009). Plant cells without detectable plastids are generated in the crumpled leaf mutant of *Arabidopsis thaliana*. *Plant Cell Physiol.* 50, 956–969.

Cline, K., and Keegstra, K. (1983). Galactosyltransferases involved in galactolipid biosynthesis are located in the outer membrane of pea chloroplast envelopes. *Plant Physiol.* 71, 366–372.

Curien, G., Bastien, O., Robert-Genthon, M., Cornish-Bowden, A., Cardenas, M. L., and Dumas, R. (2009). Understanding the regulation of aspartate metabolism using a model based on measured kinetic parameters. *Mol. Syst. Biol.* 5, 271.

Curien, G., Ravanel, S., Robert, M., and Dumas, R. (2005). Identification of six novel allosteric effectors of *Arabidopsis thaliana* aspartate kinase-homoserine dehydrogenase isoforms. Physiological context sets the specificity. *J. Biol. Chem.* 280, 41178–41183.

Dhanoa, P. K., Richardson, L. G. L., Smith, M. D., Gidda, S. K., Henderson, M. P. A., Andrews, D. W., and Mullen, R. T. (2010). Distinct pathways mediate the sorting of tail-anchored proteins to the plastid outer envelope. *PLoS ONE* 5, e10098. doi:10.1371/journal.pone.0010098

Doremus, H. D., and Jagendorf, A. T. (1985). Subcellular localization of the pathway of de novo pyrimidine nucleotide biosynthesis in pea leaves. *Plant Physiol.* 79, 856–861.

Dörmann, P., Balbo, I., and Benning, C. (1999). *Arabidopsis* galactolipid biosynthesis and lipid trafficking mediated by DGD1. *Science* 284, 2181–2184.

Dörmann, P., Hoffmann-Benning, S., Balbo, I., and Benning, C. (1995). Isolation and characterization of an *Arabidopsis* mutant deficient in the thylakoid lipid digalactosyldiacylglycerol. *Plant Cell* 7, 1801–1810.

Drea, S. C., Lao, N. T., Wolfe, K. H., and Kavanagh, T. A. (2006). Gene duplication, exon gain and neofunctionalization of OEP16-related genes in land plants. *Plant J.* 46, 723–735.

Duy, D., Soll, J., and Philippar, K. (2007). Solute channels of the outer membrane: from bacteria to chloroplasts. *Biol. Chem.* 388, 879–889.

Dyall, S. D., Brown, M. T., and Johnson, P. J. (2004). Ancient invasions: from endosymbionts to organelles. *Science* 304, 253–257.

El-Shami, M., El-Kafafi, S., Falconet, D., and Lerbs-Mache, S. (2002). Cell cycle-dependent modulation of FtsZ expression in synchronized tobacco BY2 cells. *Mol. Genet. Genomics* 267, 254–261.

Facchinelli, F., and Weber, A. P. M. (2011). The metabolite transporters of the plastid envelope: an update. *Front. Plant Sci.* 2:50. doi:10.3389/fpls.2011.00050

Ferro, M., Brugiere, S., Salvi, D., Seigneurin-Berny, D., Court, M., Moyet, L., Ramus, C., Miras, S., Mellal, M., Le Gall, S., Kieffer-Jaquinod, S., Bruley, C., Garin, J., Joyard, J., Masselon, C., and Rolland, N. (2010). AT_CHLORO, a comprehensive chloroplast proteome database with subplastidial localization and curated information on envelope proteins. *Mol. Cell. Proteomics* 9, 1063–1084.

Fischer, K. (2011). The import and export business in plastids: transport processes across the inner envelope membrane. *Plant Physiol.* 155, 1511–1519.

Fischer, K., Weber, A., Arbinger, B., Brink, S., Eckerskorn, C., and Flugge, U. I. (1994). The 24 kDa outer envelope membrane protein from spinach chloroplasts: molecular cloning, in vivo expression and import pathway of a protein with unusual properties. *Plant Mol. Biol.* 25, 167–177.

Florin, E. L., Moy, V. T., and Gaub, H. E. (1994). Adhesion forces between individual ligand-receptor pairs. *Science* 264, 415–417.

Flügge, U. I. (2000). Transport in and out of plastids: does the outer envelope membrane control the flow? *Trends Plant Sci.* 5, 135–137.

Fourrier, N., Bedard, J., Lopez-Juez, E., Barbrook, A., Bowyer, J., Jarvis, P., Warren, G., and Thorlby, G. (2008). A role for SENSITIVE TO FREEZING2 in protecting chloroplasts against freeze-induced damage in *Arabidopsis*. *Plant J.* 55, 734–745.

Frank, W., Baar, K. M., Qudeimat, E., Woriedh, M., Alawady, A., Ratnadewi, D., Gremillon, L., Grimm, B., and Reski, R. (2007). A mitochondrial protein homologous to the mammalian peripheral-type benzodiazepine receptor is essential for stress adaptation in plants. *Plant J.* 51, 1004–1018.

Friedman, J. R., Lackner, L. L., West, M., Dibenedetto, J. R., Nunnari, J., and Voeltz, G. K. (2011). ER tubules mark sites of mitochondrial division. *Science* 334, 358–362.

Froehlich, J. E., Benning, C., and Dörmann, P. (2001a). The digalactosyldiacylglycerol (DGDG) synthase DGD1 is inserted into the outer envelope membrane of chloroplasts in a manner independent of the general import pathway and does not depend on direct interaction with monogalactosyldiacylglycerol synthase for DGDG biosynthesis. *J. Biol. Chem.* 276, 31806–31812.

Froehlich, J. E., Itoh, A., and Howe, G. A. (2001b). Tomato allene oxide synthase and fatty acid hydroperoxide lyase, two cytochrome P450s involved in oxylipin metabolism, are targeted to different membranes of chloroplast envelope. *Plant Physiol.* 125, 306–317.

Gao, H. B., Kadirjan-Kalbach, D., Froehlich, J. E., and Osteryoung, K. W. (2003). ARC5, a cytosolic dynamin-like protein from plants, is part of the chloroplast division machinery. *Proc. Natl. Acad. Sci. U.S.A.* 100, 4328–4333.

Garcia, O., Bouige, P., Forestier, C., and Dassa, E. (2004). Inventory and comparative analysis of rice and *Arabidopsis* ATP-binding cassette (ABC) systems. *J. Mol. Biol.* 343, 249–265.

Gentle, I., Gabriel, K., Beech, P., Waller, R., and Lithgow, T. (2004). The Omp85 family of proteins is essential for outer membrane biogenesis in mitochondria and bacteria. *J. Cell Biol.* 164, 19–24.

Giermann, N., Schroder, M., Ritter, T., and Zrenner, R. (2002). Molecular analysis of de novo pyrimidine synthesis in solanaceous species. *Plant Mol. Biol.* 50, 393–403.

Giroud, C., Gerber, A., and Eichenberger, W. (1988). Lipids of *Chlamydomonas reinhardtii*. Analysis of molecular species and intracellular site(s) of biosynthesis. *Plant Cell Physiol.* 29, 587–595.

Glynn, J. M., Froehlich, J. E., and Osteryoung, K. W. (2008). *Arabidopsis* ARC6 coordinates the division machineries of the inner and outer chloroplast membranes through interaction with pdv2 in the intermembrane space. *Plant Cell Online* 20, 2460–2470.

Glynn, J. M., Yang, Y., Vitha, S., Schmitz, A. J., Hemmes, M., Miyagishima, S. Y., and Osteryoung, K. W. (2009). PARC6, a novel chloroplast division factor, influences FtsZ assembly and is required for recruitment of PDV1 during chloroplast division in *Arabidopsis*. *Plant J.* 59, 700–711.

Goetze, T. A., Philippar, K., Ilkavets, I., Soll, J., and Wagner, R. (2006). OEP37 is a new member of the chloroplast outer membrane Ion channels. *J. Biol. Chem.* 281, 17989–17998.

Gould, S. B., Waller, R. F., and Mcfadden, G. I. (2008). Plastid evolution. *Annu. Rev. Plant Biol.* 59, 491–517.

Gray, J. C., Hansen, M. R., Shaw, D. J., Graham, K., Dale, R., Smallman, P., Natesan, S. K. A., and Newell, C. A. (2011). Plastid stromules are induced by stress treatments acting through abscisic acid. *Plant J.* doi: 10.1111/j.1365-313X.2011.04800.x

Gray, J. C., Sullivan, J. A., Hibberd, J. M., and Hansen, M. R. (2001). Stromules: mobile protrusions and interconnections between plastids. *Plant Biol.* 3, 223–233.

Guillaumot, D., Guillon, S., Morsomme, P., and Batoko, H. (2009). ABA, porphyrins and plant TSPO-related protein. *Plant Signal. Behav.* 4, 1087–1090.

Gunning, B. E. S. (2005). Plastid stromules: video microscopy of their outgrowth, retraction, tensioning, anchoring, branching, bridging, and tip-shedding. *Protoplasma* 225, 33–42.

Guo, J., Zhang, Z., Bi, Y., Yang, W., Xu, Y., and Zhang, L. (2005). Decreased stability of photosystem I in dgd1 mutant of *Arabidopsis thaliana*. *FEBS Lett.* 579, 3619–3624.

Gutensohn, M., Schulz, B., Nicolay, P., and Flugge, U. I. (2000). Functional analysis of the two *Arabidopsis* homologues of Toc34, a component of the chloroplast protein import apparatus. *Plant J.* 23, 771–783.

Hanson, M. R., and Sattarzadeh, A. (2008). Dynamic morphology of plastids and stromules in angiosperm plants. *Plant Cell Environ.* 31, 646–657.

Hanson, M. R., and Sattarzadeh, A. (2011). Stromules: recent insights into a long neglected feature of plastid morphology and function. *Plant Physiol.* 155, 1486–1492.

Härtel, H., Dörmann, P., and Benning, C. (2000). DGD1-independent biosynthesis of extraplastidic galactolipids after phosphate deprivation in *Arabidopsis*. *Proc. Natl. Acad. Sci. U.S.A.* 97, 10649–10654.

Hashimoto, H., and Possingham, J. V. (1989). Division and DNA distribution in ribosome-deficient plastids of the barley mutant "albostrians". *Protoplasma* 149, 20–23.

Haswell, E. S., and Meyerowitz, E. M. (2006). MscS-like proteins control plastid size and shape in *Arabidopsis thaliana*. *Curr. Biol.* 16, 1–11.

Hatta, T., Bullivan, S., and Matthews, R. E. (1973). Fine-structure of vesicles induced in chloroplasts of chinese cabbage leaves by infection with turnip yellow mosaic-virus. *J. Gen. Virol.* 20, 37–50.

Heemskerk, J. W., Bogemann, G., and Wintermans, J. (1983). Turnover of galactolipids incorporated into chloroplast envelopes; an assay for galactolipid-galactolipid galactosyltransferase. *Biochim. Biophys. Acta* 754, 181–189.

Heemskerk, J. W., Storz, T., Schmidt, R. R., and Heinz, E. (1990). Biosynthesis of digalactosyldiacylglycerol in plastids from 16:3 and 18:3 plants. *Plant Physiol.* 93, 1286–1294.

Heemskerk, J. W. M., Wintermans, J. F. G. M., Joyard, J., Block, M. A., Dorne, A.-J., and Douce, R. (1986). Localization of galactolipid: galactolipid galactosyltransferase and acyltransferase in outer envelope membrane of spinach chloroplasts. *Biochim. Biophys. Acta* 877, 281–289.

Helliwell, C. A., Sullivan, J. A., Mould, R. M., Gray, J. C., Peacock, W. J., and Dennis, E. S. (2001). A plastid envelope location of *Arabidopsis* ent-kaurene oxidase links the plastid and endoplasmic reticulum steps of the gibberellin biosynthesis pathway. *Plant J.* 28, 201–208.

Hemmler, R., Becker, T., Schleiff, E., Bolter, B., Stahl, T., Soll, J., Gotze, T. A., Braams, S., and Wagner, R. (2006). Molecular properties of Oep21, an ATP-regulated anion-selective solute channel from the outer chloroplast membrane. *J. Biol. Chem.* 281, 12020–12029.

Higgins, C. F. (1992). ABC transporters: from microorganisms to man. *Annu. Rev. Cell Biol.* 8, 67–113.

Hiltbrunner, A., Grunig, K., Alvarez-Huerta, M., Infanger, S., Bauer, J., and Kessler, F. (2004). AtToc90, a new GTP-binding component of the *Arabidopsis* chloroplast protein import machinery. *Plant Mol. Biol.* 54, 427–440.

Hinnah, S. C., Hill, K., Wagner, R., Schlicher, T., and Soll, J. (1997). Reconstitution of a chloroplast protein import channel. *EMBO J.* 16, 7351–7360.

Hinnah, S. C., Wagner, R., Sveshnikova, N., Harrer, R., and Soll, J. (2002). The chloroplast protein import channel Toc75: pore properties and interaction with transit peptides. *Biophys. J.* 83, 899–911.

Holzinger, A., Buchner, O., Lutz, C., and Hanson, M. R. (2007). Temperature-sensitive formation of chloroplast protrusions and stromules in mesophyll cells of *Arabidopsis thaliana*. *Protoplasma* 230, 23–30.

Holzinger, A., Kwok, E. Y., and Hanson, M. R. (2008). Effects of arc3, arc5 and arc6 mutations on plastid morphology and stromule formation in green and nongreen tissues of *Arabidopsis thaliana*. *Photochem. Photobiol.* 84, 1324–1335.

Hölzl, G., Witt, S., Kelly, A. A., Zahringer, U., Warnecke, D., Dörmannn, P., and Heinz, E. (2006). Functional differences between galactolipids and glucolipids revealed in photosynthesis of higher plants. *Proc. Natl. Acad. Sci. U.S.A.* 103, 7512–7517.

Howe, G. A., and Schilmiller, A. L. (2002). Oxylipin metabolism in response to stress. *Curr. Opin. Plant Biol.* 5, 230–236.

Huang, J., Taylor, J. P., Chen, J.-G., Uhrig, J. F., Schnell, D. J., Nakagawa, T., Korth, K. L., and Jones, A. M. (2006). The plastid protein THYLAKOID FORMATION1 and the plasma membrane G-protein GPA1 interact in a novel sugar-signaling mechanism in *Arabidopsis*. *Plant Cell Online* 18, 1226–1238.

Huang, W., Ling, Q., Bedard, J., Lilley, K., and Jarvis, P. (2011). In vivo analyses of the roles of essential Omp85-related proteins in the chloroplast outer envelope membrane. *Plant Physiol.* 157, 147–159.

Inaba, T., and Schnell, D. J. (2008). Protein trafficking to plastids: one theme, many variations. *Biochem. J.* 413, 15–28.

Infanger, S., Bischof, S., Hiltbrunner, A., Agne, B., Baginsky, S., and Kessler, F. (2011). The chloroplast import receptor Toc90 partially restores the accumulation of Toc159 client proteins in the *Arabidopsis thaliana* ppi2 mutant. *Mol. Plant* 4, 252–263.

Inoue, K., and Keegstra, K. (2003). A polyglycine stretch is necessary for proper targeting of the protein translocation channel precursor to the outer envelope membrane of chloroplasts. *Plant J.* 34, 661–669.

Ishida, H., and Yoshimoto, K. (2008). Chloroplasts are partially mobilized to the vacuole by autophagy. *Autophagy* 4, 961–962.

Ivanova, Y., Smith, M. D., Chen, K. H., and Schnell, D. J. (2004). Members of the Toc159 import receptor family represent distinct pathways for protein targeting to plastids. *Mol. Biol. Cell* 15, 3379–3392.

Izumi, M., Wada, S., Makino, A., and Ishida, H. (2010). The autophagic degradation of chloroplasts via rubisco-containing bodies is specifically linked to leaf carbon status but not nitrogen status in *Arabidopsis*. *Plant Physiol.* 154, 1196–1209.

Jackson-Constan, D., and Keegstra, K. (2001). *Arabidopsis* genes encoding components of the chloroplastic protein import apparatus. *Plant Physiol.* 125, 1567–1576.

Jarvis, P., Chen, L. J., Li, H. M., Pete, C. A., Fankhauser, C., and Chory, J. (1998). An *Arabidopsis* mutant defective in the plastid general protein import apparatus. *Science* 282, 100–103.

Jarvis, P., Dörmann, P., Peto, C. A., Lutes, J., Benning, C., and Chory, J. (2000). Galactolipid deficiency and abnormal chloroplast development in the *Arabidopsis* MGD synthase 1 mutant. *Proc. Natl. Acad. Sci. U.S.A.* 97, 8175–8179.

Johnston, M. L., Luethy, M. H., Miernyk, J. A., and Randall, D. D. (1997). Cloning and molecular analyses of the *Arabidopsis thaliana* plastid pyruvate dehydrogenase subunits. *Biochim. Biophys. Acta* 1321, 200–206.

Jouhet, J., and Gray, J. C. (2009). Interaction of actin and the chloroplast protein import apparatus. *J. Biol. Chem.* 284, 19132–19141.

Jouhet, J., Marechal, E., Baldan, B., Bligny, R., Joyard, J., and Block, M. A. (2004). Phosphate deprivation induces transfer of DGDG galactolipid from chloroplast to mitochondria. *J. Cell Biol.* 167, 863–874.

Joyard, J., Ferro, M., Masselon, C., Seigneurin-Berny, D., Salvi, D., Garin, J., and Rolland, N. (2010). Chloroplast proteomics highlights the subcellular compartmentation of lipid metabolism. *Prog. Lipid Res.* 49, 128–158.

Kadota, A., Yamada, N., Suetsugu, N., Hirose, M., Saito, C., Shoda, K., Ichikawa, S., Kagawa, T., Nakano, A., and Wada, M. (2009). Short actin-based mechanism for light-directed chloroplast movement in *Arabidopsis. Proc. Natl. Acad. Sci. U.S.A.* 106, 13106–13111.

Kaneko, K., Yamada, C., Yanagida, A., Koshu, T., Umezawa, Y., Itoh, K., Hori, H., and Mitsui, T. (2010). Differential localizations and functions of rice nucleotide pyrophosphatase/phosphodiesterase isozymes 1 and 3. *Plant Biotechnol.* 28, 69–76.

Kaplan, F., Kopka, J., Sung, D. Y., Zhao, W., Popp, M., Porat, R., and Guy, C. L. (2007). Transcript and metabolite profiling during cold acclimation of *Arabidopsis* reveals an intricate relationship of cold-regulated gene expression with modifications in metabolite content. *Plant J.* 50, 967–981.

Kelly, A. A., and Dörmann, P. (2002). DGD2, an *Arabidopsis* gene encoding a UDP-galactose-dependent digalactosyldiacylglycerol synthase is expressed during growth under phosphate-limiting conditions. *J. Biol. Chem.* 277, 1166–1173.

Kim, D. H., Xu, Z. Y., Na, Y. J., Yoo, Y. J., Lee, J., Sohn, E. J., and Hwang, I. (2011). Small heat shock protein Hsp17.8 functions as an AKR2A cofactor in the targeting of chloroplast outer membrane proteins in *Arabidopsis. Plant Physiol.* 157, 132–146.

Kishimoto, K., Matsui, K., Ozawa, R., and Takabayashi, J. (2008). Direct fungicidal activities of C6-aldehydes are important constituents for defense responses in *Arabidopsis* against Botrytis cinerea. *Phytochemistry* 69, 2127–2132.

Köhler, R. H., and Hanson, M. R. (2000). Plastid tubules of higher plants are tissue-specific and developmentally regulated. *J. Cell Sci.* 113, 81–89.

Köhler, R. H., Schwille, P., Webb, W. W., and Hanson, M. R. (2000). Active protein transport through plastid tubules: velocity quantified by fluorescence correlation spectroscopy. *J. Cell Sci.* 113(Pt 22), 3921–3930.

Konishi, T., Shinohara, K., Yamada, K., and Sasaki, Y. (1996). Acetyl-CoA carboxylase in higher plants: most plants other than gramineae have both the prokaryotic and the eukaryotic forms of this enzyme. *Plant Cell Physiol.* 37, 117–122.

Koo, A. J., Ohlrogge, J. B., and Pollard, M. (2004). On the export of fatty acids from the chloroplast. *J. Biol. Chem.* 279, 16101–16110.

Koo, A. J. K., and Ohlrogge, J. B. (2002). The predicted candidates of *Arabidopsis* plastid inner envelope membrane proteins and their expression profiles. *Plant Physiol.* 130, 823–836.

Kouranov, A., Chen, X. J., Fuks, B., and Schnell, D. J. (1998). Tic20 and Tic22 are new components of the protein import apparatus at the chloroplast inner envelope membrane. *J. Cell Biol.* 143, 991–1002.

Kouranov, A., Wang, H., and Schnell, D. J. (1999). Tic22 is targeted to the intermembrane space of chloroplasts by a novel pathway. *J. Biol. Chem.* 274, 25181–25186.

Kovacs-Bogdan, E., Soll, J., and Bolter, B. (2010). Protein import into chloroplasts: the Tic complex and its regulation. *Biochim. Biophys. Acta* 1803, 740–747.

Kubis, S., Patel, R., Combe, J., Bedard, J., Kovacheva, S., Lilley, K., Biehl, A., Leister, D., Rios, G., Koncz, C., and Jarvis, P. (2004). Functional specialization amongst the *Arabidopsis* Toc159 family of chloroplast protein import receptors. *Plant Cell* 16, 2059–2077.

Kunst, L., Browse, J., and Somerville, C. (1988). Altered regulation of lipid biosynthesis in a mutant of *Arabidopsis* deficient in chloroplast glycerol-3-phosphate acyltransferase activity. *Proc. Natl. Acad. Sci. U.S.A.* 85, 4143–4147.

Kunz, H. H., Scharnewski, M., Feussner, K., Feussner, I., Flugge, U. I., Fulda, M., and Gierth, M. (2009). The ABC transporter PXA1 and peroxisomal beta-oxidation are vital for metabolism in mature leaves of *Arabidopsis* during extended darkness. *Plant Cell* 21, 2733–2749.

Kuroiwa, T., Kuroiwa, H., Sakai, A., Takahashi, H., Toda, K., and Itoh, R. (1998). The division apparatus of plastids and mitochondria. *Int. Rev. Cytol.* 181, 1–41.

Kusuhara, H., and Sugiyama, Y. (2007). ATP-binding cassette, subfamily G (ABCG family). *Pflugers Arch.* 453, 735–744.

Kwok, E. Y., and Hanson, M. R. (2003). Microfilaments and microtubules control the morphology and movement of non-green plastids and stromules in *Nicotiana tabacum. Plant J.* 35, 16–26.

Kwok, E. Y., and Hanson, M. R. (2004). In vivo analysis of interactions between GFP-labeled microfilaments and plastid stromules. *BMC Plant Biol.* 4, 2. doi:10.1186/1471-2229-4-2

Lee, Y. J., Kim, D. H., Kim, Y. W., and Hwang, I. (2001). Identification of a signal that distinguishes between the chloroplast outer envelope membrane and the endomembrane system in vivo. *Plant Cell* 13, 2175–2190.

Li, H., Moore, T., and Keegstra, K. (1991). Targeting of proteins to the outer envelope membrane uses a different pathway than transport into chloroplasts. *Plant Cell Online* 3, 709–717.

Liguori, L., Blesneac, I., Madern, D., Vivaudou, M., and Lenormand, J.-L. (2010). Single-step production of functional OEP24 proteoliposomes. *Protein Expr. Purif.* 69, 106–111.

Linka, N., and Weber, A. P. M. (2009). Intracellular metabolite transporters in plants. *Mol. Plant* 3, 21–53.

Linke, D., Frank, J., Pope, M. S., Soll, J., Ilkavets, I., Fromme, P., Burstein, E. A., Reshetnyak, Y. K., and Emelyanenko, V. I. (2004). Folding kinetics and structure of OEP16. *Biophys. J.* 86, 1479–1487.

Lu, B., and Benning, C. (2009). A 25-amino acid sequence of the *Arabidopsis* TGD2 protein is sufficient for specific binding of phosphatidic acid. *J. Biol. Chem.* 284, 17420–17427.

Lu, B. B., Xu, C. C., Awai, K., Jones, A. D., and Benning, C. (2007). A small ATPase protein of *Arabidopsis,* TGD3, involved in chloroplast lipid import. *J. Biol. Chem.* 282, 35945–35953.

Mackiewicz, P., and Bodyl, A. (2010). A hypothesis for import of the nuclear-encoded PsaE protein of *Paulinella chromatophora* (Cercozoa, Rhizaria) into its cyanobacterial endosymbonts/plastids via the endomembrane system. *J. Phycol.* 46, 847–859.

Marechal, E., Block, M. A., Joyard, J., and Douce, R. (1994). Comparison of the kinetic properties of MGDG synthase in mixed micelles and in envelope membranes from spinach chloroplast. *FEBS Lett.* 352, 307–310.

Mcfarlane, H. E., Shin, J. J., Bird, D. A., and Samuels, A. L. (2010). *Arabidopsis* ABCG transporters, which are required for export of diverse cuticular lipids, dimerize in different combinations. *Plant Cell* 22, 3066–3075.

Miege, C., Marechal, E., Shimojima, M., Awai, K., Block, M. A., Ohta, H., Takamiya, K., Douce, R., and Joyard, J. (1999). Biochemical and topological properties of type A MGDG synthase, a spinach chloroplast envelope enzyme catalyzing the synthesis of both prokaryotic and eukaryotic MGDG. *Eur. J. Biochem.* 265, 990–1001.

Mijaljica, D., Prescott, M., and Devenish, R. J. (2007). Different fates of mitochondria: alternative ways for degradation? *Autophagy* 3, 4–9.

Mills, W. R. (1980). Photosynthetic formation of the aspartate family of amino acids in isolated chloroplasts. *Plant Physiol.* 65, 1166–1172.

Mills, W. R., and Wilson, K. G. (1978). Amino acid biosynthesis in isolated pea chloroplasts: metabolism of labeled aspartate and sulfate. *FEBS Lett.* 92, 129–132.

Miras, S., Salvi, D., Ferro, M., Grunwald, D., Garin, J., Joyard, J., and Rolland, N. (2002). Non-canonical transit peptide for import into the chloroplast. *J. Biol. Chem.* 277, 47770–47778.

Miras, S., Salvi, D., Piette, L., Seigneurin-Berny, D., Grunwald, D., Reinbothe, C., Joyard, J., Reinbothe, S., and Rolland, N. (2007). Toc159- and Toc75-independent import of a transit sequence-less precursor into the inner envelope of chloroplasts. *J. Biol. Chem.* 282, 29482–29492.

Miyagishima, S. Y. (2005). Origin and evolution of the chloroplast division machinery. *J. Plant Res.* 118, 295–306.

Miyagishima, S. Y., Froehlich, J. E., and Osteryoung, K. W. (2006). PDV1 and PDV2 mediate recruitment of the dynamin-related protein ARC5 to the plastid division site. *Plant Cell* 18, 2517–2530.

Moellering, E. R., Muthan, B., and Benning, C. (2010). Freezing tolerance in plants requires lipid remodeling at the outer chloroplast membrane. *Science* 330, 226–228.

Murcha, M. W., Elhafez, D., Lister, R., Tonti-Filippini, J., Baumgartner, M., Philippar, K., Carrie, C., Mokranjac, D., Soll, J., and Whelan, J. (2007). Characterization of the preprotein and amino acid transporter gene family in *Arabidopsis. Plant Physiol.* 143, 199–212.

Nada, A., and Soll, J. (2004). Inner envelope protein 32 is imported into chloroplasts by a novel pathway. *J. Cell Sci.* 117, 3975–3982.

Nanjo, Y., Oka, H., Ikarashi, N., Kaneko, K., Kitajima, A., Mitsui, T., Munoz, F. J., Rodriguez-Lopez, M., Baroja-Fernandez, E., and Pozueta-Romero, J. (2006). Rice plastidial N-glycosylated nucleotide pyrophosphatase/phosphodiesterase is transported from the ER-Golgi to the chloroplast through the secretory pathway. *Plant Cell* 18, 2582–2592.

Natesan, S. K. A., Sullivan, J. A., and Gray, J. C. (2009). Myosin XI is required for actin-associated movement of plastid stromules. *Mol. Plant* 2, 1262–1272.

Nixon, P. J., Michoux, F., Yu, J., Boehm, M., and Komenda, J. (2010). Recent advances in understanding the assembly and repair of photosystem II. *Ann. Bot.* 106, 1–16.

Oelze, M. L., Kandlbinder, A., and Dietz, K. J. (2008). Redox regulation and overreduction control in the photosynthesizing cell: complexity in redox regulatory networks. *Biochim. Biophys. Acta* 1780, 1261–1272.

Oikawa, K., Kasahara, M., Kiyosue, T., Kagawa, T., Suetsugu, N., Takahashi, F., Kanegae, T., Niwa, Y., Kadota, A., and Wada, M. (2003). CHLOROPLAST UNUSUAL POSITIONING1 is essential for proper chloroplast positioning. *Plant Cell Online* 15, 2805–2815.

Oikawa, K., Yamasato, A., Kong, S. G., Kasahara, M., Nakai, M., Takahashi, F., Ogura, Y., Kagawa, T., and Wada, M. (2008). Chloroplast outer envelope protein CHUP1 is essential for chloroplast anchorage to the plasma membrane and chloroplast movement. *Plant Physiol.* 148, 829–842.

Okanenko, O. A. (2002). Plant sulfolipids. *Ukr. Biokhim. Zh.* 74, 27–36.

Okazaki, K., Kabeya, Y., Suzuki, K., Mori, T., Ichikawa, T., Matsui, M., Nakanishi, H., and Miyagishima, S. (2009). The PLASTID DIVISION1 and 2 components of the chloroplast division machinery determine the rate of chloroplast division in land plant cell differentiation. *Plant Cell* 21, 1769–1780.

Osteryoung, K. W., Stokes, K. D., Rutherford, S. M., Percival, A. L., and Lee, W. Y. (1998). Chloroplast division in higher plants requires members of two functionally divergent gene families with homology to bacterial ftsZ. *Plant Cell* 10, 1991–2004.

Park, H., Eggink, L. L., Roberson, R. W., and Hoober, J. K. (1999). Transfer of proteins from the chloroplast to vacuoles in *Chlamydomonas reinhardtii* (Chlorophyta): a pathway for degradation. *J. Phycol.* 35, 528–538.

Patel, R., Hsu, S. C., Bedard, J., Inoue, K., and Jarvis, P. (2008). The Omp85-related chloroplast outer envelope protein OEP80 is essential for viability in *Arabidopsis*. *Plant Physiol.* 148, 235–245.

Perry, S. E., and Keegstra, K. (1994). Envelope membrane-proteins that interact with chloroplastic precursor proteins. *Plant Cell* 6, 93–105.

Philippar, K., Geis, T., Ilkavets, I., Oster, U., Schwenkert, S., Meurer, J., and Soll, J. (2007). Chloroplast biogenesis: the use of mutants to study the etioplast-chloroplast transition. *Proc. Natl. Acad. Sci. U.S.A.* 104, 678–683.

Pohlmeyer, K., Soll, J., Grimm, R., Hill, K., and Wagner, R. (1998). A high-conductance solute channel in the chloroplastic outer envelope from pea. *Plant Cell* 10, 1207–1216.

Pohlmeyer, K., Soll, J., Steinkamp, T., Hinnah, S., and Wagner, R. (1997). Isolation and characterization of an amino acid-selective channel protein present in the chloroplastic outer envelope membrane. *Proc. Natl. Acad. Sci. U.S.A.* 94, 9504–9509.

Pollard, M., and Ohlrogge, J. (1999). Testing models of fatty acid transfer and lipid synthesis in spinach leaf using in vivo oxygen-18 labeling. *Plant Physiol.* 121, 1217–1226.

Pudelski, B., Kraus, S., Soll, J., and Philippar, K. (2010). The plant PRAT proteins – preprotein and amino acid transport in mitochondria and chloroplasts. *Plant Biol.* 12, 42–55.

Pyke, K. A., and Howells, C. A. (2002). Plastid and stromule morphogenesis in tomato. *Ann. Bot.* 90, 559–566.

Pyke, K. A., and Leech, R. M. (1992). Chloroplast division and expansion is radically altered by nuclear mutations in *Arabidopsis thaliana*. *Plant Physiol.* 99, 1005–1008.

Qbadou, S., Becker, T., Bionda, T., Reger, K., Ruprecht, M., Soll, J., and Schleiff, E. (2007). Toc64 – a preprotein-receptor at the outer membrane with bipartide function. *J. Mol. Biol.* 367, 1330–1346.

Rassow, J., Dekker, P. J. T., Van Wilpe, S., Meijer, M., and Soll, J. (1999). The preprotein translocase of the mitochondrial inner membrane: function and evolution. *J. Mol. Biol.* 286, 105–120.

Raynaud, C., Cassier-Chauvat, C., Perennes, C., and Bergounioux, C. (2004). An *Arabidopsis* homolog of the bacterial cell division inhibitor SulA is involved in plastid division. *Plant Cell* 16, 1801–1811.

Raynaud, C., Perennes, C., Reuzeau, C., Catrice, O., Brown, S., and Bergounioux, C. (2005). Cell and plastid division are coordinated through the prereplication factor AtCDT1. *Proc. Natl. Acad. Sci. U.S.A.* 102, 8216–8221.

Reape, T. J., Molony, E. M., and Mccabe, P. F. (2008). Programmed cell death in plants: distinguishing between different modes. *J. Exp. Bot.* 59, 435–444.

Reifarth, F., Christen, G., Seeliger, A. G., Dörmann, P., Benning, C., and Renger, G. (1997). Modification of the water oxidizing complex in leaves of the dgd1 mutant of *Arabidopsis thaliana* deficient in the galactolipid digalactosyldiacylglycerol. *Biochemistry* 36, 11769–11776.

Reiland, S., Grossmann, J., Baerenfaller, K., Gehrig, P., Nunes-Nesi, A., Fernie, A. R., Gruissem, W., and Baginsky, S. (2011). Integrated proteome and metabolite analysis of the de-etiolation process in plastids from rice (*Oryza sativa* L.). *Proteomics* 11, 1751–1763.

Reinbothe, S., Quigley, F., Springer, A., Schemenewitz, A., and Reinbothe, C. (2004). The outer plastid envelope protein Oep16: role as precursor translocase in import of protochlorophyllide oxidoreductase A. *Proc. Natl. Acad. Sci. U.S.A.* 101, 2203–2208.

Reski, R. (2009). Challenges to our current view on chloroplasts. *Biol. Chem.* 390, 731–738.

Reyes-Prieto, A., Weber, A. P. M., and Bhattacharya, D. (2007). The origin and establishment of the plastid in algae and plants. *Annu. Rev. Genet.* 41, 147–168.

Röhl, T., Motzkus, M., and Soll, J. R. (1999). The outer envelope protein OEP24 from pea chloroplasts can functionally replace the mitochondrial VDAC in yeast. *FEBS Lett.* 460, 491–494.

Rolland, N., Ferro, M., Seigneurin-Berny, D., Garin, J., Douce, R., and Joyard, J. (2003). Proteomics of chloroplast envelope membranes. *Photosynth. Res.* 78, 205–230.

Roston, R., Gao, J. P., Xu, C. C., and Benning, C. (2011). *Arabidopsis* chloroplast lipid transport protein TGD2 disrupts membranes and is part of a large complex. *Plant J.* 66, 759–769.

Roughan, P. G., and Slack, C. R. (1977). Long-chain acyl-coenzyme A synthetase activity of spinach chloroplasts is concentrated in the envelope. *Biochem. J.* 162, 457–459.

Sage, T. L., and Sage, R. F. (2009). The functional anatomy of rice leaves: implications for refixation of photorespiratory CO2 and efforts to engineer C-4 photosynthesis into rice. *Plant Cell Physiol.* 50, 756–772.

Salomon, M., Fischer, K., Flugge, U. I., and Soll, J. (1990). Sequence analysis and protein import studies of an outer chloroplast envelope polypeptide. *Proc. Natl. Acad. Sci. U.S.A.* 87, 5778–5782.

Sattarzadeh, A., Krahmer, J., Germain, A. D., and Hanson, M. R. (2009). A myosin XI tail domain homologous to the yeast myosin vacuole-binding domain interacts with plastids and stromules in *Nicotiana benthamiana*. *Mol. Plant* 2, 1351–1358.

Schattat, M., Barton, K., Baudisch, B., Klosgen, R. B., and Mathur, J. (2011). Plastid stromule branching coincides with contiguous endoplasmic reticulum dynamics. *Plant Physiol.* 155, 1667–1677.

Schleiff, E., Eichacker, L. A., Eckart, K., Becker, T., Mirus, O., Stahl, T., and Soll, J. (2003a). Prediction of the plant beta-barrel proteome: a case study of the chloroplast outer envelope. *Protein Sci.* 12, 748–759.

Schleiff, E., Jelic, M., and Soll, J. (2003b). A GTP-driven motor moves proteins across the outer envelope of chloroplasts. *Proc. Natl. Acad. Sci. U.S.A.* 100, 4604–4609.

Schnell, D. J., Kessler, F., and Blobel, G. (1994). Isolation of components of the chloroplast protein import machinery. *Science* 266, 1007–1012.

Schnurr, J. A., Shockey, J. M., De Boer, G. J., and Browse, J. A. (2002). Fatty acid export from the chloroplast. Molecular characterization of a major plastidial acyl-coenzyme A synthetase from *Arabidopsis*. *Plant Physiol.* 129, 1700–1709.

Schwenkert, S., Soll, J., and Bolter, B. (2010). Protein import into chloroplasts-how chaperones feature into the game. *Biochim. Biophys. Acta* 1808, 901–911.

Shaw, D. J., and Gray, J. C. (2011). Visualisation of stromules in transgenic wheat expressing a plastid-targeted yellow fluorescent protein. *Planta* 233, 961–970.

Shine, W. E., Mancha, M., and Stumpf, P. K. (1976). Fat metabolism in higher plants. The function of acyl thioesterases in the metabolism of acyl-coenzymes A and acyl-acyl carrier proteins. *Arch. Biochem. Biophys.* 172, 110–116.

Shiojiri, K., Kishimoto, K., Ozawa, R., Kugimiya, S., Urashimo, S., Arimura, G., Horiuchi, J., Nishioka, T., Matsui, K., and Takabayashi, J. (2006). Changing green leaf volatile biosynthesis in plants: an approach for improving plant resistance against both herbivores and pathogens. *Proc. Natl. Acad. Sci. U.S.A.* 103, 16672–16676.

Shockey, J. M., Fulda, M. S., and Browse, J. A. (2002). *Arabidopsis* contains nine long-chain acyl-coenzyme A synthetase genes that participate in fatty acid and glycerolipid metabolism. *Plant Physiol.* 129, 1710–1722.

Siddique, M. A., Grossmann, J., Gruissem, W., and Baginsky, S. (2006). Proteome analysis of bell pepper (*Capsicum annuum* L.) chromoplasts. *Plant Cell Physiol.* 47, 1663–1673.

Singh, B. K., and Shaner, D. L. (1995). Biosynthesis of branched chain amino acids: from test tube to field. *Plant Cell* 7, 935–944.

Soll, J., Bolter, B., Wagner, R., and Hinnah, S. C. (2000). . . . response: the chloroplast outer envelope: a molecular sieve? *Trends Plant Sci.* 5, 137–138.

Soll, J., and Schleiff, E. (2004). Protein import into chloroplasts. *Nat. Rev. Mol. Cell Biol.* 5, 198–208.

Somerville, C., and Browse, J. (1991). Plant lipids: metabolism, mutants, and membranes. *Science* 252, 80–87.

Stanga, J. P., Boonsirichai, K., Sedbrook, J. C., Otegui, M. S., and Masson, P. H. (2009). A role for the TOC complex in *Arabidopsis* root gravitropism. *Plant Physiol.* 149, 1896–1905.

Steiner, J. M., Yusa, F., Pompe, J. A., and Loffelhardt, W. (2005). Homologous protein import machineries in chloroplasts and cyanelles. *Plant J.* 44, 646–652.

Steinkamp, T., Hill, K., Hinnah, S. C., Wagner, R., Rohl, T., Pohlmeyer, K., and Soll, J. (2000). Identification of the pore-forming region of the outer chloroplast envelope protein OEP16. *J. Biol. Chem.* 275, 11758–11764.

Suetsugu, N., Yamada, N., Kagawa, T., Yonekura, H., Uyeda, T. Q. P., Kadota, A., and Wada, M. (2010). Two kinesin-like proteins mediate actin-based chloroplast movement in *Arabidopsis thaliana*. *Proc. Natl. Acad. Sci. U.S.A.* 107, 8860–8865.

Sugiyama, A., Shitan, N., Sato, S., Nakamura, Y., Tabata, S., and Yazaki, K. (2006). Genome-wide analysis of ATP-binding cassette (ABC) proteins in a model legume plant, *Lotus japonicus*: comparison with *Arabidopsis* ABC protein family. *DNA Res.* 13, 205–228.

Sun, Q., Zybailov, B., Majeran, W., Friso, G., Olinares, P. D., and Van Wijk, K. J. (2009). PPDB, the plant proteomics database at Cornell. *Nucleic Acids Res.* 37, D969–D974.

Sun, X., Feng, P., Xu, X., Guo, H., Ma, J., Chi, W., Lin, R., Lu, C., and Zhang, L. (2011). A chloroplast envelope-bound PHD transcription factor mediates chloroplast signals to the nucleus. *Nat. Commun.* 2, 477–487.

Sveshnikova, N., Grimm, R., Soll, J., and Schleiff, E. (2000). Topology studies of the chloroplast protein import channel Toc75. *Biol. Chem.* 381, 687–693.

Takahashi, H., Kopriva, S., Giordano, M., Saito, K., and Hell, R. (2011). Sulfur assimilation in photosynthetic organisms: molecular functions and regulations of transporters and assimilatory enzymes. *Annu. Rev. Plant Biol.* 62, 157–184.

Thorlby, G., Fourrier, N., and Warren, G. (2004). The sensitive to freezing2 gene, required for freezing tolerance in *Arabidopsis thaliana*, encodes a beta-glucosidase. *Plant Cell* 16, 2192–2203.

Tietje, C., and Heinz, E. (1998). Uridine-diphospho-sulfoquinovose: diacylglycerol sulfoquinovosyltransferase activity is concentrated in the inner membrane of chloroplast envelopes. *Planta* 206, 72–78.

Tranel, P. J., Froehlich, J., Goyal, A., and Keegstra, K. (1995). A component of the chloroplastic protein import apparatus is targeted to the outer envelope membrane via a novel pathway. *EMBO J.* 14, 2436–2446.

Tranel, P. J., and Keegstra, K. (1996). A novel, bipartite transit peptide targets OEP75 to the outer membrane of the chloroplastic envelope. *Plant Cell* 8, 2093–2104.

Trojan, A., and Gabrys, H. (1996). Chloroplast distribution in *Arabidopsis thaliana* (L.) depends on light conditions during growth. *Plant Physiol.* 111, 419–425.

Tu, S.-L., Chen, L.-J., Smith, M. D., Su, Y.-S., Schnell, D. J., and Li, H.-M. (2004). Import pathways of chloroplast interior proteins and the outer-membrane protein OEP14 converge at Toc75. *Plant Cell Online* 16, 2078–2088.

Tu, S.-L., and Li, H.-M. (2000). Insertion of OEP14 into the outer envelope membrane is mediated by proteinaceous components of chloroplasts. *Plant Cell Online* 12, 1951–1960.

Tyra, H. M., Linka, M., Weber, A. P., and Bhattacharya, D. (2007). Host origin of plastid solute transporters in the first photosynthetic eukaryotes. *Genome Biol.* 8, R212.

Uchiyama, Y., Shibata, M., Koike, M., Yoshimura, K., and Sasaki, M. (2008). Autophagy-physiology and pathophysiology. *Histochem. Cell Biol.* 129, 407–420.

Ueda, H., Yokota, E., Kutsuna, N., Shimada, T., Tamura, K., Shimmen, T., Hasezawa, S., Dolja, V. V., and Hara-Nishimura, I. (2010). Myosin-dependent endoplasmic reticulum motility and F-actin organization in plant cells. *Proc. Natl. Acad. Sci. U.S.A.* 107, 6894–6899.

Van Besouw, A., and Wintermans, J. F. (1978). Galactolipid formation in chloroplast envelopes. I. Evidence for two mechanisms in galactosylation. *Biochim. Biophys. Acta* 529, 44–53.

Van Doorn, W. G., and Woltering, E. J. (2005). Many ways to exit? Cell death categories in plants. *Trends Plant Sci.* 10, 117–122.

Vancanneyt, G., Sanz, C., Farmaki, T., Paneque, M., Ortego, F., Castanera, P., and Sanchez-Serrano, J. J. (2001). Hydroperoxide lyase depletion in transgenic potato plants leads to an increase in aphid performance. *Proc. Natl. Acad. Sci. U.S.A.* 98, 8139–8144.

Vanhee, C., Zapotoczny, G., Masquelier, D., Ghislain, M., and Batoko, H. (2011). The *Arabidopsis* multistress regulator TSPO is a heme binding membrane protein and a potential scavenger of porphyrins via an autophagy-dependent degradation mechanism. *Plant Cell* 23, 785–805.

Villarejo, A., Buren, S., Larsson, S., Dejardin, A., Monne, M., Rudhe, C., Karlsson, J., Jansson, S., Lerouge, P., Rolland, N., Von Heijne, G., Grebe, M., Bako, L., and Samuelsson, G. (2005). Evidence for a protein transported through the secretory pathway en route to the higher plant chloroplast. *Nat. Cell Biol.* 7, 1224–1231.

Von Braun, S. S., and Schleiff, E. (2008). The chloroplast outer membrane protein CHUP1 interacts with actin and profilin. *Planta* 227, 1151–1159.

Von Loeffelholz, O., Kriechbaumer, V., Ewan, R. A., Jonczyk, R., Lehmann, S., Young, J. C., and Abell, B. M. (2011). OEP61 is a chaperone receptor at the plastid outer envelope. *Biochem. J.* 438, 143–153.

Von Zychlinski, A., Kleffmann, T., Krishnamurthy, N., Sjolander, K., Baginsky, S., and Gruissem, W. (2005). Proteome analysis of the rice etioplast – metabolic and regulatory networks and novel protein functions. *Mol. Cell. Proteomics* 4, 1072–1084.

Wallas, T. R., Smith, M. D., Sanchez-Nieto, S., and Schnell, D. J. (2003). The roles of Toc34 and Toc75 in targeting the Toc159 preprotein receptor to chloroplasts. *J. Biol. Chem.* 278, 44289–44297.

Wallsgrove, R. M., and Mazelis, M. (1980). The enzymology of lysine biosynthesis in higher plants: complete localization of the regulatory enzyme dihydrodipicolinate synthase in the chloroplasts of spinach leaves. *FEBS Lett.* 116, 189–192.

Wang, Q., Sullivan, R. W., Kight, A., Henry, R. L., Huang, J. R., Jones, A. M., and Korth, K. L. (2004). Deletion of the chloroplast-localized thylakoid formation1 gene product in *Arabidopsis* leads to deficient thylakoid formation and variegated leaves. *Plant Physiol.* 136, 3594–3604.

Waters, M. T., Fray, R. G., and Pyke, K. A. (2004). Stromule formation is dependent upon plastid size, plastid differentiation status and the density of plastids within the cell. *Plant J.* 39, 655–667.

Weber, A. P. M. (2004). Solute transporters as connecting elements between cytosol and plastid stroma. *Curr. Opin. Plant Biol.* 7, 247–253.

Weber, A. P. M., Linka, M., and Bhattacharya, D. (2006). Single, ancient origin of a plastid metabolite translocator family in Plantae from an endomembrane-derived ancestor. *Eukaryotic Cell* 5, 609–612.

Weber, A. P. M., and Linka, N. (2011). Connecting the plastid: transporters of the plastid envelope and their role in linking plastidial with cytosolic metabolism. *Annu. Rev. Plant Biol.* 62, 53–77.

Weber, A. P. M., and Osteryoung, K. W. (2010). From endosymbiosis to synthetic photosynthetic life. *Plant Physiol.* 154, 593–597.

Weber, A. P. M., Schneidereit, J., and Voll, L. M. (2004). Using mutants to probe the in vivo function of plastid envelope membrane metabolite transporters. *J. Exp. Bot.* 55, 1231–1244.

Weber, A. P. M., and Von Caemmerer, S. (2010). Plastid transport and metabolism of C(3) and C(4) plants – comparative analysis and possible biotechnological exploitation. *Curr. Opin. Plant Biol.* 13, 257–265.

Whippo, C. W., Khurana, P., Davis, P. A., Deblasio, S. L., Desloover, D., Staiger, C. J., and Hangarter, R. P. (2011). THRUMIN1 is a light-regulated actin-bundling protein involved in chloroplast motility. *Curr. Biol.* 21, 59–64.

Wilson, M. E., Jensen, G. S., and Haswell, E. S. (2011). Two mechanosensitive channel homologs influence division ring placement in *Arabidopsis* chloroplasts. *Plant Cell* 23, 2939–2949.

Xu, C., Fan, J., Riekhof, W., Froehlich, J. E., and Benning, C. (2003). A permease-like protein involved in ER to thylakoid lipid transfer in *Arabidopsis*. *EMBO J.* 22, 2370–2379.

Xu, C., Moellering, E. R., Muthan, B., Fan, J., and Benning, C. (2010). Lipid transport mediated by *Arabidopsis* TGD proteins is unidirectional from the endoplasmic reticulum to the plastid. *Plant Cell Physiol.* 51, 1019–1028.

Xu, C. C., Fan, J. L., Cornish, A. J., and Benning, C. (2008). Lipid trafficking between the endoplasmic reticulum and the plastid in *Arabidopsis* requires the extraplastidic TGD4 protein. *Plant Cell* 20, 2190–2204.

Yang, Y., Glynn, J. M., Olson, B. J., Schmitz, A. J., and Osteryoung, K. W. (2008). Plastid division: across time and space. *Curr. Opin. Plant Biol.* 11, 577–584.

Yoon, H. S., Hackett, J. D., Ciniglia, C., Pinto, G., and Bhattacharya, D. (2004). A molecular timeline for the origin of photosynthetic eukaryotes. *Mol. Biol. Evol.* 21, 809–818.

Zhao, L., Katavic, V., Li, F., Haughn, G. W., and Kunst, L. (2010). Insertional mutant analysis reveals that long-chain acyl-CoA synthetase 1 (LACS1), but not LACS8, functionally overlaps with LACS9 in *Arabidopsis* seed oil biosynthesis. *Plant J.* 64, 1048–1058.

Zrenner, R., Stitt, M., Sonnewald, U., and Boldt, R. (2006). Pyrimidine and purine biosynthesis and degradation in plants. *Annu. Rev. Plant Biol.* 57, 805–836.

Zybailov, B., Rutschow, H., Friso, G., Rudella, A., Emanuelsson, O., Sun, Q., and Van Wijk, K. J. (2008). Sorting signals, N-terminal modifications and abundance of the chloroplast proteome. *PLoS ONE* 3, e1994. doi:10.1371/journal.pone.0001994

Conflict of Interest Statement: The authors declare that the research was conducted in the absence of any commercial or financial relationships that could be construed as a potential conflict of interest.

Received: 24 October 2011; accepted: 29 November 2011; published online: 14 December 2011.

Citation: Breuers FKH, Bräutigam A and Weber APM (2011) The plastid outer envelope – a highly dynamic interface between plastid and cytoplasm. Front. Plast Sci. ***2****:97. doi: 10.3389/fpls.2011.00097*

This article was submitted to Frontiers in Plant Physiology, a specialty of Frontiers in Plant Science.

III. Results and Discussion

Publication 2 (Research): Dynamic remodeling of the plastid envelope membrane – a tool for chloroplast envelope *in vivo* localization

Status: **published** (January 2012)

Authors: **Frederique K. H. Breuers, Andrea Bräutigam, Stefan Geimer, Ulla Y. Welzel, Giovanni Stefano, Luciana Renna, Federica Brandizzi, and Andreas P. M. Weber**

Journal: "**Frontiers in plant science**"

Impact factor: **not yet available**

1. Co-Author

Own contribution: 75%

- Experimental design
- Preliminary experiments (cloning, expression study, material preparation)
- Data elicitation and selection
- Writing the manuscript

frontiers in
PLANT SCIENCE

ORIGINAL RESEARCH ARTICLE
published: 23 January 2012
doi: 10.3389/fpls.2012.00007

Dynamic remodeling of the plastid envelope membranes – a tool for chloroplast envelope *in vivo* localizations

Frederique K. H. Breuers[1†], Andrea Bräutigam[1†], Stefan Geimer[2†], Ulla Y. Welzel[2], Giovanni Stefano[3], Luciana Renna[3], Federica Brandizzi[3] and Andreas P. M. Weber[1]*

[1] *Institute for Plant Biochemistry, Heinrich Heine University Düsseldorf, Düsseldorf, Germany*
[2] *Electron Microscopy Laboratory, Institute for Cell Biology, University of Bayreuth, Bayreuth, Germany*
[3] *Plant Research Laboratory, Department of Energy, Michigan State University, East Lansing, MI, USA*

Edited by:
Patrick Xuechun Zhao, Samuel Roberts Noble Foundation, USA

Reviewed by:
Vagner Benedito, West Virginia University, USA
Haiquan Li, University of Illinois at Chicago, USA

***Correspondence:**
Andreas P. M. Weber, Institute for Plant Biochemistry, Heinrich Heine University, Geb. 26.03.01, Universitätsstrasse 1, D-40225 Düsseldorf, Germany.
e-mail: andreas.weber@uni-duesseldorf.de

[†] *Frederique K. H. Breuers, Andrea Bräutigam and Stefan Geimer have contributed equally to this work.*

Two envelope membranes delimit plastids, the defining organelles of plant cells. The inner and outer envelope membranes are unique in their protein and lipid composition. Several studies have attempted to establish the proteome of these two membranes; however, differentiating between them is difficult due to their close proximity. Here, we describe a novel approach to distinguish the localization of proteins between the two membranes using a straightforward approach based on live cell imaging coupled with transient expression. We base our approach on analyses of the distribution of GFP-fusions, which were aimed to verify outer envelope membrane proteomics data. To distinguish between outer envelope and inner envelope protein localization, we used AtTOC64–GFP and AtTIC40–GFP, as respective controls. During our analyses, we observed membrane proliferations and loss of chloroplast shape in conditions of protein over-expression. The morphology of the proliferations varied in correlation with the suborganellar distribution of the over-expressed proteins. In particular, while layers of membranes built up in the inner envelope membrane, the outer envelope formed long extensions into the cytosol. Using electron microscopy, we showed that these extensions were stromules, a dynamic feature of plastids. Since the behavior of the membranes is different and is related to the protein localization, we propose that *in vivo* studies based on the analysis of morphological differences of the membranes can be used to distinguish between inner and outer envelope localizations of proteins. To demonstrate the applicability of this approach, we demonstrated the localization of AtLACS9 to the outer envelope membrane. We also discuss protein impact on membrane behavior and regulation of protein insertion into membranes, and provide new hypotheses on the formation of stromules.

Keywords: chloroplast envelope, membrane proliferation, membrane protein, outer envelope membrane, inner envelope membrane, LACS9, stromule

INTRODUCTION

The defining organelle of plant cells is the plastid. Plant plastids derive from a single primary endosymbiosis event, and are delimited by an outer and an inner envelope membrane. These membranes are the gateway for protein (Strittmatter et al., 2010), lipid (Benning, 2009), and metabolite flux (Linka and Weber, 2010; Breuers et al., 2011; Facchinelli and Weber, 2011; Weber and Linka, 2011) between plastid and cytosol. Further, the membranes are the location of several biosynthetic processes, like membrane lipid biosynthesis (Benning, 2009). During the past decade, several proteomics analyses (e.g., Ferro et al., 2003, 2010; Rolland et al., 2003; Bräutigam et al., 2008a,b; Bräutigam and Weber, 2009; Sun et al., 2009; Joyard et al., 2010) contributed to a better understanding of the protein composition of the envelope membranes and thus provided new platforms to increase knowledge on the functions and evolutionary role of these permeable barriers.

In the last decades, the concept of the chloroplast envelope membranes has changed from a static border to a highly dynamic interface between the plastids and the cytosol. For example, thin, stroma filled structures surrounded by both envelope membranes have been observed extruding from the plastid under natural conditions in a wide variety of plant species (Gunning, 2005; Holzinger et al., 2007a,b; Sage and Sage, 2009). Further, they have been found in plant cells transformed with constructs encoding stroma-targeted and envelope GFP-fusion proteins (Köhler et al., 1997a,b; Tirlapur et al., 1999; Köhler and Hanson, 2000; Shiina et al., 2000; Arimura et al., 2001; Pyke and Howells, 2002; Hanson and Sattarzadeh, 2008; Shaw and Gray, 2011). These structures are called stromules, which stands for stroma filled tubules (Köhler et al., 1997a,b; Köhler and Hanson, 2000; Hanson and Köhler, 2001). Several functions have been proposed for stromules, such as increasing surface area, connecting chloroplasts (and possibly other organelles), a role in signaling pathways, and

adaption to temperature and light stress (for a recent review: Hanson and Sattarzadeh, 2011). Despite the observation of stromules in non-transformed plant cells via light and electron microscopy, GFP-fusions have remained the predominant tool for observing stromule formation *in vivo*.

The localization of plastid proteins to distinct subcompartments of the chloroplast, such as stroma, envelope membranes, and thylakoids, via GFP-fusion proteins is challenging for several reasons. Stromal proteins are relatively easy to distinguish from envelope localizations, because envelope localized proteins form a ring like structure around the chloroplast. In contrast, distinguishing between localization in the outer envelope or inner envelope is challenging due to their close proximity. Here, we demonstrate that a combination of membrane dynamics and GFP-fusion proteins provides an efficient tool for distinguishing between inner and outer envelope proteins, using the long chain fatty acid CoA synthetase AtLACS9 as an example. AtLACS9 is the only investigated protein with LACS activity in the chloroplast and has been shown to account for 90% of the LACS activity in the chloroplast (Schnurr et al., 2002; Shockey et al., 2002); however, its location has not been conclusively demonstrated to date. While LACS activity has been described in outer envelopes of spinach chloroplasts (Roughan and Slack, 1977), the *in vivo* LACS9 was non-specifically described as envelope localized (Schnurr et al., 2002; Koo et al., 2004; Sun et al., 2009; Zhao et al., 2010).

MATERIALS AND METHODS

PLANT GROWTH CONDITION

Nicotiana benthamiana plants were grown for 4–6 weeks in a green house, while *Nicotiana tabacum* plants were grown for 4–6 weeks in a growth chamber using a 16 h/8 h day/night cycle with temperatures of 27˚C/24˚C.

CLONING

The genes for AtTOC64-III (At3g17970), AtLACS9 (At1g77590), AtTic40 (At5g16620), AtTPT (At5g46110), AtAPG1 (At3g63410), and AtLrgB (At1g32080) were amplified from cDNA and cloned into the plant expression vector pMDC83 (Curtis and Grossniklaus, 2003) for C-terminal GFP-fusion. In addition AtLACS9 was cloned into pUBC-GFP (Grefen et al., 2010) as Ubiquitin10 promoter driven construct in C-terminal GFP fusion, pABindGFP (Bleckmann et al., 2010) as β-estradiol inducible promoter driven construct in C-terminal GFP-fusion, and pMDC32 (Curtis and Grossniklaus, 2003) as untagged 35 S-promoter driven constructs.

AGROBACTERIUM TUMEFACIENS PREPARATION

Agrobacterium tumefaciens [GV3101(pMP90)] (Koncz and Schell, 1986) was transformed with the plasmids, and grown on LB plates (5 g yeast extract, 10 g tryptone, 5 g NaCl, 1 ml 1 M NaOH in 1 l) or YEB plates (1 g yeast extract, 5 g tryptone, 5 g beef extract, 5 g sucrose, 0.5 g $MgSO_4 \times 7\,H_2O$, in 1 l) containing rifampicin (50–150 μg/ml), gentamycin, (25–50 μg/ml), and either kanamycin (25–50 μg/ml; pMDC83 and pMDC32) or spectinomycin (100 μg/ml; pUBC-GFP and pABindGFP), depending on the plasmid resistance. Colonies were grown for 48 h in a 30˚C chamber and used for transformation of *Nicotiana* leaves.

AGROBACTERIUM TUMEFACIENS MEDIATED TRANSFORMATION OF *N. TABACUM* FOR *IN PLANTA* STUDIES

Colonies were inoculated in 5 ml liquid cultures of LB containing antibiotics (see above) and grown under constant shaking of 220 rpm and 30˚C in Innova incubation shakers in culture tubes for 16–24 h. A 1-ml aliquot of the cell cultures was harvested by centrifugation and re-suspended in fresh infiltration buffer [IF; 2 mM Na_3PO_4, 50 mM MES/KOH (pH 7.6), 5 mg/ml glucose, 200 mM acetosyringone]. Bacteria ($OD_{600} = 0.05$) were used for infiltration into *N. tabacum* leaves, as described earlier (Batoko et al., 2000). After infiltration, all plants were kept in growth chamber under conditions of 16 h/8 h day/night cycle with temperatures of 27˚C/24˚C.

AGROBACTERIUM TUMEFACIENS MEDIATED TRANSFORMATION OF *N. BENTHAMIANA* FOR PROTOPLAST STUDIES

Colonies were streaked-out on new plates and grown for additional 24 h in a 30˚C chamber. Liquid cultures of YEB medium containing antibiotics (see above) of 12 ml were grown under constant shaking of 220 rpm and 30˚C in Innova incubation shakers in 125 ml Erlenmeyer flasks over night. Cells were harvested by centrifugation and re-suspended in fresh activation medium [containing 10 mM MES/KOH (pH 5.6), 10 mM $MgCl_2$, and 150 μM acetosyringone]. Bacteria containing protein expression vectors ($OD_{600} = 0.4$) were mixed together with a p19 helper strain ($OD_{600} = 0.3$; Voinnet et al., 2003). The mixture was incubated for 2 h at room temperature and infiltrated into *N. benthamiana* leaves. After infiltration, all plants were kept in the greenhouse until the end of analysis (adapted from Wydro et al., 2006; Gehl et al., 2009).

PROTOPLAST ISOLATION

Four to seven leaf disks with a diameter of 0.8 cm of transfected *N. benthamiana* were cut with a cork borer and transferred into a 10-ml syringe containing 2 ml of cell wall digestion solution (CWDS; 1.5% cellulase R-10, 0.4% macerozyme R-10, 0.4 M mannitol, 20 mM KCl, 20 mM MES (pH 5.6), 10 mM $CaCl_2$, 0.1% BSA). The enzyme solution was infiltrated into the intercellular space of the leaf disks. Leaf disks were than transferred to a 2-ml Eppendorf tube with the enzyme solution and incubated for 2–4 h at 20–25˚C. Protoplasts were shaken out of the digested tissue and pelleted by gravity upon removal of undigested tissue with a pipette tip. CWDS was exchanged by minus-enzymes-solution (−ES; 0.4 M mannitol, 20 mM KCl, 20 mM MES (pH 5.6), 10 mM $CaCl_2$, 0.1% BSA) and used to wash the isolated protoplasts (adapted from Yoo et al., 2007).

MICROSCOPIC ANALYSIS

Protoplasts and plant tissue were analyzed by an inverted or an upright Zeiss LSM 510 META confocal laser-scanning microscope. GFP and chlorophyll were excited by the 488-nm laser line of an Argon laser and the emission was collected at 505–550 nm and at >650 nm, respectively. Differential interference contrast (DIC) microscopic analysis was done via a Nikon Eclipse T inverse microscope. Pictures were taken via a b/w-ProgResMF™-camera by Jenoptik.

TRANSMISSION ELECTRON MICROSCOPY

Leaf pieces (about 1–2 mm^2) were cut from infiltrated *N. benthamiana* leaves and incubated in fixation buffer (2.5% glutaraldehyde and 3% formaldehyde in 50 mM sodium cacodylate, pH 7.3) at room temperature and a pressure of 20 mbar for 60 min. The fixation buffer was replaced, and the samples were fixed overnight at 4˚C. After three 10-min washes in distilled water, the samples were osmicated in 1% osmium tetroxide (in distilled water) for 60–100 min at 4˚C, rinsed three times for 10 min each in distilled water and incubated in 1% uranyl acetate (in distilled water) at 4˚C overnight. After three washes of 10 min each in distilled water the samples were embedded in 1% Difco™Agar noble (Becton, Dickinson and Company, Sparks, MD, USA), dehydrated using increasing concentrations of ethanol and embedded in glycidyl ether 100 (formerly Epon 812; Serva, Heidelberg, Germany) with propylene oxide as intermediate solvent following standard procedures. Polymerization was carried out for 48 h at 65˚C. Ultrathin sections (~60 nm) were cut with a diamond knife (type ultra 35˚; Diatome, Biel, Suisse) on an EM UC6 ultramicrotome (Leica Microsystems, Wetzlar, Germany) and mounted on single-slot Pioloform-coated copper grids (Plano, Wetzlar, Germany). The sections were stained with uranyl acetate and lead citrate (Reynolds, 1963) and viewed with a JEM-2100 transmission electron microscope (JEOL, Tokyo, Japan) operated at 80 kV. Micrographs were taken using a 4080 × 4080 or 1350 × 1040 pixels charge-coupled device camera (UltraScan 4000 or Erlangshen ES500W respectively, Gatan, Pleasanton, CA, USA) and Gatan Digital Micrograph software (version 1.70.16). Image brightness and contrast were adjusted and figures assembled using Adobe Photoshop 8.0.1.

RESULTS

DISTINCT STRUCTURES ARE OBSERVED WHEN EXPRESSING ATTOC64 AND ATTIC40 IN TRANSIENTLY TRANSFORMED TOBACCO CELLS

To examine labeling patterns of inner and outer envelope membrane proteins, we performed *in vivo* localization studies using fluorescent-tagged fusion proteins in *N. benthamiana*. Since it is known that an N-terminal transit peptide, or at least a signal sequence, is needed to insert envelope proteins into the membrane (Bionda et al., 2010), we fused the fluorescent tag to the C-terminus of the proteins of interest. As a control for the outer envelope, we used AtTOC64-III, a co-receptor and co-chaperone of the TOC (Translocon of the outer chloroplast membrane) complex (Sohrt and Soll, 2000; Qbadou et al., 2007). As a control for the inner envelope, we used AtTIC40, a component of the TIC (Translocon of the inner chloroplast membrane) complex (Chou, 2003; Singh et al., 2008). As cytosolic control we expressed GFP driven by a 35 S-promoter (**Figure 1A**).

By analyzing the distribution of 35S:AtTOC64–GFP, we detected GFP signal in bright circular structures surrounding the chlorophyll autofluorescence (**Figure 1B**). This distribution is consistent with previous observations by Bae et al. (2008) and with that of other outer envelope proteins such as CHUP1 (e.g., Oikawa et al., 2003, 2008; Schmidt Von Braun and Schleiff, 2008) and OEP7 (Lee et al., 2001). However, we also observed GFP labeled extensions looping out from the envelope circles (**Figure 1B**).

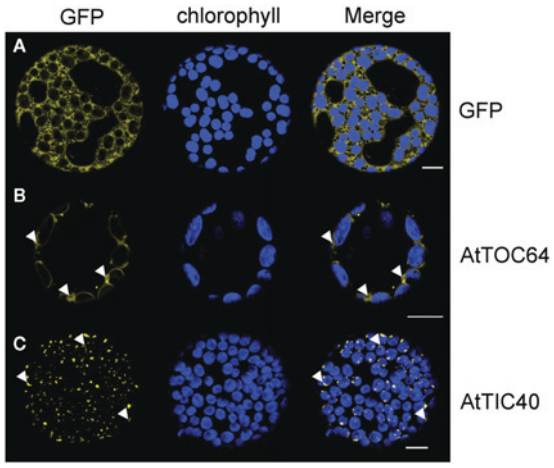

FIGURE 1 | GFP-fusion protein expression patterns in *N. benthamiana* protoplasts. Confocal microscopic analysis on isolated protoplasts of *N. benthamiana* leaves after 35 S-promoter driven *in planta* expression of GFP-fusion proteins. Pictures were taken 48 h after infiltration. GFP fluorescence (GFP) in yellow, chlorophyll autofluorescence (chlorophyll) in blue and an overlay (merge) of representative protoplasts are shown. **(A)** Expression pattern of cytosolic GFP. **(B)** Expression pattern of AtTOC64-III-GFP in ring structures around the chlorophyll autofluorescence with slide GFP labeled extensions (arrowheads). **(C)** Expression pattern of AtTIC40–GFP in dots associated with the autofluorescence. Crescent moon-like structures can be seen (arrowheads). Size bars: 10 μm.

Next we analyzed the distribution of 35S:AtTIC40–GFP and observed GFP labeling patterns. The GFP signal was clearly distinct from that of AtTOC64–GFP. We detected GFP as small dots and crescent moon-like structures associated with the chlorophyll autofluorescence (**Figure 1C**). In addition to these most frequently observed patterns, some protoplasts expressed GFP in circles around the chloroplast. Filamentous extrusions from the chloroplast were never observed. We hypothesized that the observed differences between the labeling patterns might be due to different expression levels within the transient expression system employed in our study. To test this hypothesis, we conducted a time course analysis of the expression pattern after introduction of the tagged proteins into transiently transformed cells.

ABERRANT MEMBRANE STRUCTURE FORMATION IS DEPENDENT ON THE PROTEIN AMOUNT

Agrobacterium mediated transient transfection of plant cells is based on the insertion of T-DNA into the cell genome. Afterward, protein is constantly synthesized and thus protein concentration is increasing in a time dependent manner (Wydro et al., 2006). Hence, when our constructs were inserted into the cell genome, we were able to observe different protein loading in the respective membrane at different time points. AtTIC40–GFP and AtTOC64–GFP expression were monitored 48, 72, and 96 h after leaf infiltration. We took pictures of representative expression patterns for each time point and each protein. At least 50 transfected protoplasts were evaluated for each sample and the experiments

were done at least three times independently for each expressed protein.

Fortyeight hours after infiltration with *Agrobacterium* with AtTIC40–GFP the expression pattern was congruent with the observations outlined above (**Figure 2A**). In addition to GFP dots the crescent moon structures were highly abundant in the transfected protoplasts (**Figure 2A** zoom). In protoplasts isolated from leaves at 3 days after infiltration, a circular pattern surrounding the chloroplast dominated the protoplast samples (**Figure 2B**). However, most of the circles were incomplete and surrounded no more than half of the autofluorescence. Small areas between such half circles remained free of GFP signal (**Figure 2B** zoom). After an additional 24 h, we observed full circles (**Figure 2C**). Most of the protoplasts also contained minor loop-like structures evolving from the circles (**Figure 2C** zoom).

After 2 days expressing 35S:AtTOC64–GFP, we observed chlorophyll autofluorescence surrounded by circular GFP fluorescence; most likely illuminating the predominant shape of the outer envelope membrane (**Figure 3**). However, some protoplasts already contained labeled loop-like deformations (**Figure 3A** zoom). These deformations became more abundant when we expressed AtTOC64–GFP for an additional 24 h. We observed various labeled thin tubular structures evolving from the chloroplast-surrounding circles that partially connected different chloroplasts (**Figure 3B**). These structures became even more abundant in the protoplasts after 96 h of expression (**Figure 3C**). A network of thin tubules could be detected protruding through the entire cell. We observed labeled tubules of up to 40 μm spanning through the protoplast and connecting individual chloroplasts with each other (**Figures 3B,C** zoom).

The structures observed after expressing the inner envelope protein AtTIC40 or outer envelope protein AtTOC64 indicated that the membranes were altered. We hypothesized that these alteration were due to the high protein amounts produced in the transiently transformed cells and not due to the intrinsic properties of the expressed proteins.

INNER MEMBRANE ALTERATION IS INDEPENDENT OF THE PROTEIN PROPERTIES

To test this hypothesis, we designed fluorophore expression vectors for additional inner membrane proteins, such as AtTPT, the triosephosphate carrier in the inner envelope membrane (Fischer et al., 1994); AtAPG1, the membrane-associated protein catalyzing the methylation of demethylplastoquinol to plastoquinone-9 (Dreses-Werringloer et al., 1991; Motohashi et al., 2003); and AtLrgB, a highly abundant protein of unknown molecular function (Yang et al., 2012). In all cases the observed patterns were similar to those observed with AtTIC40–GFP, punctate structures around the chloroplast (**Figure 4A**), crescent moon structures (**Figure 4B**) and out loops (**Figure 4C**). We thus conclude that the observed

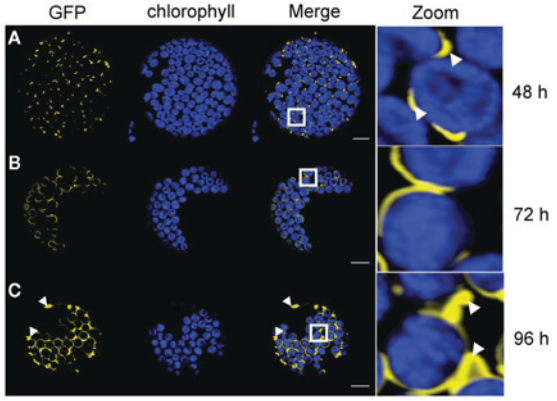

FIGURE 2 | Time course analysis of expression patterns for AtTIC40–GFP in *N. benthamiana* protoplasts. Time based confocal microscopic analysis on isolated protoplasts of *N. benthamiana* leaves after 35 S-promoter driven *in planta* expression of AtTIC40–GFP. GFP fluorescence (GFP) in yellow, chlorophyll autofluorescence (chlorophyll) in blue, an overlay (merge) and a magnification (zoom) of representative protoplasts are shown. The white box indicates the merged region magnified under zoom. **(A)** Expression pattern 2 days (48 h) after *Agrobacterium* infiltration shows short crescent moon-like structures (arrowheads) and dots associated with the chloroplasts. GFP signal slightly departs from chlorophyll autofluorescence. **(B)** Expression pattern 3 days (72 h) after *Agrobacterium* infiltration displays half circles around the chloroplasts. **(C)** Expression pattern 4 days (96 h) after *Agrobacterium* infiltration shows partially full circles surrounding the chloroplasts, interrupted circles, and scattered extensions (arrowheads). Size bars: 10 μm.

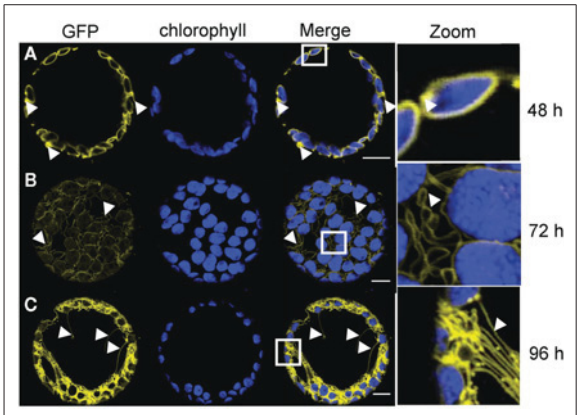

FIGURE 3 | Time course analysis of expression patterns for AtTOC64-III-GFP in *N. benthamiana* protoplasts. Time based confocal microscopic analysis on isolated protoplasts of *N. benthamiana* leaves after 35 S-promoter driven *in planta* expression of AtTOC64-III-GFP. GFP fluorescence (GFP) in yellow, chlorophyll autofluorescence (chlorophyll) in blue, an overlay (merge) and a magnification (zoom) of representative protoplasts are shown. The white box indicates the merged region magnified under zoom. **(A)** Expression pattern 2 days (48 h) after *Agrobacterium* infiltration shows ring structures surrounding the chloroplasts with slight extensions proliferating from the ring. **(B)** Expression pattern 3 days (72 h) after *Agrobacterium* infiltration displays along the chloroplast associated circles extensions of different length. Extensions are connecting the chloroplasts with each other. **(C)** Expression pattern 4 days (96 h) after *Agrobacterium* infiltration shows a network of GFP labeled structures surrounding the chloroplasts and spanning though the entire protoplasts. Size bars: 10 μm.

membrane deformations are independent of the function and the biochemical properties of the inner envelope proteins but due to the increased protein amounts.

LACS9 IS A CHLOROPLAST OUTER ENVELOPE PROTEIN

To investigate to which of the envelope membrane layers AtLACS9 was targeted, we expressed 35S:AtLACS9–GFP in *N. benthamiana* leaves for subsequent protoplast isolation. After 48 h we observed circular structures around the chloroplast (**Figure 5A**), as previously seen for AtTOC64-III expression (**Figure 2A**). Also for AtLACS9, we saw small loops protruding into the cytosol (**Figure 5A** zoom). After 72 h of expression the majority of evaluated protoplasts showed increased amounts of loop structures and thin tubules arising form the chloroplast (**Figure 5B**). The expression pattern 4 days after infiltration was dominated by an extensive system of tubular structures connecting the GFP labeled circles around the chloroplast (**Figure 5C**). All these observations were congruent with the expression patterns previously observed for the outer envelope protein AtTOC64-III. We hence classified AtLACS9 as a chloroplast outer envelope protein.

EXPERIMENTAL CONDITIONS DO NOT AFFECT THE MEMBRANE ALTERATION

In all cases, we isolated protoplasts from transiently transformed tobacco leaves before microscopic observation of the GFP labeling pattern. It was thus possible that the protoplast isolation procedure, involving cell wall digestions with cellulase and macerozyme might have influenced the observed patterns. To exclude a possible effect of cell wall digestion on the observed membrane alterations, we performed *in planta* analyses on the outer envelope protein AtLACS9 and the inner envelope protein AtTIC40. We chose *N. tabacum* as our model for these experiments and focused on expression in leaf epidermis cells. In the case of AtLACS9–GFP we observed the formation of thin extensions arising from a GFP labeled plastids (**Figure 6A**), congruent with observations obtained with chloroplasts in protoplasts. This expression pattern differed from that of AtTIC40–GFP, which was expressed in dot like structures attached to the chloroplasts (**Figure 6B**). Also this observation was congruent with our findings in the protoplast assays. Therefore we conclude that the digestion of the cell wall during protoplast isolation was unlikely to affect the membrane alterations induced by expression of GFP-tagged proteins. Similarly, an effect of the p19 helper strain (Voinnet et al., 2003) used in the *N. benthamiana* transfection but not used in the *N. tabacum* plant, could be excluded. Further, these experiments demonstrate that the nature of the induced structures is also observed in intact cells. Another recent study that was using protoplast transfection instead of *Agrobacterium*-infiltration of leaves observed similar structures when transfecting cells with various

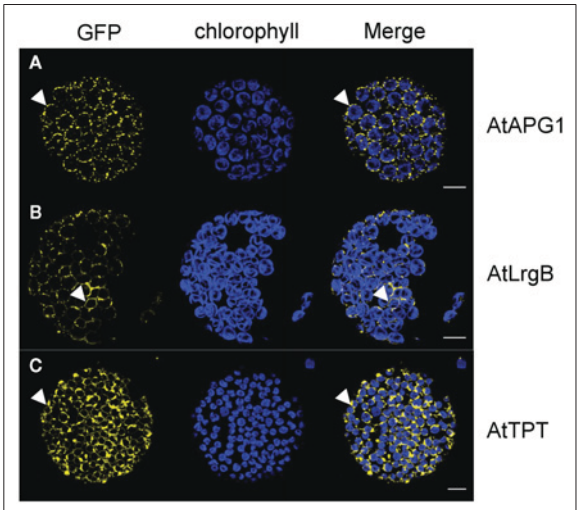

FIGURE 4 | GFP-fusion inner envelope protein expression patterns in *N. benthamiana* protoplasts. Confocal microscopic analysis on isolated protoplasts of *N. benthamiana* leaves after 35 S-promoter driven *in planta* expression of GFP-fusion proteins. Pictures were taken 72 h after infiltration. GFP fluorescence (GFP) in yellow, chlorophyll autofluorescence (chlorophyll) in blue and an overlay (merge) of representative protoplasts are shown. **(A)** Expression pattern of AtAPG1–GFP in dot structures associated with the chloroplast. **(B)** Expression pattern of AtLrgB–GFP in interrupted ring structures around the chlorophyll autofluorescence. **(C)** Expression pattern of AtTPT–GFP in circle structures with slide extensions proliferating from the circle. Size bars: 10 μm.

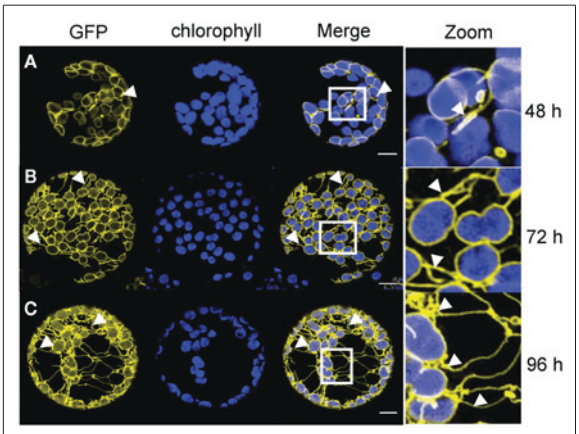

FIGURE 5 | Time course analysis of expression patterns for AtLACS9–GFP in *N. benthamiana* protoplasts. Time based confocal microscopic analysis on isolated protoplasts of *N. benthamiana* leaves after 35 S-promoter driven *in planta* expression of AtLACS9–GFP. GFP fluorescence (GFP) in yellow, chlorophyll autofluorescence (chlorophyll) in blue, an overlay (merge) and a magnification (zoom) of representative protoplasts are shown. The white box indicates the merged region magnified under zoom. **(A)** Expression pattern 2 days (48 h) after *Agrobacterium* infiltration shows ring structures surrounding the chloroplasts with slight extensions proliferating from the ring. **(B)** Expression pattern 3 days (72 h) after *Agrobacterium* infiltration displays more pronounced extensions in addition to ring like structures surrounding the chloroplasts. **(C)** Expression pattern 4 days (96 h) after *Agrobacterium* infiltration shows a network of GFP labeled structures surrounding the chloroplasts, spanning though the entire protoplasts and connecting chloroplasts. Size bars: 10 μm.

tagged inner envelope and outer envelope proteins (Machettira et al., 2012).

The expression of an untagged AtLACS9 led to the formation of tubular structures protruding from the chloroplast (**Figure 7**). This demonstrated that the membrane alteration is not due to the GFP-fusion. We achieved similar results to those described above with constructs driven by the ubiquitin10 promoter and β-estradiol inducible promoter (data not shown). Thus, the observed alterations were not due to an effect of the 35 S cauliflower mosaic virus promoter.

INVESTIGATING THE IDENTITY OF STRUCTURAL ALTERATIONS

The tubular structures we observed during expression of the outer envelope proteins AtTOC64 and AtLACS9 were reminiscent of the previously described stromules (e.g., Köhler and Hanson, 2000; Hanson and Köhler, 2001). Stromules are stroma filled extensions from plastids that are surrounded by the inner and outer envelope membranes. Previous work on the inner envelope protein AtTIC40 reported similar structures compared to those observed in our study and it was concluded that the inner envelope proliferated in several layers when expressing this protein from the chloroplast genome. It had also been shown that the outer envelope was not affected by these proliferations (Singh et al., 2008).

To further investigate the induced structures, we performed transmission electron microscopy on transiently transformed *N. benthamiana* leaves, expressing AtLACS9–GFP or AtTIC40–GFP. The analysis showed that chloroplast of transfected cells expressing AtLACS9 had extensions filled with stroma that were surrounded by two membranes (**Figures 8A–C**), the inner and the outer envelope. We further observed direct connections between distinct chloroplasts via such stroma filled extensions (**Figure 8A** and insert). In addition, organelles like mitochondria (**Figure 8B**) and

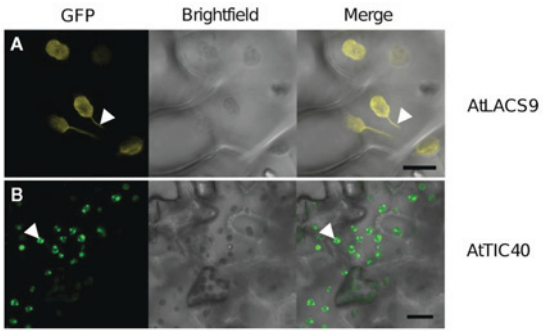

FIGURE 6 | In *planta* expression pattern of outer and inner envelope proteins. GFP-fusion protein expression patterns in intact leave cells of *N. tabacum*, 48 h after *Agrobacterium* infiltration. GFP fluorescence (GFP) in yellow, bright-field photo (bright-field) in black/white and an overlay (merge) of representative leave areas are shown. **(A)** Expression of outer envelope protein AtLACS9–GFP in intact epidermis cells led GFP signal to co-localize with chloroplasts and stromule formation (arrowhead). **(B)** Expression pattern of the inner envelope protein AtTIC40–GFP shows dot structures associated with the chloroplasts (arrowhead). Also slight GFP rings can be seen around the chloroplasts. Size bars: 20 μm.

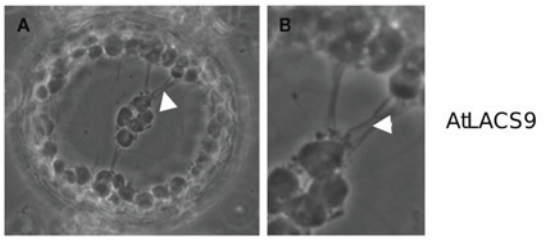

FIGURE 7 | AtLACS9 w/o GFP expression in *N. benthamiana* leaf protoplast. Protoplast of a transfected *N. benthamiana* leaf cell expressing AtLACS9 driven by a 35 S-promoter. **(A)** Chloroplasts are connected by a system of strings (arrowhead). **(B)** Close-up of the connections between the chloroplasts.

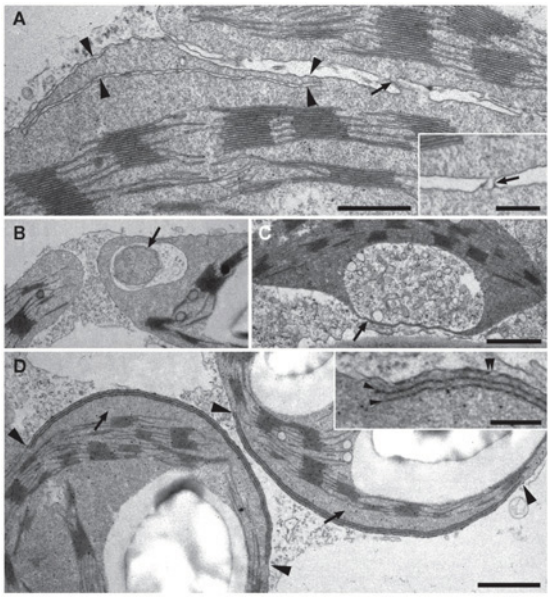

FIGURE 8 | Analysis of transient transfected *N. benthamiana* leave cells by transmission electron microscopy. Ultrastructural analysis of leave material of *N. benthamiana* plants transiently transfected with the constructs 35S:AtLACS9–GFP **(A–C)** or 35S:AtTIC40–GFP **(D)**. [**(A)**; and inset] Stroma filled connection sites (arrows) between chloroplasts in AtLACS9 transfected tobacco cells. The lower chloroplast displays a thin, stroma filled extension (arrowheads). Scale bar in **(A)** 0.5 μm, scale bar in the inset: 0.2 μm. **(B)** An AtLACS9–GFP containing chloroplast enclosing a mitochondrion (arrow) by a stroma filled extension. **(C)** A chloroplast of an AtLACS9–GFP expressing tobacco cell displaying a very thin, stroma filled tube. Scale bar in **(C)** [applies also to **(B)**]: 1 μm. [**(D)** and inset] Chloroplasts of AtTIC40–GFP transfected tobacco cells displaying areas with layers of inner envelope membrane (between arrowheads). The inset shows a higher magnification of additional layers of inner envelope membrane (arrowheads). A double arrowhead labels the outer and inner envelope membranes in close proximity. The proliferated membrane withdraws from the thylakoid membrane and generates a thylakoid free area (arrows). Scale bar in **(D)** 1 μm, scale bar in the inset: 0.25 μm.

peroxisomes appeared to be surrounded by stroma filled loops of the chloroplast (**Figure 8C**). These latter observations were comparable with ultrastructural analyses of rice leaves (Sage and Sage, 2009). We concluded that the structures observed by confocal microscopy were stromules, because they contain stroma and are surrounded by the inner and outer envelope membranes (Köhler and Hanson, 2000).

The structures observed in AtTIC40-transfected cells were remarkably different from those of the outer envelope protein-transfected cells. Additional membrane layers were observed in distinct areas (**Figure 8D** and insert). These proliferations affected only a part of the inner envelope, while the majority of the inner envelope surface appeared unaffected and did not proliferate. These results are consistent with a previous study in which AtTIC40 was expressed from the chloroplast genome and lead to proliferation of inner envelope membrane (Singh et al., 2008). In addition to the proliferations in distinct areas, the folded membrane with drew from the chloroplast center creating a thylakoid free area (**Figure 8D**). These effects could also be seen in confocal microscopy pictures, where the GFP signal the chlorophyll autofluorescence were separated by a gap (**Figure 2A** zoom).

The results of the ultrastructural analysis by transmission electron microscopy indicated that the inner and outer envelope membranes reacted differently to over-expression of some of their protein constituents. In the case of the inner envelope membrane, membrane proliferations were formed that extended in several layers into the stroma without affecting the outer envelope membrane. In the case of the outer envelope membrane, membrane proliferation led to the formation of stromule-like structures that contained both the inner and the outer envelope membrane. Thus, proliferation of the outer envelope membrane was accompanied by a simultaneous proliferation of the inner envelope membrane.

DISCUSSION

In this study we showed that envelope membranes reproducibly proliferate in distinct patterns as increasing amounts of proteins are inserted into the membranes due to over-expression of envelope membrane proteins. We suggest that the structures observed after over-expression of envelope membrane proteins were indicative of the localization of the protein to either the inner or the outer envelope membrane, thereby providing a tool for assessing the localization of unknown proteins. Using a set of different inner envelope proteins we demonstrated that the proliferation of the inner envelope previously described by Singh et al. (2008), who expressed AtTic40 from the chloroplast genome, could also be achieved by nuclear expression and was likely due to the protein amount in the membrane and not to the protein function or structure.

Our work localized the protein AtLACS9 to the chloroplast outer envelope. We were able to show that AtLACS9 indeed labeled stromules in support of previous observations (Schnurr et al., 2002). Several plant species, such as rice (Sage and Sage, 2009) and the arctic–alpine plant *Oxyria digyna* (Gunning, 2005; Holzinger et al., 2007a,b) contain stromule-like structures in their mesophyll cells. However, the formation of stromules was shown to be much more frequent in non-green tissues (Köhler and Hanson, 2000; Pyke and Howells, 2002; Waters et al., 2004; Natesan et al., 2005; Hanson and Sattarzadeh, 2008). Here, we show that stromule formation can also be induced by over-expression of outer envelope proteins. Using the outer envelope proteins AtLACS9 and AtTOC64-III, we were able to show that the formation is independent of the function or structure of the protein. Hence we posit that the proliferation of the membrane was a direct effect of the protein content in the membrane, as outlined above for inner envelope proteins. Furthermore, we report that inner and outer envelope membrane was differentially affected by over-expression of their protein constituents. This may also indicate that the membrane structures were controlled by different regulatory mechanisms. Similar results have been recently obtained using transiently transfected protoplasts (Machettira et al., 2012).

STROMULES – CONTROLLED PLASTID SHAPE LOSS

It is debated whether filament-forming proteins, such as the stroma-localized plastid division protein FtsZ and the cytosolic actin filaments are involved in plastid shape maintenance and the formation of stromules (Kwok and Hanson, 2003; Hanson and Sattarzadeh, 2008, 2011; Martin et al., 2009; Natesan et al., 2009; Reski, 2009; Sattarzadeh et al., 2009). It can be assumed that the inner envelope membrane is the surface for these plastid internal structural elements, while the outer envelope is the surface for interaction with the cytoskeleton.

The withdrawal of the folded inner envelope from the chloroplast center (**Figure 8D**) represented a shape loss of the organelle, a departure from the usually stable lens shape. Withdrawal of the folded up inner envelope from the thylakoid was observed in both electron micrographs (**Figure 8D**) and live cell imaging (**Figure 2A** zoom), which indicated that it was not a preparation artifact. If there is indeed an inner "plastoskeleton" as suggested (compare Reski, 2009; Hanson and Sattarzadeh, 2011), the loss of the normal shape of the chloroplast might be related to a loss of connection sides between the plastoskeleton and the membrane. The membrane populations of the thylakoids and the inner envelope not only remained separate; they were spaced even further apart upon proliferation. Excess inner envelope membrane did not traffic toward the thylakoids (**Figure 8D**). The outer envelope did not proliferate in concert with the inner envelope (**Figure 8D**). Two alternative hypotheses explaining these observations could be envisaged: (i) limiting membrane amount of the outer envelope limited membrane expansion and thus shape loss. (ii) Alternatively, either an internal or external skeleton held plastid shape constant, thus forcing the inner envelope to proliferate in layers.

Observing the outer envelope allows differentiation between these hypotheses. The outer envelope membrane proliferated in the form of stromule-like extensions, a different kind of shape loss of the chloroplast. Since both over-expression of inner and of outer envelope proteins promoted plastid shape loss, albeit different types, it was not the limited membrane amount which maintained plastid shape. We were able to show that in the plastid extensions the inner envelope and stroma were present. It was previously proposed that the formation of stromules is due to an interaction of internal pressure of the chloroplast and/or an external pulling by the cytoskeleton (compare Hanson and Sattarzadeh, 2011). Starting from this premise, the proliferation of the outer membrane induces or even forces pulling from an extra-plastidial

component. Presumably, the proliferation of outer envelope causes the loss of a stabilizing factor residing on the cytosolic side. Following this model, inner envelopes proliferated to accommodate stromule formation induced by the outer envelope. This hypothesis leads to the question of whether the external factors involved in maintaining plastid shape provide the majority of chloroplast stability. Such cytosolic factors might provide the driving force of stromule formation under natural conditions.

IMPLICATION FOR FUTURE RESEARCH

The results presented here allow localization of envelope proteins and provide new observations on stromule formation. The differential response of the inner and the outer envelope may also provide a tool to investigate the regulation of envelope formation. Singh et al. (2008) observed the same structures as reported here in stably transformed *N. tabacum* plants over-expressing the Tic40 protein from the chloroplast genome. The insertion of the protein expressed from the chloroplast genome is independent of the TIC/TOC translocon complexes and possibly represents the reason why inner envelope proliferation was never reported for stable expression from the nuclear genome. This would indicate that the TIC/TOC complex is actively involved in the regulation of membrane protein concentration and indirectly prevents the membrane from accumulating excess protein amounts. The protein load appears to be the signal for the plant to commit additional membrane lipids to the inner envelope. Singh et al. (2008) observed increased amounts of other inner envelope proteins when over-expressing the Tic40 protein from the chloroplast, but no increase in outer envelope proteins. Since we found that outer envelope proliferation is accompanied by a proliferation of the inner envelope (**Figures 8A–C**), we speculate that the proliferation of the outer membrane is associated with increased inner envelope protein levels. Altered protein levels of nuclear encoded proteins indicate that the protein load in the plastid envelope is communicated to the nucleus (Singh et al., 2008). Recently, a chloroplast envelope protein was found that is proposed to be involved in the signaling between chloroplast and nucleus (Sun et al., 2011). Investigating the expression levels of this protein or similar proteins while over-expressing outer or inner envelope proteins might pinpoint possible regulators involved in the regulation of protein abundance in envelope membranes.

Our observations on the proliferation of the inner envelope membrane and the outer envelope membrane (**Figure 8**) raises the question of whether the proliferation is only due to increased protein amount or also due to an increase in lipid content of the membrane. Unlike the plastid envelopes, the mitochondrial inner membrane (Guidotti, 1972) and the thylakoid membranes (Block et al., 1983) are described as naturally protein dense membrane structures of organelles. Both membranes are either folded (thylakoids; Hodge et al., 1955) or display out-looping formations (mitochondrial inner membrane; Palade, 1953). These structures are similar to the observations for the inner and outer envelope of plastids when over-expressing their respective proteins. Therefore, an increase of membrane lipid production would not necessarily be a prerequisite for proliferating the membrane systems. Analyzing the protein to (plastid-) lipid ratio in inducible stable lines before and after induction of membrane proliferation could answer that question.

ACKNOWLEDGMENTS

This work was funded by a grant of the Deutsche Forschungsgemeinschaft (WE2231/4-1 to APMW) in the framework of the *Arabidopsis* Functional Genomics Network (AFGN).We thank the German-American Fulbright Commission, Alisandra Denton, and Sebastian Breuers for supporting this work in diverse ways.

REFERENCES

Arimura, S., Hirai, A., and Tsutsumi, N. (2001). Numerous and highly developed tubular projections from plastids observed in tobacco epidermal cells. *Plant Sci.* 160, 449–454.

Bae, W., Lee, Y. J., Kim, D. H., Lee, J., Kim, S., Sohn, E. J., and Hwang, I. (2008). AKr2A-mediated import of chloroplast outer membrane proteins is essential for chloroplast biogenesis. *Nat. Cell Biol.* 10, 220–227.

Batoko, H., Zheng, H. Q., Hawes, C., and Moore, I. (2000). A Rab1 GTPase is required for transport between the endoplasmic reticulum and Golgi apparatus and for normal Golgi movement in plants. *Plant Cell* 12, 2201–2217.

Benning, C. (2009). Mechanisms of lipid transport involved in organelle biogenesis in plant cells. *Annu. Rev. Cell Dev. Biol.* 25, 71–91.

Bionda, T., Tillmann, B., Simm, S., Beilstein, K., Ruprecht, M., and Schleiff, E. (2010). Chloroplast import signals: the length requirement for translocation *in vitro* and *in vivo*. *J. Mol. Biol.* 402, 510–523.

Bleckmann, A., Weidtkamp-Peters, S., Seidel, C. A., and Simon, R. (2010). Stem cell signaling in *Arabidopsis* requires CRN to localize CLV2 to the plasma membrane. *Plant Physiol.* 152, 166–176.

Block, M. A., Dorne, A. J., Joyard, J., and Douce, R. (1983). Preparation and characterization of membrane fractions enriched in outer and inner envelope membranes from spinach chloroplasts. II. Biochemical characterization. *J. Biol. Chem.* 258, 13281–13286.

Bräutigam, A., Hofmann-Benning, S., and Weber, A. P. M. (2008a). Comparative proteomics of chloroplast envelopes from C3 and C4 plants reveals specific adaptations of the plastid envelope to C4 photosynthesis and candidate proteins required for maintaining c4 metabolite fluxes. *Plant Physiol.* 148, 568–579.

Bräutigam, A., Shrestha, R. P., Whitten, D., Wilkerson, C. G., Carr, K. M., Froehlich, J. E., and Weber, A. P. M. (2008b). Comparison of the use of a species-specific database generated by pyrosequencing with databases from related species for proteome analysis of pea chloroplast envelopes. *J. Biotechnol.* 136, 44–53.

Bräutigam, A., and Weber, A. P. M. (2009). Proteomic analysis of the proplastid envelope membrane provides novel insights into small molecule and protein transport across proplastid membranes. *Mol. Plant* 2, 1247–1261.

Breuers, F. K. H., Bräutigam, A., and Weber, A. P. M. (2011). The plastid outer envelope – a highly dynamic interface between plastid and cytoplasm. *Front. Plant Sci.* 2:97. doi:10.3389/fpls.2011.00097

Chou, M.-L. (2003). Tic40, a membrane-anchored co-chaperone homolog in the chloroplast protein translocon. *EMBO J.* 22, 10.

Curtis, M. D., and Grossniklaus, U. (2003). A gateway cloning vector set for high-throughput functional analysis of genes in planta. *Plant Physiol.* 133, 462–469.

Dreses-Werringloer, U., Fischer, K., Wachter, E., Link, T. A., and Flugge, U. I. (1991). cDNA sequence and deduced amino-acid-sequence of the precursor of the 37-Kda inner envelope membrane polypeptide from spinach-chloroplasts – its transit peptide contains an amphiphilic alpha-helix as the only detectable structural element. *Eur. J. Biochem.* 195, 361–368.

Facchinelli, F., and Weber, A. P. M. (2011). The metabolite transporters of the plastid envelope: an update. *Front. Plant Sci.* 2:50. doi:10.3389/fpls.2011.00050

Ferro, M., Brugiere, S., Salvi, D., Seigneurin-Berny, D., Court, M., Moyet, L., Ramus, C., Miras, S., Mellal, M., Le Gall, S., Kieffer-Jaquinod, S., Bruley, C., Garin, J., Joyard, J., Masselon, C., and Rolland, N. (2010). AT_CHLORO, a comprehensive chloroplast proteome database with subplastidial localization and curated information on envelope proteins. *Mol. Cell. Proteomics* 9, 1063–1084.

Ferro, M., Salvi, D., Brugiere, S., Miras, S., Kowalski, S., Louwagie, M., Garin, J., Joyard, J., and Rolland, N. (2003). Proteomics of the chloroplast envelope membranes from *Arabidopsis thaliana*. *Mol. Cell. Proteomics* 2, 325–345

Fischer, K., Arbinger, B., Kammerer, B., Busch, C., Brink, S., Wallmeier, H., Sauer, N., Eckerskorn, C., and Flugge, U. I. (1994). Cloning and in-vivo expression of functional triose phosphate/phosphate translocators from C-3-plants and C-4-plants – evidence for the putative participation of specific amino-acid-residues in the recognition of phosphoenolpyruvate. *Plant J.* 5, 215–226.

Gehl, C., Waadt, R., Kudla, J., Mendel, R. R., and Hansch, R. (2009). New GATEWAY vectors for high throughput analyses of protein-protein interactions by bimolecular fluorescence complementation. *Mol. Plant* 2, 1051–1058.

Grefen, C., Donald, N., Hashimoto, K., Kudla, J., Schumacher, K., and Blatt, M. R. (2010). A ubiquitin-10 promoter-based vector set for fluorescent protein tagging facilitates temporal stability and native protein distribution in transient and stable expression studies. *Plant J.* 64, 355–365.

Guidotti, G. (1972). Membrane proteins. *Annu. Rev. Biochem.* 41, 731–752.

Gunning, B. E. S. (2005). Plastid stromules: video microscopy of their outgrowth, retraction, tensioning, anchoring, branching, bridging, and tip-shedding. *Protoplasma* 225, 33–42.

Hanson, M. R., and Köhler, R. H. (2001). GFP imaging: methodology and application to investigate cellular compartmentation in plants. *J. Exp. Bot.* 52, 529–539.

Hanson, M. R., and Sattarzadeh, A. (2008). Dynamic morphology of plastids and stromules in angiosperm plants. *Plant Cell Environ.* 31, 646–657.

Hanson, M. R., and Sattarzadeh, A. (2011). Stromules: recent insights into a long neglected feature of plastid morphology and function. *Plant Physiol.* 155, 1486–1492.

Hodge, A. J., Mclean, J. D., and Mercer, F. V. (1955). Ultrastructure of the lamellae and grana in the chloroplast of *Zea Mays* L. *J. Biophys. Biochem. Cytol.* 1, 605.

Holzinger, A., Buchner, O., Lutz, C., and Hanson, M. R. (2007a). Temperature-sensitive formation of chloroplast protrusions and stromules in mesophyll cells of *Arabidopsis thaliana*. *Protoplasma* 230, 23–30.

Holzinger, A., Wasteneys, G. O., and Lutz, C. (2007b). Investigating cytoskeletal function in chloroplast protrusion formation in the arctic-alpine plant *Oxyria digyna*. *Plant Biol.* 9, 400–410.

Joyard, J., Ferro, M., Masselon, C., Seigneurin-Berny, D., Salvi, D., Garin, J., and Rolland, N. (2010). Chloroplast proteomics highlights the subcellular compartmentation of lipid metabolism. *Prog. Lipid Res.* 49, 128–158.

Köhler, R., Hanson, M., and Wildman, S. (1997a). Pictures in cell biology – plastid interconnections imaged by fluorescence and phase contrast. *Trends Cell Biol.* 7, 392–392.

Köhler, R. H., Cao, J., Zipfel, W. R., Webb, W. W., and Hanson, M. R. (1997b). Exchange of protein molecules through connections between higher plant plastids. *Science* 276, 2039–2042.

Köhler, R. H., and Hanson, M. R. (2000). Plastid tubules of higher plants are tissue-specific and developmentally regulated. *J. Cell Sci.* 113, 81–89.

Koncz, C., and Schell, J. (1986). The promoter of Tl-DNA gene 5 controls the tissue-specific expression of chimeric genes carried by a novel type of *Agrobacterium* binary vector. *Mol. Gen. Genet.* 204, 383–396.

Koo, A. J., Ohlrogge, J. B., and Pollard, M. (2004). On the export of fatty acids from the chloroplast. *J. Biol. Chem.* 279, 16101–16110.

Kwok, E. Y., and Hanson, M. R. (2003). Microfilaments and microtubules control the morphology and movement of non-green plastids and stromules in *Nicotiana tabacum*. *Plant J.* 35, 16–26.

Lee, Y. J., Kim, D. H., Kim, Y. W., and Hwang, I. (2001). Identification of a signal that distinguishes between the chloroplast outer envelope membrane and the endomembrane system *in vivo*. *Plant Cell* 13, 2175–2190.

Linka, N., and Weber, A. P. M. (2010). Intracellular metabolite transporters in plants. *Mol. Plant* 3, 21–53.

Machettira, A. B., Groß, L. E., Tillmann, B., Weis, B. L., Englich, G., Sommer, M. S., Königer, M., and Schleiff, E. (2012). Protein induced modulation of chloroplast membrane morphology. *Front. Plant Sci.* 2:118. doi: 10.3389/fpls.2011.00118

Martin, A., Lang, D., Hanke, S. T., Mueller, S. J. X., Sarnighausen, E., Vervliet-Scheebaum, M., and Reski, R. (2009). Targeted gene knockouts reveal overlapping functions of the five *Physcomitrella* patens FtsZ isoforms in chloroplast division, chloroplast shaping, cell patterning, plant development, and gravity sensing. *Mol. Plant* 2, 1359–1372.

Motohashi, R., Ito, T., Kobayashi, M., Taji, T., Nagata, N., Asami, T., Yoshida, S., Yamaguchi-Shinozaki, K., and Shinozaki, K. (2003). Functional analysis of the 37 kDa inner envelope membrane polypeptide in chloroplast biogenesis using a Ds-tagged *Arabidopsis* pale-green mutant. *Plant J.* 34, 719–731.

Natesan, S. K. A., Sullivan, J. A., and Gray, J. C. (2005). Stromules: a characteristic cell-specific feature of plastid morphology. *J. Exp. Bot.* 56, 787–797.

Natesan, S. K. A., Sullivan, J. A., and Gray, J. C. (2009). Myosin XI is required for actin-associated movement of plastid stromules. *Mol. Plant* 2, 1262–1272.

Oikawa, K., Kasahara, M., Kiyosue, T., Kagawa, T., Suetsugu, N., Takahashi, F., Kanegae, T., Niwa, Y., Kadota, A., and Wada, M. (2003). Chloroplast unusual positioning1 is essential for proper chloroplast positioning. *Plant Cell* 15, 2805–2815.

Oikawa, K., Yamasato, A., Kong, S. G., Kasahara, M., Nakai, M., Takahashi, F., Ogura, Y., Kagawa, T., and Wada, M. (2008). Chloroplast outer envelope protein CHUP1 is essential for chloroplast anchorage to the plasma membrane and chloroplast movement. *Plant Physiol.* 148, 829–842.

Palade, G. E. (1953). An electron microscope study of the mitochondrial structure. *J. Histochem. Cytochem.* 1, 188–211.

Pyke, K. A., and Howells, C. A. (2002). Plastid and stromule morphogenesis in tomato. *Ann. Bot.* 90, 559–566.

Qbadou, S., Becker, T., Bionda, T., Reger, K., Ruprecht, M., Soll, J., and Schleiff, E. (2007). Toc64 - A preprotein-receptor at the outer membrane with bipartide function. *J. Mol. Biol.* 367, 1330–1346.

Reski, R. (2009). Challenges to our current view on chloroplasts. *Biol. Chem.* 390, 731–738.

Reynolds, E. S. (1963). Use of lead citrate at high pH as an electron-opaque stain in electron microscopy. *J. Cell Biol.* 17, 208–212.

Rolland, N., Ferro, M., Seigneurin-Berny, D., Garin, J., Douce, R., and Joyard, J. (2003). Proteomics of chloroplast envelope membranes. *Photosyn. Res.* 78, 205–230.

Roughan, P. G., and Slack, C. R. (1977). Long-chain acyl-coenzyme A synthetase activity of spinach chloroplasts is concentrated in the envelope. *Biochem. J.* 162, 457–459.

Sage, T. L., and Sage, R. F. (2009). The functional anatomy of rice leaves: implications for refixation of photorespiratory CO2 and efforts to engineer C-4 photosynthesis into rice. *Plant Cell Physiol.* 50, 756–772.

Sattarzadeh, A., Krahmer, J., Germain, A. D., and Hanson, M. R. (2009). A Myosin XI tail domain homologous to the yeast myosin vacuole-binding domain interacts with plastids and stromules in *Nicotiana benthamiana*. *Mol. Plant* 2, 1351–1358.

Schmidt Von Braun, S., and Schleiff, E. (2008). The chloroplast outer membrane protein CHUP1 interacts with actin and profilin. *Planta* 227, 1151–1159.

Schnurr, J. A., Shockey, J. M., De Boer, G. J., and Browse, J. A. (2002). Fatty acid export from the chloroplast. Molecular characterization of a major plastidial acyl-coenzyme A synthetase from *Arabidopsis*. *Plant Physiol.* 129, 1700–1709.

Shaw, D. J., and Gray, J. C. (2011). Visualisation of stromules in transgenic wheat expressing a plastid-targeted yellow fluorescent protein. *Planta* 233, 961–970.

Shiina, T., Hayashi, K., Ishii, N., Morikawa, K., and Toyoshima, Y. (2000). Chloroplast tubules visualized in transplastomic plants expressing green fluorescent protein. *Plant Cell Physiol.* 41, 367–371.

Shockey, J. M., Fulda, M. S., and Browse, J. A. (2002). *Arabidopsis* contains nine long-chain acyl-coenzyme A synthetase genes that participate in fatty acid and glycerolipid metabolism. *Plant Physiol.* 129, 1710–1722.

Singh, N. D., Li, M., Lee, S. B., Schnell, D., and Daniell, H. (2008). *Arabidopsis* Tic40 expression in tobacco chloroplasts results in massive proliferation of the Inner envelope membrane and upregulation of associated proteins. *Plant Cell* 20, 3405–3417.

Sohrt, K., and Soll, J. (2000). Toc64, a new component of the protein translocon of chloroplasts. *J. Cell Biol.* 148, 1213–1221.

Strittmatter, P., Soll, J., and Bolter, B. (2010). The chloroplast protein import machinery: a review. *Methods Mol. Biol.* 619, 307–321.

Sun, Q., Zybailov, B., Majeran, W., Friso, G., Olinares, P. D., and Van Wijk, K. J. (2009). PPDB, the plant proteomics database at Cornell. *Nucleic Acids Res.* 37, D969–D974.

Sun, X., Feng, P., Xu, X., Guo, H., Ma, J., Chi, W., Lin, R., Lu, C.,

and Zhang, L. (2011). A chloroplast envelope-bound PHD transcription factor mediates chloroplast signals to the nucleus. *Nat. Commun.* 2, 477.

Tirlapur, U. K., Dahse, I., Reiss, B., Meurer, J., and Oelmuller, R. (1999). Characterization of the activity of a plastid-targeted green fluorescent protein in *Arabidopsis*. *Eur. J. Cell Biol.* 78, 233–240.

Voinnet, O., Rivas, S., Mestre, P., and Baulcombe, D. (2003). An enhanced transient expression system in plants based on suppression of gene silencing by the p19 protein of tomato bushy stunt virus. *Plant J.* 33, 949–956.

Waters, M. T., Fray, R. G., and Pyke, K. A. (2004). Stromule formation is dependent upon plastid size, plastid differentiation status and the density of plastids within the cell. *Plant J.* 39, 655–667.

Weber, A. P. M., and Linka, N. (2011). Connecting the plastid: transporters of the plastid envelope and their role in linking plastidial with cytosolic metabolism. *Annu. Rev. Plant Biol.* 62, 53–77.

Wydro, M., Kozubek, E., and Lehmann, P. (2006). Optimization of transient *Agrobacterium*-mediated gene expression system in leaves of *Nicotiana benthamiana*. *Acta Biochim. Pol.* 53, 289–298.

Yang, Y., Jin, H., Chen, Y., Lin, W., Wang, C., Chen, Z., Han, N., Bian, H., Zhu, M., and Wang, J. (2012). A chloroplast envelope membrane protein containing a putative LrgB domain related to the control of bacterial death and lysis is required for chloroplast development in *Arabidopsis thaliana*. *New Phytol.* 193, 81–95.

Yoo, S. D., Cho, Y. H., and Sheen, J. (2007). *Arabidopsis* mesophyll protoplasts: a versatile cell system for transient gene expression analysis. *Nat. Protoc.* 2, 1565–1572.

Zhao, L., Katavic, V., Li, F., Haughn, G. W., and Kunst, L. (2010). Insertional mutant analysis reveals that long-chain acyl-CoA synthetase 1 (LACS1), but not LACS8, functionally overlaps with LACS9 in *Arabidopsis* seed oil biosynthesis. *Plant J.* 64, 1048–1058.

Conflict of Interest Statement: The authors declare that the research was conducted in the absence of any commercial or financial relationships that could be construed as a potential conflict of interest.

Received: 26 October 2011; accepted: 05 January 2012; published online: 23 January 2012.

Citation: Breuers FKH, Bräutigam A, Geimer S, Welzel UY, Stefano G, Renna L, Brandizzi F and Weber APM (2012) Dynamic remodeling of the plastid envelope membranes – a tool for chloroplast envelope in vivo localizations. Front. Plant Sci. ***3****:7. doi: 10.3389/fpls.2012.00007*

This article was submitted to Frontiers in Technical Advances in Plant Science, a specialty of Frontiers in Plant Science.

Addendum 1: The impact of lipids on the envelope proliferation

Status: **unpublished** (2013)

Authors: **Frederique K.H. Breuers, Andrea Bräutigam, and Andreas P.M. Weber**

1. Author

Own contribution: 95%

- Experimental design
- Preliminary experiments
- Data elicitation and selection
- Writing the manuscript

Abstract

In the last decades, the dynamic nature of the chloroplast envelopes under natural condition as well as under artificial induction has been under continuous investigation. However, the analyses have been of a more descriptive nature and lacked a clear explanation for the appearance of, for example, thin tubules out-looping form the plastid. The recent findings that these structures can be induced by overexpressing proteins residing in the outer envelope membrane of the plastid and the divergent folded envelope structures can be induced by overexpressing inner envelope proteins, offered a tool for analysis of their origin. Using inducible *Arabidopsis* overexpression lines for outer envelope and inner envelope proteins, fatty acid analyses were performed to investigate the impact of membrane lipids on the expansion/proliferation process of the envelope membranes. Even though, the results of this study remain inconclusive, it indicates that fatty acid production plays a subordinate role in proliferation processes.

Introduction

The primary chloroplast and its "non-green" relatives are surrounded by two envelope membranes, the inner envelope (IE) and the outer envelope (OE). Most recently, since the description of stromules – stroma filled tubules – by the Hanson group (e.g. Köhler et al, 1997; Gray et al., 2001; Gray et al., 2011; Hanson and Sattarzadeh, 2011) the dynamics of the envelope membranes became accessible. Recent studies described these membranes as highly dynamic in reacting to an alteration of protein amounts (Breuers et al., 2012; Machettira et al., 2012). In these fluorophore based studies, the transient expression of proteins of the envelope membranes led to proliferation of the membranes in envelope specific manners. These effects were independent of function or insertion modality of the tested proteins. Thus, the proliferation was solely by the amount of protein.

The over-expression of IE proteins led to the folding of the IE in several layers, which was detectable by electron microscopy. In confocal microscopic analyses, these folded areas could be viewed as fluorophore labeled crescent-moon like structures attached to the chlorophyll autofluorescence. On the contrary, OE protein over-expression led to fluorophore labeled thin tubule-like structures out-looping from the plastid. Ultrastructure analyses revealed that these out-loop contained OE as well as IE and stroma. Hence, these structures were identified as stromules (Breuers et al., 2012). In other words, this stromule formation included the proliferation of both envelope membranes at the same time. This discrepancy between the proliferation properties caused by IE and OE proteins became a localization tool for envelope proteins.

While it is indisputable, that the expansions of the membranes require material, the origins of this material remain unsolved. It is hypothesized, that the proliferation processes require more membrane lipids and therefore an enhanced fatty acid (FA) production. Similar to the differences in the proliferation properties – single IE proliferation or co-proliferation of IE and OE – the increase in FA levels is likely different between IE and OE protein overexpression lines.

To investigate these hypotheses, comparative analysis of FA levels in OE and IE overexpression lines were carried out. The protein AtWBC7 (White-Brown-Complex protein 7) was chosen as representative for the OE proteins. While the function of AtWBC7 remained unexplored, it was found to be located to the OE (Schleiff et al., 2003; Diploma thesis F.K.H. Breuers). A function in the transfer of hydrophobic particles across the OE can be hypothesized, since two of its homologs in the plasma membrane display this function (Mcfarlane et al., 2010; Breuers et al., 2011). For investigation of lipid impact on the IE proliferation, AtTIC40 was chosen. This 40 kDa sized component of the IE protein translocon complex (TIC) plays a crucial role in protein insertion into the IE (Chiu and Li, 2008). The protein is anchored via a single domain in the IE (Kovacheva et al., 2005; Bedard et al., 2007) and its validity as

proliferation inducer was demonstrated in previous studies (Singh et al., 2008; Breuers et al., 2012). As negative control for the proliferation process, a stromal localized protein was chosen named AtcpRNA (for chloroplast ribosomal RNA metabolism associated). This protein was chosen as control, since it was shown by an in-house study to localize inside the plastid (Diploma thesis Breuers, F.K.H.), supported by two publications of Belligni and Mayfield (2008) and Bollenbach et al. (2009).

These three proteins were introduced into *A. thaliana* in pABindGFP expression vectors, with their full coding sequence N-terminal fused to GFP and under control of a β-estradiol inducible promoter (Figure 1). Wild type plants were used as a negative control in the FA analysis.

Results and Discussion

The previous investigations on the membrane dynamics were motivated by the need for a protein localization tool in a transient system. Therefore, unstable factors like the infiltration of agrobacteria into leaves, the various counts of insertions of the genes of interest into the plant genome and the starting time of protein biosynthesis did not present critical factors. However, these factors disqualified the transient system for comparable lipid analysis.

Establishing the system of choice: β-estradiol inducible constructs in Arabidopsis thaliana

Previous and recent studies found that the expression of GFP labeled envelope protein in a stable manner only displayed green fluorescent circles around the plastid, regardless of whether the localization was to the IE or OE (e.g. Schnurr et al., 2002; Seigneurin-Berny et al., 2006; Yamasaki et al., 2013). A proliferation of membranes was not described. This indicated that the plant regulatory systems prevent membrane proliferation when the T-DNA insertion appears prior to early plant development. Thus, a system needed to be found that was stable, but allowed a

proliferation process. To this end, constructs were designed containing β-estradiol inducible promoters in front of the genes of interest. In order to visualize the expected proliferation process, GFP was fused at the C-terminus (Figure 1). These constructs were stably transformed into *Arabidopsis thaliana*. This design allowed an insertion of the construct into the plant genome without contamination by Agrobacteria during the fatty acid (FA) isolation procedure. Thereby, each cell contained the same count of construct insertions and protein biosynthesis could be simultaneously induced in every cell by applying β-estradiol.

Expression patterns of the induced over-expresser lines are comparative to previous observations

To verify that the chosen system possessed similar proliferation properties as the transient tobacco system, protein expression was induced in single leaves of the stable inducible lines by brushing a 20 mM β-estradiol solution on the ventral leaf surface. GFP signal in these leaves were detected via confocal microscopy 24 and 48 hours after induction (Figure 2). After 24 hours of expressing AtTIC40-GFP in the inducible over-expression lines (oxAtTIC40), GFP signal appeared in crescent-moon-like structures associated with chloroplasts (Figure 2A), which further increased in brightness and area after 48 hours (Figure 2B). These results were comparable to

Figure 1: Inducible construct design for plant transformation based on the pABindGFP vector (adapted from Bleckmann et al., 2010).

T-DNA construct for inducible expression of translational fusions of genes of interest (GOI) with a C-terminal GFP. G10-90: Constitutive promoter; XVE: chimeric transcription factor that activates transcription from the lexA-46 35S promoter upon estradiol induction. Hygomycin resistance is driven by a 35S promoter (Hygr).

those achieved in the transient tobacco system (Breuers et al., 2012) Also the OE protein expressing lines displayed results comparable to those observed in the transient system. Contrasting to the AtTIC40 results, 24 hours after induction of the expression of AtWBC7-GFP, green signal could be detected thinly surrounding the chloroplasts of the inducible over-expression lines (oxAtWBC7; Figure 2C). After an additional 24 hours, stromule formation could be detected (Figure 2D). These results

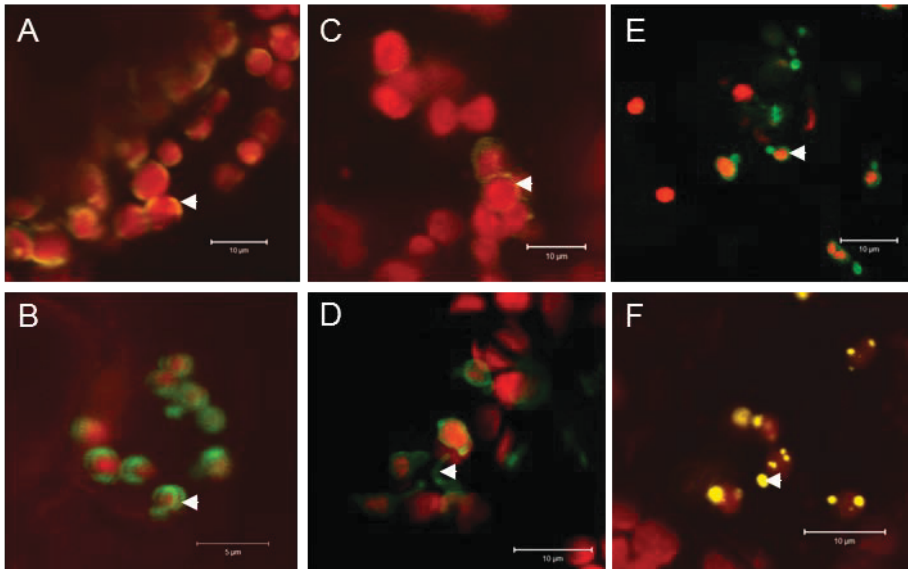

Figure 2: Expression patterns in stable inducible *Arabidopsis* lines after β-estradiol induction

A) Crescent-moon-like GFP signal surrounding plastids of AtTIC40-GFP after 24 hours and **B)** after 48 hours. **C)** AtWBC7-GFP signal thinly surrounding plastids after 24 hours and **D)** out-looping stromules after 48 hours. **E)** Colocalizing GFP and chlorophyll autofluorescence in oxcpRNA lines after 24 hours. GFP signal can be also detected outside the chloroplast. **F)** AtcpRNA-GFP aggregations alongside of plastids. **Green**: GFP signal**; red**: chlorophyll autofluorescence

indicated that the stable *Arabidopsis* system represented a valid setup for comparative FA analysis.

The GFP signal of the negative control lines, expressing the stromal protein construct AtcpRNA-GFP (oxcpRNA), co-localized with the chlorophyll autofluorescence (Figure 2E). Sometimes, the signal was not equally distributed across the whole chloroplast signal, but denser in dot-like structures on or alongside the chlorophyll autofluorescence (Figure 2F). This might indicate protein aggregation in the stroma

or cytosol due to its unnaturally high concentration and potentially the malfunction of protein transport systems. However, it cannot be excluded that AtcpRNA naturally associated with the chloroplast surface, since this protein was recently under controversial discussion. A study of Fettke et al. (2011) named this protein HIP1.3 (heteroglycan-interaction protein 1.3) and described an association of this protein with the OE from the cytosolic side. However, observations indicating changes in envelope membranes could not be observed. Hence, the oxcpRNA lines were used as negative membrane proliferation control.

No differences in the FA content nor FA distribution between over-expresser lines

The data analysis of the FA methyl esters (FAME) and therefore, of the total FA content of the sample leaves revealed no significant changes (Figure 3). A statistical analysis via a two way ANOVA test, followed by a Bonferroni posttest revealed that the visual increase in the FA levels of the oxTIC40 samples and the fluctuation in the oxWBC7 samples were not significant.

Even though, no significant changes in the total FA could be detected, a change in the FA composition remained possible. *Arabidopsis* and other '16:3'-plants present an approximately fifty-fifty usage of prokaryotic and eukaryotic FA in membrane lipids (Browse et al., 1986; Kelly and Dörmann, 2004). However, in stress situations, such as phosphate deprivation (Härtel et al., 2000) or freezing stress (Moellering et al., 2010) these plants shift their FA usage in the direction of the eukaryotic pathway, according to the localization of involved enzymes. FA from the plastid/prokaryotic pathway are remarkably different to these produced extra-plastidic in the eukaryotic pathway (Ohlrogge and Browse, 1995). Membrane lipids like MGDG or DGDG contain predominantly 18:2 FAs when they derive from the eukaryotic pathway, while plastidic lipids contain 18:1 and 16:0/16:3 FAs (Browse et al., 1986; Härtel et al., 2000; Kelly and Dörmann., 2004). The proliferation process induced by unnaturally high protein amounts in the envelope membranes were expected to be a stress situation for the plants. Thus, it was hypothesized that the FA composition shifts

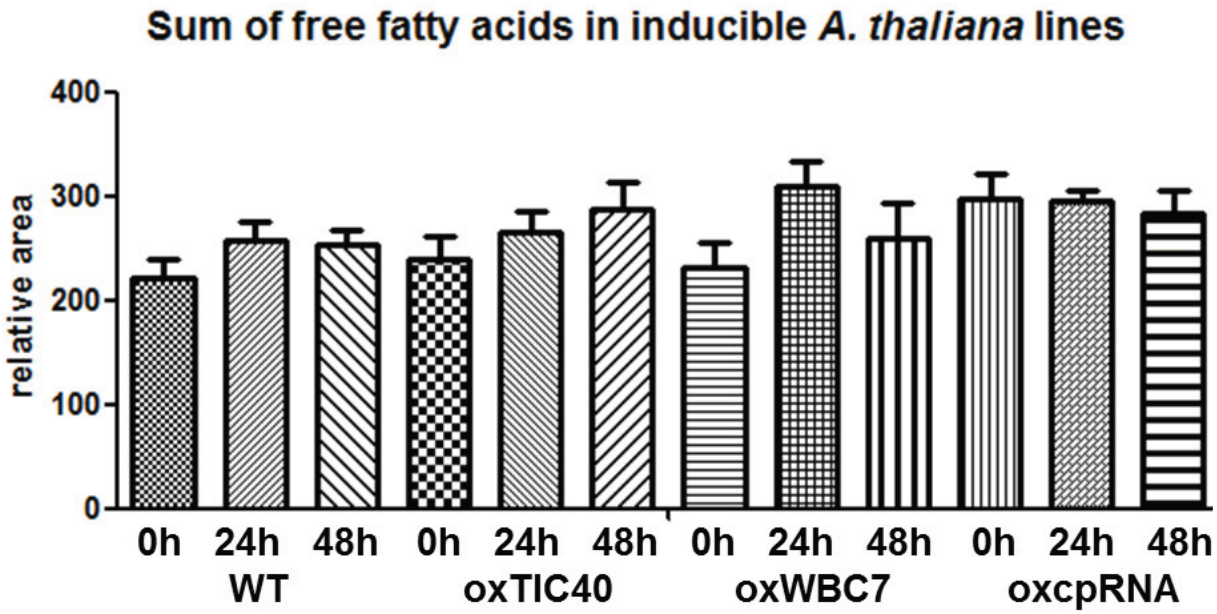

Figure 3: Sum of free fatty acids in inducible *A. thaliana* lines

Results of a GC MS component analysis of free fatty acids in WT, inducible inner envelope protein over-expresser (oxTIC40), inducible outer envelope protein over-expresser (oxWBC7), and inducible stromal protein over-expresser (oxcpRNA) lines at three different time points (t=0h, 24h, 48 h). All lines display no significant time dependent changes in fatty acid levels.

from plastidic to more extraplastidic FA compounds. Even though, a visible increase in the portion of 18:3 FA was observed in oxcpRNA lines (Figure 4B) and in oxWBC7 (Figure 4 D), a similar increase could be found in the control WT plants (Figure 4 A). Furthermore, these slight level changes are mainly covered by the decreases in the levels of 18:2 and 18:0 levels. However, statistical analysis via a combined ANOVA and Bonferroni posttest revealed no significant changes in the superior FA in any of the over-expression plants. Furthermore, the FA compound 18:1 was not detectable in the GC/MS analysis. This problem was already described by Browse et al. (1986) as related to the combined elution of 18:1 and 16:3 FAs during the chromatography process. The 16:0 and 16:3 portions of 30% and 15%, respectively, remained unaffected in all lines and at all time points, indicating that plastid FA production was unaffeced at all.

Conclusive Statement and implications

The lipid analysis of the inducible *Arabidopsis* transformants did not prove nor disprove the hypothesis that lipids are involved in the rapid envelope proliferation. However, the results might indicate that an increase in membrane lipids is not needed in the fast proliferation process. It may be accepted, that the proliferation is only due to the increased protein amounts in the membranes. Therefore, a change in protein to lipid ratio might indicate an 'imitation' of other known protein-dense membrane types like the out-looping mitochondrial inner membrane (Palade et al., 1953; Guidotti, 1972) or the folded thylakoid membrane (Hodge et al., 1955; Block et al., 1983) by the plastid envelopes.

However, it must be assumed that FAME analyses are not sensitive enough to detect changes in membrane lipid production. This relies on the fact that the FAME analysis results in a combination of all free FAs (FFA) from leaf tissue. Provided that acute membrane lipid production is served from a potential FFA pool or from the diacylglycerol (DAG) pool (Ohlrogge and Browse, 1995; Maréchal et al., 1997; Joyard et al., 2004), which is on a steady-state level, changes could not be detected. Hence, a pre-separation of membrane lipids via thin layer chromatography and the subsequent analysis of the lipid components would be more effective to investigate the involvement of membrane lipids in membrane alterations.

Material and Methods

Cloning

The coding sequences of AtWBC7 (At2g01320), AtTic40 (At5g16620), and cpRNA (At1g09340) were amplified from cDNA and cloned into the plant expression vector pABindGFP (Bleckmann et al., 2010) as ß-estradiol-inducible-promoter driven construct with a C-terminal GFP fusion (Figure 1) using the Invitrogen Gateway® system.

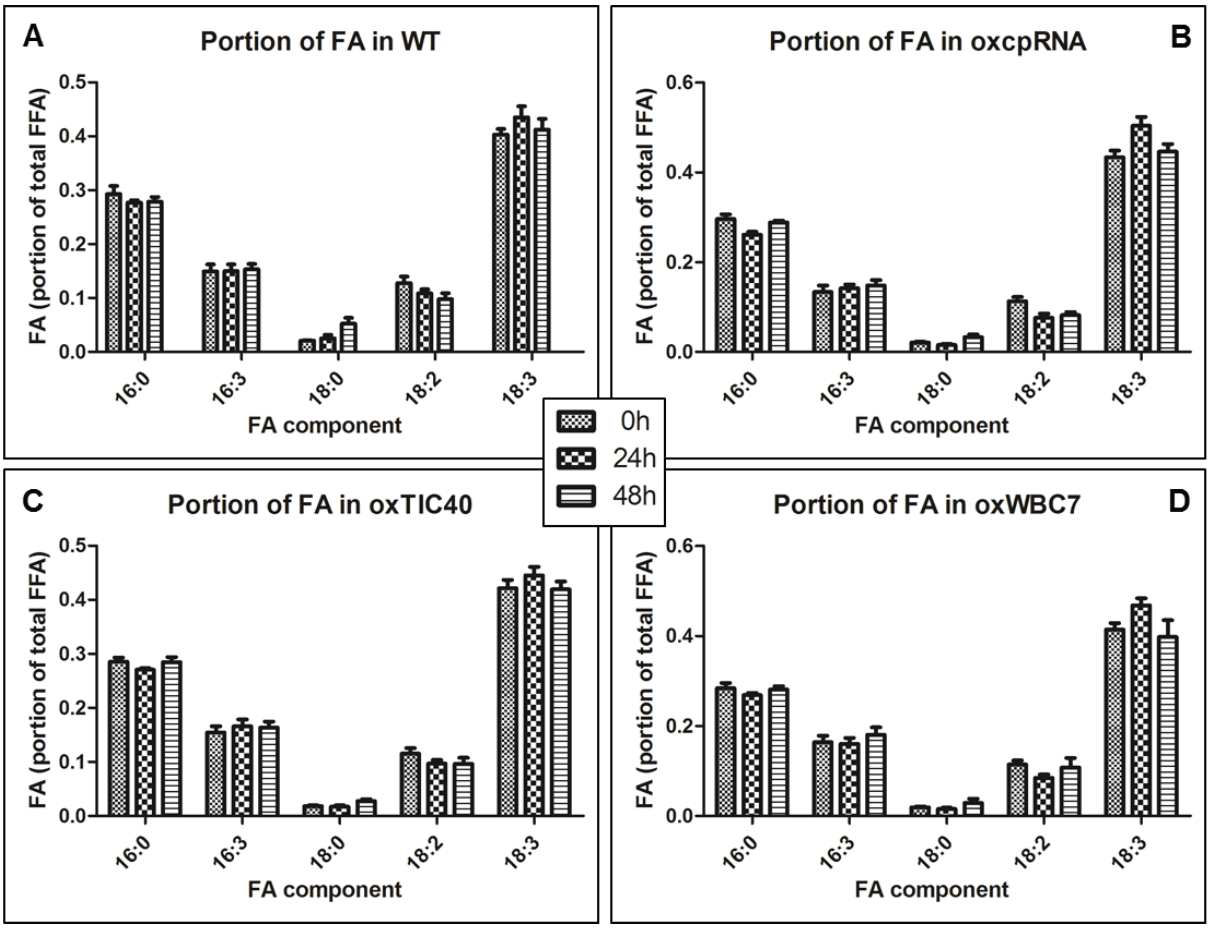

Figure 4: Portion of fatty acid components on total free fatty acid levels subjected to expression time of proteins.

Time-dependent development of major fatty acids in **A)** wild type (WT) plants and in expression line **B)** oxcpRNA, **C)** oxTIC40, and **D)** oxWBC7. Visible changes are statistically not significant.

Processing plant material

Constructs were introduced into *A. thaliana* via the floral dip method (Clough and Bent, 1998) using the *Agrobacteria* strain GV3101/ pMP90 (Koncz and Schell, 1986).Seeds from these transformation events were positively selected on plates containing the antibiotic hygromycin at a concentration of 30 µg / ml. Survivors were screened via PCR at the gDNA level for the insertion of the complete construct, including promoter and GFP. Positive seedlings were grown for an additional four to six weeks. Afterwards, the protein expression was induced in single leaves by

brushing a 20 mM β-estradiol solution on the ventral leaf surface. GFP signal in these leaves were detected via confocal microscopy 24 and 48 hours after induction.

Confocal microscopic analysis

Confocal microscopy was performed on leave slices of *Arabidopsis* using an upright Zeiss LSM 510 META confocal laser-scanning microscope. GFP and chlorophyll were excited by the 488 nm laser line of an Argon laser and the emission was collected at 505-550 nm and at > 650 nm, respectively. Pictures were processed using the LSM Image Browser (Zeiss).

Fatty acid methyl ester (FAME) isolation and analysis

The fatty acid composition of *Arabidopsis* leaves was analyzed via fatty acid methyl esterification followed by GC-TOF detection (adapted protocol from Browse et al., 1986). The fatty acids from triacyl glycerols and membrane lipids were converted to fatty acid methyl esters (FAMEs) by acid catalyzed trans-methylation. Therefore, single leaves were taken from *Arabidopsis*, weighted out and transferred into screw-mountable glass test tubes containing 1 ml 3M methanolic HCl mixed with 10 μg/ml internal C17:0 internal standard for MS analysis. Test tubes were secured with Teflon sealed screw cap. Samples were incubated at 90°C for 60 min in a heating block and afterwards chilled to room temperature. Samples were further processed by adding 1 ml hexane and 1 ml 1% sodium chloride. Samples were vortexed for 10 sec and afterwards centrifuged for 5 min on 2000 rcf. The upper hexane phase containing the FAMEs were carefully removed via a glass Pasteur pipet and transferred into screw cap vials (Agilent Technologies; #5182-0714). For the GC-TOF analysis, samples were diluted to a concentration of 1:10. The detection was performed using Agilent 7890A gas chromatograph coupled to Waters GCT-TOP Premier mass spectrometer equipped with an ALEX (Automatic Liner Exchange) and a MPS2 (Multi-Purpose Sampler) for automatized sampling. Quantification and identification of the detected fatty acids was carried out with QuanLynx and MassLynx V4.1 (Waters) respectively.

Peaks were integrated and the resulting areas used for determination of relative changes in the abundance of fatty acids. Fatty acid quantities were normalized in regard to the internal standard and to the leaf weighted portion. All samples were analyzed in in minimum three biological replicates.

Statistical analysis and graphical follow up

QuanJynx and MassLynx processed data were saved in a Microsoft™ Excel sheet. Data were calculated according to leaf weight and internal 17:0 standard. Afterward, data were transferred to PRISM5.0a (GraphPad, www.graphpad.com/prism /prism.htm) for graphical layout and statistical analysis. Data were analysed via an ANOVA test followed by a Bonferroni posttest to evaluate statistical significance of differences between the data. Data would have been accepted as significantly different at a *P* value of < 0.05.

References

Bedard, J., Kubis, S., Bimanadham, S., and Jarvis, P. (2007). Functional similarity between the chloroplast translocon component, Tic40, and the human co-chaperone, Hsp70-interacting protein (Hip). *J. Biol. Chem.* 282**,** 21404-21414.

Beligni, M., and Mayfield, S. (2008). Arabidopsis thaliana mutants reveal a role for CSP41a and CSP41b, two ribosome-associated endonucleases, in chloroplast ribosomal RNA metabolism. *Plant Mol.Biol.* 67**,** 389-401.

Bleckmann, A., Weidtkamp-Peters, S., Seidel, C.A., and Simon, R. (2010). Stem cell signaling in Arabidopsis requires CRN to localize CLV2 to the plasma membrane. *Plant Physiol* 152**,** 166-176.

Bollenbach, T.J., Sharwood, R.E., Gutierrez, R., Lerbs-Mache, S., and Stern, D.B. (2009). The RNA-binding proteins CSP41a and CSP41b may regulate transcription and translation of chloroplast-encoded RNAs in Arabidopsis. *Plant Mol.Biol.* 69**,** 541-552.

Breuers, F.K.H., Braeutigam, A., Geimer, S., Welzel, U.Y., Stefano, G., Renna, L., Brandizzi, F., and Weber, A.P.M. (2012). Dynamic remodeling of the plastid envelope membranes ? a tool for chloroplast envelope in vivo localizations. *Frontiers in Plant Science* 3.

Breuers, F.K.H., Braeutigam, A., and Weber, A.P.M. (2011). The plastid outer envelope - a highly dynamic interface between plastid and cytoplasm. *Frontiers in Plant Science* 2.

Browse, J., Mccourt, P.J., and Somerville, C.R. (1986a). Fatty acid composition of leaf lipids determined after combined digestion and fatty acid methyl ester formation from fresh tissue. *Anal. Biochem.* 152**,** 141-145.

Browse, J., Warwick, N., Somerville, C.R., and Slack, C.R. (1986b). Fluxes through the prokaryotic and eukaryotic pathways of lipid synthesis in the '16:3' plant Arabidopsis thaliana. *Biochem J* 235**,** 25-31.

Chiu, C.C., and Li, H.M. (2008). Tic40 is important for reinsertion of proteins from the chloroplast stroma into the inner membrane. *Plant J.* 56**,** 793-801.

Clough, S.J., and Bent, A.F. (1998). Floral dip: a simplified method for Agrobacterium-mediated transformation of Arabidopsis thaliana. *Plant J.* 16**,** 735-743.

Fettke, J., Nunes-Nesi, A., Fernie, A.R., and Steup, M. (2011). Identification of a novel heteroglycan-interacting protein, HIP 1.3, from Arabidopsis thaliana. *Journal of Plant Physiology* 168**,** 1415-1425.

Gray, J.C., Hansen, M.R., Shaw, D.J., Graham, K., Dale, R., Smallman, P., Natesan, S.K.A., and Newell, C.A. (2011). Plastid stromules are induced by stress treatments acting through abscisic acid. *The Plant Journal***,** no-no.

Gray, J.C., Sullivan, J.A., Hibberd, J.M., and Hansen, M.R. (2001). Stromules: Mobile protrusions and interconnections between plastids. *Plant Biol.* 3**,** 223-233.

Guidotti, G. (1972). Membrane proteins. *Annu Rev Biochem* 41**,** 731-752.

Hanson, M.R., and Sattarzadeh, A. (2011). Stromules: Recent Insights into a Long Neglected Feature of Plastid Morphology and Function. *Plant Physiol.* 155**,** 1486-1492.

Härtel, H., Dormann, P., and Benning, C. (2000). DGD1-independent biosynthesis of extraplastidic galactolipids after phosphate deprivation in Arabidopsis. *Proc. Natl. Acad. Sci. U. S. A.* 97**,** 10649-10654.

Hodge, A.J., Mclean, J.D., and Mercer, F.V. (1955). Ultrastructure of the lamellae and grana in the chloroplasts of zea mays L. *Journal of Biophysical and Biochemical Cytology* 1**,** 605-&.

Joyard, J., Maréchal, E., Miège, C., Block, M., Dorne, A.-J., and Douce, R. (2004). "Structure, Distribution and Biosynthesis of Glycerolipids from Higher Plant Chloroplasts," in *Lipids in Photosynthesis: Structure, Function and Genetics,* eds. S. Paul-André & M. Norio. Springer Netherlands), 21-52.

Kelly, A., and Dormann, P. (2004). Green light for galactolipid trafficking. *Curr. Opin. Plant Biol.* 7**,** 262-269.

Kohler, R.H., Cao, J., Zipfel, W.R., Webb, W.W., and Hanson, M.R. (1997). Exchange of protein molecules through connections between higher plant plastids. *Science* 276**,** 2039-2042.

Koncz, C., and Schell, J. (1986). The Promoter of Tl-DNA Gene 5 Controls the Tissue-Specific Expression of Chimeric Genes Carried by a Novel Type of Agrobacterium Binary Vector. *Mol. Gen. Genet.* 204**,** 383-396.

Kovacheva, S., Bedard, J., Patel, R., Dudley, P., Twell, D., Rios, G., Koncz, C., and Jarvis, P. (2005). In vivo studies on the roles of Tic110, Tic40 and Hsp93 during chloroplast protein import. *Plant J.* 41**,** 412-428.

Machettira, A.B., Groß, L.E., Tillmann, B., Weis, B.L., Englich, G., Sommer, M.S., Köniğer, M., and Schleiff, E. (2012). Protein induced modulation of chloroplast membrane morphology. *Frontiers in Plant Science* 2.

Maréchal, E., Block, M.A., Dorne, A.J., Douce, R., and Joyard, J. (1997). Lipid synthesis and metabolism in the plastid envelope. *Physiol. Plant.* 100**,** 65-77.

Mcfarlane, H.E., Shin, J.J., Bird, D.A., and Samuels, A.L. (2010). Arabidopsis ABCG transporters, which are required for export of diverse cuticular lipids, dimerize in different combinations. *Plant Cell* 22**,** 3066-3075.

Moellering, E.R., Muthan, B., and Benning, C. (2010). Freezing tolerance in plants requires lipid remodeling at the outer chloroplast membrane. *Science* 330**,** 226-228.

Ohlrogge, J., and Browse, J. (1995). Lipid biosynthesis. *Plant Cell* 7**,** 957-970.

Palade, G.E. (1953). An electron microscope study of the mitochondrial structure. *J Histochem Cytochem* 1**,** 188-211.

Schleiff, E., Eichacker, L.A., Eckart, K., Becker, T., Mirus, O., Stahl, T., and Soll, J. (2003). Prediction of the plant beta-barrel proteome: A case study of the chloroplast outer envelope. *Protein Science* 12**,** 748-759.

Schnurr, J.A., Shockey, J.M., De Boer, G.J., and Browse, J.A. (2002). Fatty acid export from the chloroplast. Molecular characterization of a major plastidial acyl-coenzyme A synthetase from Arabidopsis. *Plant Physiol.* 129**,** 1700-1709.

Seigneurin-Berny, D., Gravot, A., Auroy, P., Mazard, C., Kraut, A., Finazzi, G., Grunwald, D., Rappaport, F., Vavasseur, A., Joyard, J., Richaud, P., and Rolland, N. (2006). HMA1, a New Cu-ATPase of the Chloro plast Envelope, Is Essential for Growth under Adverse Light Conditions. *J. Biol. Chem.* 281**,** 2882-2892.

Singh, N.D., Li, M., Lee, S.B., Schnell, D., and Daniell, H. (2008). Arabidopsis Tic40 Expression in Tobacco Chloroplasts Results in Massive Proliferation of the Inner Envelope Membrane and Upregulation of Associated Proteins. *Plant Cell* 20, 3405-3417.

Yamasaki, K., Motomura, Y., Yagi, Y., Nomura, H., Kikuchi, S., Nakai, M., and Shiina, T. (2013). Chloroplast envelope localization of EDS5, an essential factor for salicylic acid biosynthesis in Arabidopsis thaliana. *Plant Signal Behav* 8.

Addendum 2: The plastid outer envelope protein OMP24 – A novel putative pore?

Status: **unpublished** (2013)

Authors: **Frederique K.H. Breuers, Nadine Schwarz, Peter Jahns, and Andreas P.M. Weber**

1. Author

Own contribution: 90%

- Experimental design
- Preliminary experiments
- Data elicitation and selection
- Writing the manuscript

Abstract

The plastid outer envelope (OE) possesses quite wide transport ability for metabolites. This is facilitated by a few transport pores interspersing the membrane. While four of these pores are known, the existence of additional pores is certain. The 24 kDa OE protein of spinach (SoOMP24), for example, is a putative novel pore. Its high abundance in spinach chloroplasts points to a dominant role in plants. Furthermore, some biochemical similarities if not necessarily the sequence similarity between SoOMP24 and the known PsOEP24 indicate a role in transport across the OE. However, while the *Arabidopsis* homolog AtOMP24 presents similar properties, it is less abundant and mainly expressed during early seedling development and seed drying. A bioinformatics analysis of the structural features of both proteins found two α-helical areas, of which one is located in the common area of both, SoOMP24 and AtOMP24. Results of CD spectrometric analyses supported the presence of α-helical structures. Functional investigations of the proteins via a yeast complementation assay to test for transport activity of the proteins was inconclusive due to interference from the vector backbone. Therefore, the transporter hypothesis could not be confirmed. Conclusively, the results provide strong evidences for structural and functional equality of the *Arabidopsis* and spinach protein. However, the function remains unsolved.

Introduction

The plastid outer envelope (OE) was thought to be a molecular sieve for molecules larger than 10 kDa. The exploration of high abundance pore forming proteins in the OE rejected this view (Pohlmeyer et al., 1997; Flügge, 2000; Soll et al., 2000). The four known OE pores (OEPs) – classified by their molecular size as OEP16 (Pohlmeyer et al., 1997), OEP21, OEP24 (Pohlmeyer et al., 1998), and OEP37 (Schleiff et al., 2003) – were initially identified in *Pisum sativum* (Ps; pea). Later, the investigations of these proteins was extended to other plants, including the model plant *Arabidopsis*

(compare Duy et al., 2007). Examination of the transport pores in these species might extend the understanding of the OE transport ability.

The pore with the broadest transport function in the OE is PsOEP24. It facilitates transport of TP, hexose-phosphates, sugar, ATP, Pi, dicarboxylates and charged amino acids (Pohlmeyer et al., 1998). This transport ability paired with the high abundance in the OE of pea resulted in the expectation that OEP24 also would be a major transporter in other plants. Homologs of this protein were found in the model plant *Arabidopsis thaliana* (AtOEP24s; Duy et al., 2007) and in other sequenced plant species. However, the AtOEP24s show overall low expression in whole plant tissue (Figure 2 B and C, Winter et al., 2007); a fact conflicting with the picture of the vital 'everything transporter'. Even though, the three other known pore-forming OEPs are found in *Arabidopsis*, the low abundance of the OEP24 suggests the need of additional transporters.

A study on spinach revealed a highly abundant protein in the OE named E24 or OMP24 (outer membrane protein of 24 kDa; *here*: SoOMP24; Joyard et al., 1983; Fischer et al., 1994). While it does not show any sequence similarity to the OEP24 proteins, it shows similarity in the biochemical properties. Like the known pea transport pore, the spinach protein presents approximately 50% hydrophobicity and is resistant to proteolysis – evidence for integral membrane proteins (Fischer et al., 1994). Abundance and biochemical properties led to the hypothesis, that SoOMP24 is

```
SoOMP24 MAEGQHTTAVTTGNPEASRQEQNNPFFFLSLIPKFLLQPFNNIKNKGDSEKSVKRVDGEE
AtOMP24 MAEEAQVD--RSNGSDSSSPPIKLPPFITNLFAFLQPKPP-----PATIDANAPKPTGEK
        ***  :.    :...::*    : * *: .*:. :  :*       .  : .. :  **:

SoOMP24 GSGSYTKTPDVVRFPATQP-EVAPLKLENE-DAQEDTNPLILWQIYALGGFIVLKWAWGK
AtOMP24 EP--LKSTYETVTFPYNPPKSAEPIKFEAEPSSGRTSNSVILWQVYALGGFLVLKWAWAR
         .   ..* :.* ** . * .. *:*:* * .: . :*.:****:******:******.:

SoOMP24 WQERKANNG---SSGEDQPQPPPSATAPAPAED-
AtOMP24 WNERNERSDKKEATGDDDQKDDDEDDQSSDGHED
        *:**: ...   ::*:*: :   .   .: ..:
```

Figure 1: Alignment of SoOMP24 and AtOMP24

Closest similarity between SoOMP24 and AtOMP24 exists in the area of amino acid 90 to 120 (bar).

a transport pore, and potentially similar in function to OEP24. However, the structure and function of SoOMP24 remain unknown.

To investigate SoOMP24 and the hypothesis that this protein is a transport pore, the following study takes the approach for a functional analysis following the investigators of PsOEP24 (Röhl et al., 1999). Furthermore, the first steps into the structural elucidation of OMP24 proteins were taken via circular dichroism (CD) spectroscopy.

Results and Discussion

Screening for homologs with higher potential for genetic analysis

Spinach is unsuitable to investigate a proteins' function with genetic methods, since it is un-sequenced. Therefore, an *in silico* screen was performed to find homologs of SoOMP24 in a more suitable species, preferably *Arabidopsis*. Overall, the screen resulted in only a few homologs in sequenced plants (Supplemental Figure 1). However, an *Arabidopsis* protein could be found, presenting 47% sequence identity to the spinach protein. Therefore, the protein, encoded at locus At3g52230, was named AtOMP24. The most conserved region was found in the area of the amino acids 90 and 120 (Figure 1). In a bioinformatics analysis, this area was also predicted to contain secondary structure elements (compare Figure 9, red bars), indicating a functional relevance of this area.

SoOMP24 and AtOMP24 are OE proteins

To postulate that both proteins are OE transporters, the localization of the proteins needed to be verified. Therefore, C-terminal GFP (green fluorescent protein) tagged versions of these proteins were transiently expressed in tobacco leaves. Life cell imaging analysis of transformed cells via confocal microscopy revealed that the expression of SoOMP24-GFP resulted in fluorescence in close proximity to the chloroplasts. Besides circular structures, covering the plastids, out-looping

protrusions could also be detected (Figure 2 A). Similar structures could be observed for AtOMP24-GFP (Figure 2 B). These labeling patterns are typical for over-expressed OE proteins (Breuers et al., 2012, Machettira et al., 2012) and so verified the localization of SoOMP24 and AtOMP24 to the OE.

The OMP24 pair shows comparative relationship to OEP24 triplet

While SoOMP24 was shown to be an abundant OE protein in green tissue (Joyard et al., 1983; Fischer et al., 1994), AtOMP24 showed a relatively low expression profile in whole plant tissue, but peaked to a level of 2500 absolute count in expression during the late seed development and in dry seeds (Figure 3 A).

If one compares these findings to the transport pore of pea, PsOEP24 and its *Arabidopsis* homologs, intersections can be found. The pea protein is one of the most abundant proteins in the chloroplast OE (Pohlmeyer et al., 1997). Contrastingly, AtOEP24.1 and AtOEP24.2 (Figure 3 B and C) show only low overall expression in *Arabidopsis*. However, the distinct expression pattern in developmental tissue, like

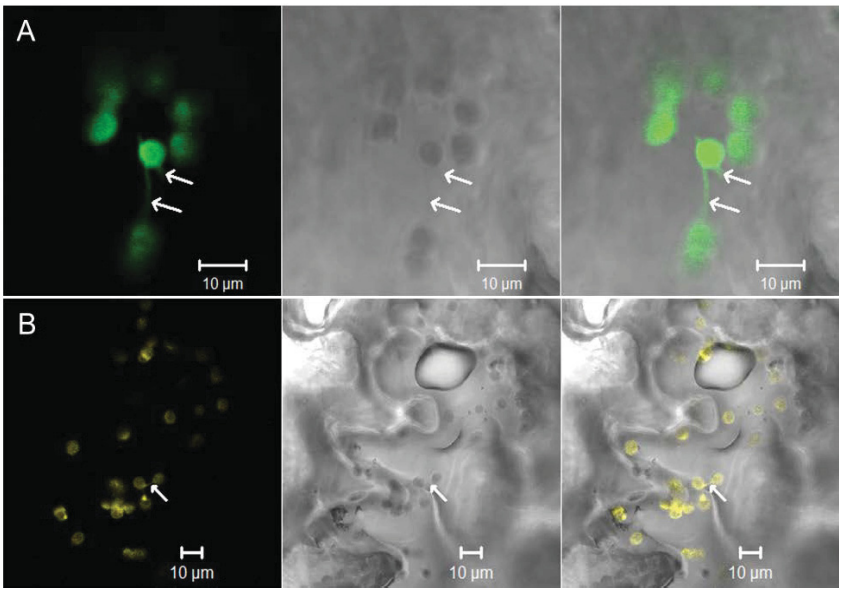

Figure 2: Life cell imaging to localize OMP24 to the OE

A) SoOMP24-GFP covers chloroplasts but also display thin protrusions (white arrows) extending from the chloroplasts**. B)** AtOMP24-GFP surrounds chloroplasts and protursions extending from the plastids (white arrow). From the left to the right: GFP fluorescence, brightfield, merged picture.

seeds and early seedling stages (AtOEP24.1) or seeds and shoot apex (AtOEP24.2), indicate a role in plant development. Even though, no primary results were published about these proteins, Duy et al. (2007) noted that PsOEP24 homologs in *Arabidopsis* were necessary for pollen germination or late seed development. Furthermore, Duy et al. (2007) stated that the *Arabidopsis* proteins fulfill the same processes as the pea protein except that it is performed at a different developmental stage. The similarity between the demonstrated parameters of the OEP24 triplet and the OMP24 pair permits the intuitive assumption of functional similarity between OEP24 and OMP24.

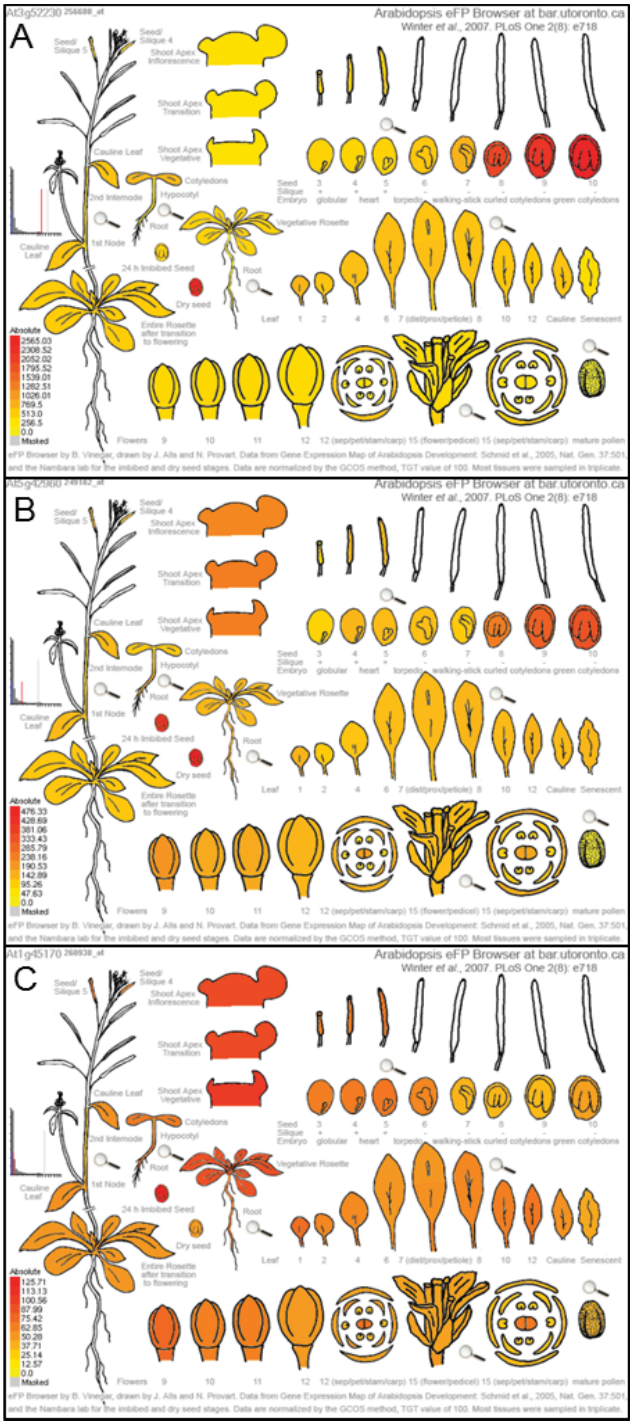

Figure 3: Overall low expression levels of AtOMP24 and AtOEP24s according to the efp-browser (Winter et al., 2007)

A) Expression levels of AtOMP24; red color indicates highest expression level in late seedling development and in dry seeds. Maximal absolute expression count: ~2560. B) Expression levels of AtOEP24.1; red color indicates highest expression in late seedling development and in seeds. Maximal absolute expression count: ~480 C) Expression levels of AtOEP24.2; red color indicates highest expression in shoot apex and seeds. Maximal

Reverse genetics analysis on AtOMP24 KO lines

To take the first steps in the functional analysis of the protein the T-DNA insertion Gabi_Kat line

226C05 was ordered, grown and analyzed for homozygosity. This line carried a T-DNA insertion in the second exon of the AtOMP24 gene at position 330 base pairs of the coding sequence (Figure 4 A). While this insertion might not result in a complete lack of the protein production, the insertion inside the predicted structural element (compare Figure 9) was expected to seriously interfere with the protein function.

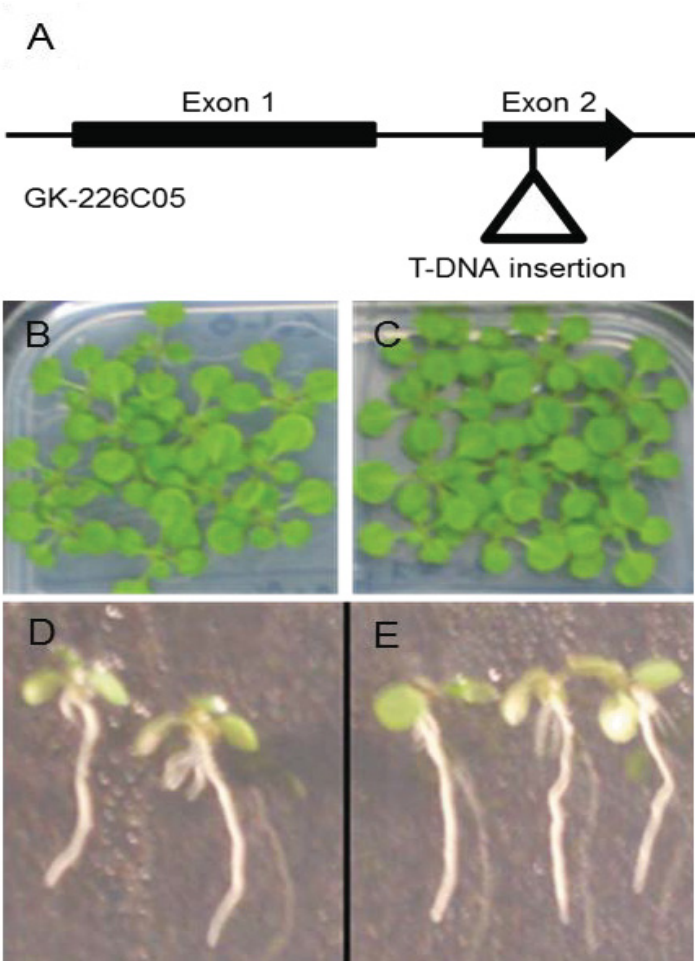

Figure 4: GK-226C05 insertion line in comparison to WT plants

A) Scheme of the T-DNA insertion in GK-226C05. **B) and D)** Columbia-0 wildtype (Wt) plants and **C) and E)** GK-226C05 mutants grown on ½ MS plates.

Even though, homozygous lines could be detected, no aberrant visual phenotype could be observed for the T-DNA insertion lines (Figure 4 C) in comparison to WT plants (Figure 4 B). Based on the highest expression signals in dry seeds and early seedlings a focused analysis was performed on the early developmental stages of seedlings. However, neither cotyledon not root showed a delay in development or organ deformation in mutants (Figure 4 E) compared to the WT control plants (Figure 4 D). These results indicate that AtOMP24 is not vital for plant development under standard growth conditions or that its function can be covered by another protein. However, the results did not provide new insights into the function of the protein.

Heat stress and unfavorable carbon source dictate mutant growth

Still the hypothesis remained that OMP24 proteins are candidates for transport pores like PsOEP24, so the procedure used by the investigators of PsOEP24 was followed up. Röhl et al. (1999) described that PsOEP24 functionally complemented the mitochondrial outer membrane VDAC1 channel in yeast. The ΔVDAC1 mutants did not grow on minimal yeast medium containing glycerin as sole carbon source at a temperature of 37°C (Blachly-Dyson et al., 1997). However, transformation with PsOEP24 restored growth of this mutant to WT level (Röhl et al., 1999).

In this study, the yeast deletion strain Y17374 (Euroscarf) was used as the ΔVDAC1 mutant and analyzed for the described growth defect. While this strain did not show any deficiency in growth when supplied with glucose and incubated at 30°C (Figure 5 A), stress conditions affected the mutant yeast strain. Mutant growth was already slightly impaired, when it was grown on 37°C (Figure 5 B). However, this effect became more pronounced when glycerol was the sole carbon source. While the mutant was still able to grow at 30°C (Figure 5 C), no growth could be detected when

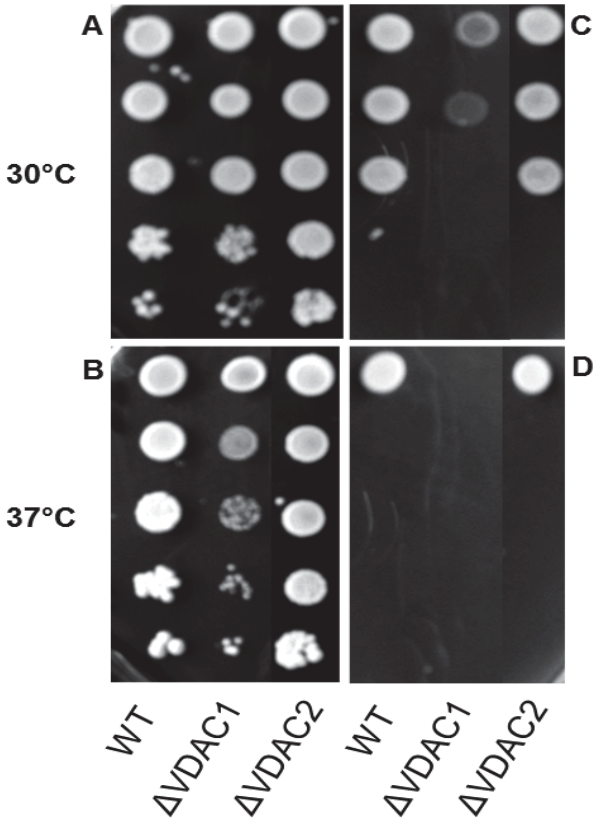

Figure 5: Drop-test to investigate growth of mutant yeast strains

Each picture **A) to D)** line up the drop tests for the WT stain, ΔVDAC1 mutant strain and ΔVDAC2 mutant strain from the left to the right. **A) and B)** display growth of the strains on minimal medium with 2% glucose as carbon source at 30°C and 37°C, respectively. **C) and D)** display growth of the strains on minimal medium with 2 % glycerol as sole carbon source at 30°C and 37°C, respectively. Drop concentration form top tp the buttom: OD_{600} = 3; 1:10; 1:100; 1:1000; 1:10000.

the mutant was grown at 37°C (Figure 5 D). Due to the also strongly impaired growth of the control strains at 37°C (Figure 5 D), complementation experiments were performed at 30°C and when glycerol was the sole carbon source (Figure 5 C).

The mutant defective in the second yeast VDAC, ΔVDAC2 (strain Y12273; Euroscarf), was also analyzed. It was described that a lack of VDAC2 only led to a growth defect in ΔVDAC1/ΔVDAC2 double mutant but displayed WT growth in single mutants (Blachly-Dyson et al., 1997). Similarly, in this study ΔVDAC2 displayed the described WT growth phenotype under all tested conditions (Figure 5). Therefore, it was used as a positive growth control in exchange for the WT strain, when geneticin was used as antibiotic in the growth media.

Vector backbone interferes with the complementation assay

To investigate whether OMP24 proteins fulfill the function of the VDAC1 channel, transformed ΔVDAC1 mutants were grown for seven days at 30°C using glycerol

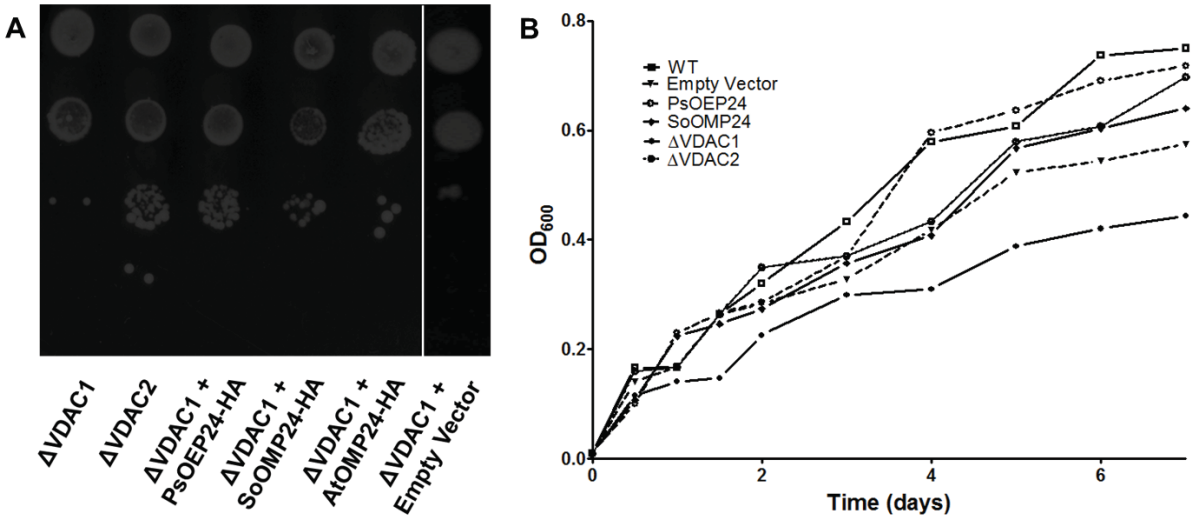

Figure 6: Yeast complementation study

A) Yeast drop-test on minimal medium containing 2% glycerol as sole carbon source. Line 1 and 2 display untransformed mutant strains ΔVDAC1 and ΔVDAC2, respectively. Lines 3 to 5 demonstrate growth of mutant ΔVDAC1 transformed with constructs for PsOEP24, SoOMP24, AtOMP24 expression, respectively. Line 6 displays growth of ΔVDAC1 with the empty vector backbone pAG426GPD-ccdB-HA. B) Growth curves for the in A) described lines in liquid minimal medium with 2% glycerol s single carbon source.

containing minimal medium. The mutants transformed with SoOMP24, AtOMP24, and the positive control PsOEP24 in the yeast expression vector pAG426GPD-HA, led to a slight improvement of yeast growth (Figure 6 A). Nevertheless, none of the proteins restored growth to WT levels. ΔVDAC1 mutants transformed with the empty vector pAG426GPD-ccdB-HA displayed no improvement in growth on minimal media plates, indeed the colonies appeared to be slightly sicker than the mutant ones (Figure 6 A).

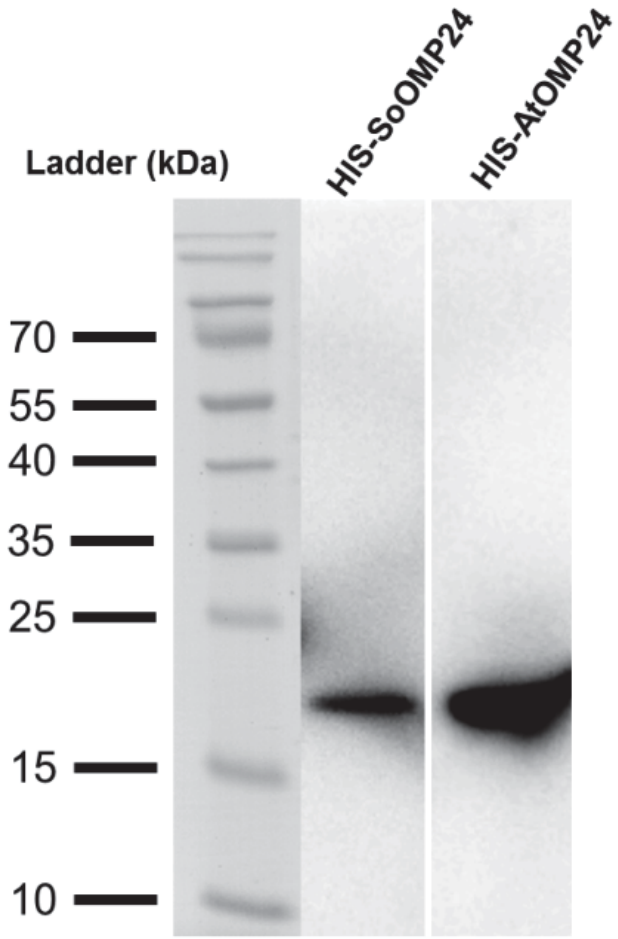

Figure 7: Immunoblot of heterologous expressed HIS-tagged OMP24 proteins

Immuno-detection via HIS-antibody identified a band in a height of approximately 22 kDa for both proteins AtOMP24 and SoOMP24.

To confirm the drop test data semi-quantitatively, liquid cultures were inoculated, grown at 30°C for 7 days and evaluated every day. In these liquid cultures, complementation with PsOEP24 resulted in a WT like growth rate. While SoOMP24 complementation also resulted in enhanced growth compared to the ΔVDAC1 mutant, the growth rate did not reach WT levels. Besides, the empty vector carrying mutant strain grew better than the ΔVDAC1 strain (Figure 6 B), even though it grew slightly slower than the other transformants. These results indicate an impact of the vector backbone on yeast growth, interfering with the system to test the hypothesized protein function of the

OMP24 proteins. Therefore, the transport pore hypothesis must not be rejected but further investigated.

OMP24 proteins show discrepancy in calculated and experimental size

Since the structure of the proteins could allow inferences on the function, N-terminal HIS-tagged SoOMP24 and AtOMP24 were heterologously expressed in *E.coli* cells. Proteins were isolated and fractionated to detect their localization in the *E. coli* cells. The heterologous protein was localized to the cytosolic fraction (Supplemental Figure 2). Furthermore, the observations revealed that the described size of 24 kDa (Joyard et al., 1983) could not be reached. For both proteins, the calculated size was approximately 16 kDa. This result was consistent with the published result that SoOMP24 run higher on a SDS page (Joyard et al., 1983; Fischer et al., 1994). Fischer et al. (1994) demonstrated that authentic SoOMP24 exhibits a size of 21.2 kDa or 23 kDa when tagged with HIS residues. In this study a size of approximately 22 kDa could be observed for both HIS tagged proteins (Figure 7), verifying the previous data (Fischer et al., 1994). In addition, these results demonstrated that, while AtOMP24 and SoOMP24 show only 47% sequence identity, both possess similar abnormal amino acid compositions, leading to an abnormal flow level on a gel. This abnormal run furthermore indicates the proteins remain secondary structure, even under denaturing conditions.

Purification of OMP24 proteins expose potential for polymerization

Processing the HIS-AtOMP24 protein suspension through a Ni-NTA column resulted in highly concentrated HIS-tagged protein of approximately 22 kDa in the first elution fraction (Figure 8 A). Subsequently, the fraction was gel-filtrated, using an ÄKTA Prime system (GE Healthcare), intending to reduce potential contaminations of far lighter and far heavier proteins. The chromatogram detected that the majority of proteins flowed faster through the filtration column than expected for a 22 kDa sized protein (Supplemental Figure 3 A), yet a subsequent SDS page analysis of the

respective fractions revealed a high abundance of the 22 kDa protein (Supplemental Figure 3 B).

Similar results were found for the HIS-SoOMP24. The first Ni-NTA elution fraction contained the approximately 22 kDA sized protein (Figure 8 B). This fraction was processed through a Centricon (Milipore) with a 30 kDa cutoff, to clean the 22 kDA protein from larger sized contaminations and to concentrate the protein. However, subsequent SDS page analysis of the resulting fractions arise that the 22 kDa sized protein remained in the upper part of the Centricon (Supplemental Figure 4), indicating an aggregation of the protein in the not-denaturing settings. Since this aggregation also took place in presence of high concentrations of sodium cholate, the interaction between the aggregating proteins might be rather specific. If so, the aggregation could be polymerization with critical impact on protein function. Supporting this hypothesis, a 16 kDa (or even 22 kDA) sized protein could not build a transport pore as a single protein (Pohlmeyer et al., 1997). Therefore, a homo-dimerization would be an advantage in building such a pore, as was described for the amino acid pore OEP16

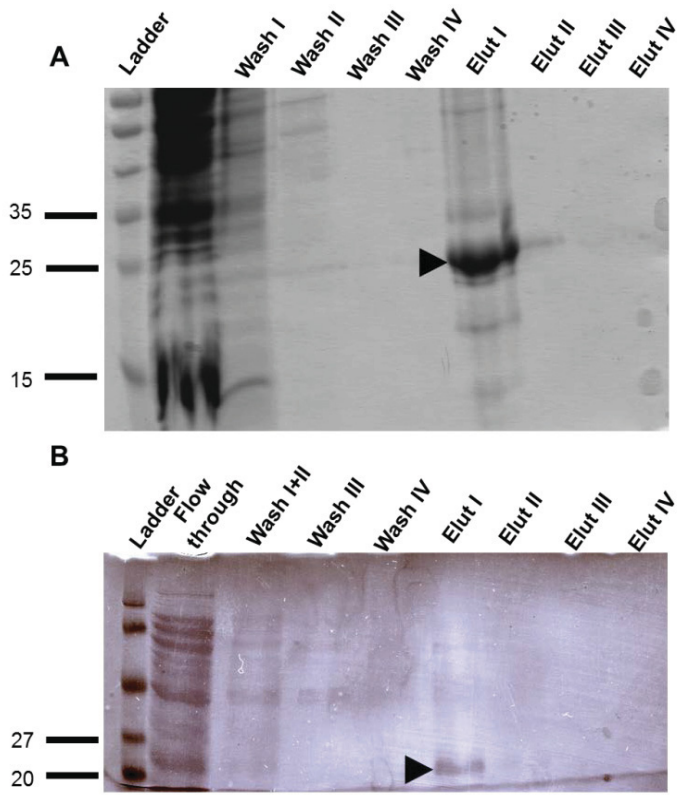

Figure 8: SDS page of Ni-NTA processed HIS-tagged OMP24 proteins

A) Commassie gel for Ni-NTA purification of HIS-AtOMP24 resulting in high concentrated 22 kDa protein in the first elution fraction (arrowhead).B) Commassie gel for Ni-NTA purification of HIS-SoOMP24 resulting in high concentrated 22 kDa protein in the first elution fraction (arrowhead).

(Pohlmeyer et al., 1997; Steinkamp et al., 2000; Linke et al., 2004). However, the polymerization hypothesis should be investigated further via two-dimensional gel electrophoresis, since the aggregation does not present a valid proof for polymerization.

Even though, the aggregation interfered with the purification process, highly concentrated protein solutions were obtained. These solutions were dialyzed to exchange the elution buffer to 50 mM sodium phosphate buffer for the further CD spectrometric analysis.

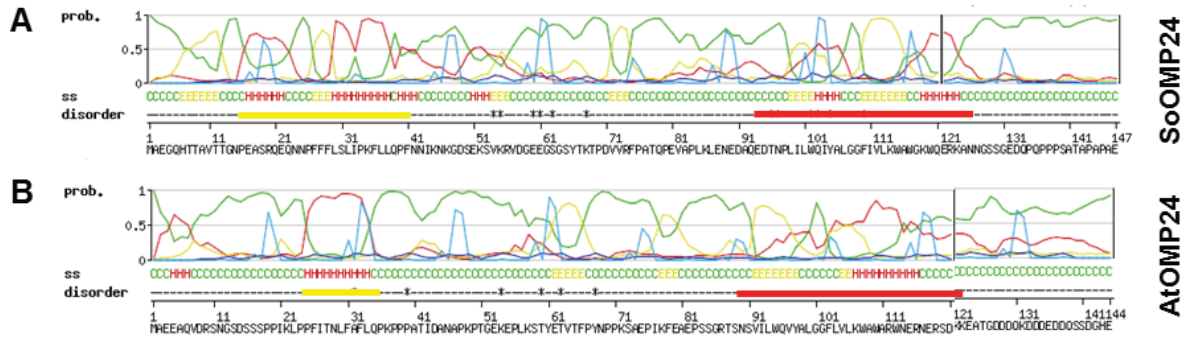

Figure 9: Bioinformatical analysis of OMP24 protein sequences for secondary structural elements by InterProScan

A) Analysis of SoOMP24 protein sequence and **B)** analysis of AtOMP24 protein sequence display secondary structural elements random coil (C), β-sheet (E), and α-helices (H). Both proteins display structural elements at the N-terminus (yellow bars) and at the C-terminus (red bars.

CD spectrometric analysis

Preliminary bioinformatics secondary structure analysis via InterProScan (Zdobnov and Apweiler, 2001) revealed a high proportion of random coiled areas in both proteins (Figure 9). However, the structural elements β-sheets and α-helices were also predicted by the program, especially in the most similar region between both proteins (amino acids 90-120; Figure 9 red bars). The nature of these structures was not clear, since both β-sheets and α-helices are indicated by the program in comparable amounts in this area. Besides, both proteins displayed potential for α-

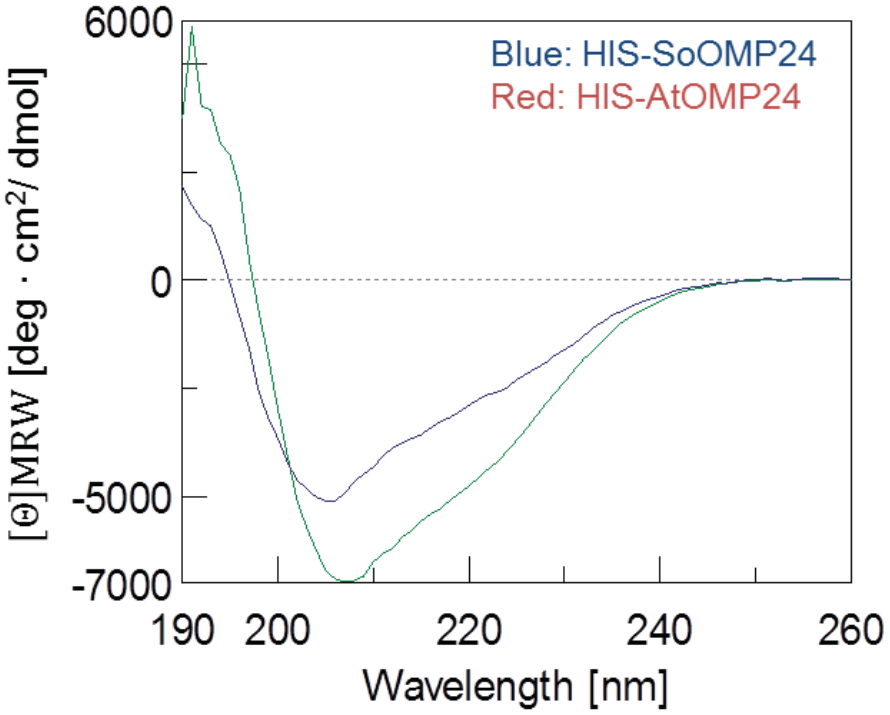

Figure 10: CD spectrometric analysis of HIS-tagged OMP24 proteins

The blue line demonstrates the spectrum of heterologous expressed HIS-tagged SoOMP24 protein in 50 mM NaPi buffer. The red line demonstrated the spectrum of heterologous expressed HIS-tagged AtOMP24 protein in 50 mM NaPi buffer. Both spectra display a minimum at 209 nm and a maximum at 190 nm.

helical structures in the N-terminal region of SoOMP24 (Figure 9 A, yellow bar) and on a smaller scale for AtOMP24 (Figure 9 B, yellow bar). To deepen the information, a first biophysical analysis via CD spectrometry was performed on the heterologous expressed N-terminal HIS tagged SoOMP24 and AtOMP24.

Both protein spectra showed local maxima at a wavelength of approx. 190 nm and a local minimum at approx. 209 nm (Figure 10). These ware defining parameters for α-helical protein structures (Kelly et al., 2005). However, both spectra were lacking in the typical second local minimum of α-helical proteins at 222 nm. This lack could be explained by the high portion of random coiled areas in the protein. This structural element presents local maxima at 212 nm and local minima at 195 nm. The maximum of the random coil could interfere with the minimum typical for the α-helix. Beside this graphical score, bioinformatics evaluation of the spectrometric data with the

K2D3 tool (Kelly et al., 2005; Louis-Jeune et al., 2012), identified the proteins to >91% as α-helical (Supplemental Figure 5).

Conclusive statements and future perspective

This study allows three clear statements about the OMP24 proteins. First, the proteins are both outer envelope proteins. Second, both proteins show abnormal running properties on SDS gels, indicating strong secondary structural elements. And third, the secondary structure of both proteins is α-helical. However, the transport pore hypothesis could neither proven nor disproven. The data of the complementation assay were not conclusive, since the vector backbone influenced the experiment. Furthermore, the growth analysis of the *Arabidopsis* mutants indicate no vital function of the protein on the plant – at least not under standardized growth conditions.

In opposition to the pore hypothesis is the fact that the large majority of the known broad spectrum transport pores in eukaryotes as well as prokaryotes are β-barrel formed (reviewed in Duy et al., 2007). Only a small portion display α-helical structure, such as the OEP16 protein (Pohlmeyer et al., 1997; Linke et al., 2004). Notable, this protein displays not a broad, but rather a specific transport activity for amino acids (Pohlmeyer et al., 1997, 1998) and so, is an exception among the OE transporters.

Particularly, the resistance against denaturing conditions, indicated by the SDS page analysis and the abnormal composition of amino acids might be contrary to the pore hypothesis. The assumption that the polarity index of 49% point on a pore forming feature, may need to be rejected in favor of another hypothesis. Amphipathic α-helices can present the same polarity distribution. While hydrophobic amino acids are orientated to the one side of the helix, polar residues form the other side. This kind of protein structure allows the protein to embed into a membrane without spanning it. Known for containing amphipathic α-helical areas are the dehydrins

(reviewed in Close, 1996) and LEA (late embryogenesis abundant) proteins. These proteins provide resistance against stress to cell compartments of plants (and invertebrates (eg. Browne et al., 2002)). The predicted 51 LEA proteins in Arabidopsis are predominantly abundant in seeds but also in every other plant tissue, especially, when stress is provided (Hundertmak and Hincha, 2008). A recent study on the mitochondrial LEA protein LEAM also demonstrated that it provides desiccation tolerance to plant seeds (Tolleter et al., 2010).

The expression profile of the AtOMP24 demonstrates the strongest levels of expression in dried seeds and at developmental stages, when the seeds change from internal to external resource supply (compare Figure 3a). Even though, the sequence of AtOMP24 and LEA proteins does not show sequence similarity, expression profile and properties are comparable. Therefore, it is tempting to speculate, that the OMP24 proteins provide stress tolerance to the plant by structural protecting the plastid OE. A focused analysis on the germination efficiency of *atomp24* mutant seeds and an analysis of the effects of stress conditions on germinating seeds might lead to supporting results for this hypothesis. Further, an analysis of the effect of heterologously expressed SoOMP24 and AtOMP24 on the stability of liposomes as performed by Tolleter et al. (2010) would help to evaluate the hypothesis that OMP24s are LEA-like OE protectors.

Material and Methods

Cloning of OMP24 genes for complementation

The Gateway system compatible vector pAG426GPD-ccdB-HA from the Linquist Lab was used to investigate the function of the SoOMP24 and AtOMP24 via a yeast complementation approach (Alberti et al., 2007). To produce appropriate templates for the amplification of the target genes, RNA was isolated from leaves of spinach and *A. thaliana*, and cDNA synthesis were performed via SuperScript® III reverse transcriptase (Invitrogen). Gateway compatible attB-sites were introduced into the

amplicons using the forward primer 5′-ggggACAAGTTTGTACAAAAAAGCAGGC TccaccATGGCTGAAGAAGCTCAAGTAGATC-3′ and the reverse primer 5′-ggACCACTTTGTACAAGAAAGCTGGGTcGTCTTCATGCCCATCAGATGATT-3′ for AtOMP24, and the forward primer 5′-ggggACAAGTTTGTACAAAAAAG CAGGCTccaccATGGCAGAAGGACAACACACC-3′ and the reverse primer 5′-ggAC CACTTTGTACAAGAAAGCTGGGTcATCTCAGCTGGAGCAGGG-3′ for SoOMP24. Cloning of the genes was performed via the Gateway® system using pDONR207 as the Entry vector, BP clonase mix II (Invitrogen; 75 µg pDONR207, 75 µg amplicon and 0.5 µl BP clonase mix II) for the BP reaction, and LR clonase mix II (75 µg Destination vector, 75 µg Entry vector and 0.5 µl LR clonase mix II) for the final reaction. Final vectors were sequenced and used in the complementation study.

For the control PsOEP24, RNA was isolated from four week old *Pisum sativum* plants. cDNA synthesis, amplification and cloning of PsOEP24 was processed as described for OMP24 genes. For the amplification the primers 5′- ggggACAAGTTTGTACAAA AAAGCAGGCTccaccATGAAGGCCGCTTTGAAGGGC-3′ (forward) and 5′-ggACC ACTTTGTACAAGAAAGCTGGGTCATCTCAAAATTCAATGTGG-3′ (reverse) were used.

Cloning of OMP24 genes for recombinant protein expression

A restriction enzyme and ligase based cloning approach was used to transfer AtOMP24 and SoOMP24 into the *E. coli* protein expression vector pET15b (Novagen). cDNA of spinach and *Arabidopsis* was used as template for PCR amplification of the genes using Fusion DNA polymerase. A BamHI cutting site was introduced with the forward primers 5′-CACACCATATGGCTGAAGAAGCTCAAGTAGATC-3′ for AtOMP24 and 5′-CACACCATATGATGGCAGAAGGACAACACACC-3′ for SoOMP24. An NdeI cutting site was introduced with the reverse primers 5′-CACACGGATCCGTCTTCATGCCCATCAGATGATT-3′ for AtOMP24 and 5′-CACACGGATCCATCCTCAGCTGGAG CAGGG-3′ for SoOMP24. Amplicons were ligated into the sub-clone vector pJet1.2 for propagation. Inserts were cut out and

ligated into pET15b. Selection was processed on LB plates containing 0.1 mg/ml Ampicillin. Resulting vectors were transformed in chemo-competent *E. coli* cells of the BL21DE strain for protein expression.

Yeast complementation

The yeast strains ΔVDAC1 (Y17374; Euroscarf), ΔVDAC2 (Y12273; Euroscarf), and wildtype (Y10000; Euroscarf) were transform with the complementation constructs using the lithium acetate method (compare Schiestl and Gietz, 1989). Selection were performed on uracil lacking drop out plates (SD uracil) and grown for 3-4 days at 30°C. Drop tests were performed using overnight liquid cultures, washed with water, and used in a concentration of OD_{600} of 3. Dilutions from 1:10 to 1:10000 were dropped on plates and grown for 3 days (glucose plates, 30°C) or 7 days (glycerol plates, 30°C). Growth analyses of liquid cultures were started by inoculating media to an OD_{600} of 0.01. Cultures were grown for 3 to 5 days and sampled from every 1.5 to 12 hours.

Expression and purification of recombinant SoOMP24-HIS and AtOMP24-HIS

Proteins were expressed using BL21DE cells carrying either plasmids SoOMP24/pet15b or AtOMP24/pET15b. The expression was carried out at 37°C. Initially, overnight cultures were diluted to an OD_{600} of 0.1 and incubated until they reached an OD_{600} of 0.6. Expression was induced by adding 1 mM IPTG to the culture. Cultures were grown for additional 5 h. Cells were harvested by centrifugation at 5000 rcf and 4°C for 20 min. Cell pellet was washed by resuspending in ddH_2O and finally resuspended in 4 ml/g pellet lysis buffer (20mM sodium phosphate buffer, pH 7.4; cOmplete EDTA-free protease inhibitor (1 tablet per 50 ml; Roche); 1% Triton X-100; 1 mg/ml Lysozym (Sigma-Aldrich; #L7651); 0.1 mg/ml DNAse I (AppliChem; #A3778)). Lysis reaction was incubated for 30 min on room temperature under constant shaking. Suspension was sonicated 3x 45 sec on ice and afterwards processed 2 to 3 times through a FrenchPress® system (Thermo

Fischer; Pressure: 1500 bar). Cell lysate was centrifuged for 30 min (40000 x rcf, 4°C) and supernatant was transferred on a 5 ml Ni-NTA column (Qiagen; #30210) and processed via gravity flow. Column was washed subsequently with 5 ml B1 (40mM Tris-HCl, pH 8.0; 300mM NaCl + 1% Triton X-100); 5 ml B2 (40mM Tris-HCl, pH 8.0; 300mM NaCl + 50mM NaCholate), and 10 ml CV B3 (B2 + 10mM Imidazole). To elute the histidine tagged protein from the Ni-NTA column, the column was washed four times with 5 ml elution buffer 1 (EB1; B2 + 300mM Imidazole). Two additional elution steps were done with 5 ml EB2 (B2 + 750mM Imidazole) each. All flow through was collected and stored at 4°C.

Cell fractionation

To analyze the localization of the expressed protein, the cell lysate was fractionated by differential centrifugation. Therefore, 1 ml cell lysate was centrifuged for 10 min at 10000 rcf. The supernatant was further centrifuged (20 min; 100000 rcf). This procedure resulted in the pellet fraction containing the bacterial membranes and the supernatant containing the cytosolic components. The pellet from the first centrifugation was re-suspended in 1 ml lysis buffer and centrifuged for 5 min on 1100 rcf. This procedure resulted in the liquid fraction containing lighter cell components like inclusion bodies and the pellet fraction containing cell debris (e.g. crushed cell walls). The pellet fraction was re-suspended in 1 ml lysis buffer. Each fraction was separately analyzed via SDS-PAGE.

Circular dichroism spectrometry

Circular dichroism (CD) spectra were measured by using Jasco-J-815 spectropolarimeter (Jasco Labor- und Datentechnik GmbH, Gross-Umstadt, Germany). The spectra were recorded at 20°C in a quartz cell with a 0.1 cm optical length path. Scans were performed at a rate of 0.2 nm/sec and averaged (n = 20) to improve the signal/noise ratio. Proteins were buffered in 50 mM sodium phosphate

pH 7.5. Both samples (SoOMP24 and AtOMP24) were adjusted to the same protein concentration: 175 ± 15 μg protein.

References

Blachly-Dyson, E., Song, J., Wolfgang, W.J., Colombini, M., and Forte, M. (1997). Multicopy suppressors of phenotypes resulting from the absence of yeast VDAC encode a VDAC-like protein. *Mol Cell Biol* 17**,** 5727-5738.

Breuers, F.K.H., Braeutigam, A., Geimer, S., Welzel, U.Y., Stefano, G., Renna, L., Brandizzi, F., and Weber, A.P.M. (2012). Dynamic remodeling of the plastid envelope membranes ? a tool for chloroplast envelope in vivo localizations. *Frontiers in Plant Science* 3.

Close, T.J. (1996). Dehydrins: Emergence of a biochemical role of a family of plant dehydration proteins. *Physiol. Plant.* 97**,** 795-803.

Duy, D., Soll, J., and Philippar, K. (2007). Solute channels of the outer membrane: from bacteria to chloroplasts. *Biol. Chem.* 388**,** 879-889.

Fischer, K., Weber, A., Arbinger, B., Brink, S., Eckerskorn, C., and Flugge, U.I. (1994). The 24 kDa outer envelope membrane protein from spinach chloroplasts: molecular cloning, in vivo expression and import pathway of a protein with unusual properties. *Plant Mol Biol* 25**,** 167-177.

Flügge, U.I. (2000). Transport in and out of plastids: does the outer envelope membrane control the flow? *Trends Plant Sci* 5**,** 135-137.

Hundertmark, M., and Hincha, D. (2008). LEA (Late Embryogenesis Abundant) proteins and their encoding genes in Arabidopsis thaliana. *BMC Genomics* 9**,** 118.

John, B., Alan, T., and Ann, B. (2002). Anhydrobiosis: Plant desiccation gene found in a nematode. *Nature* 416**,** 38-38.

Joyard, J., Billecocq, A., Bartlett, S.G., Block, M.A., Chua, N.H., and Douce, R. (1983). Localization of Polypeptides to the Cytosolic Side of the Outer Envelope Membrane of Spinach-Chloroplasts. *J. Biol. Chem.* 258**,** 6.

Kelly, S.M., Jess, T.J., and Price, N.C. (2005). How to study proteins by circular dichroism. *Biochimica et Biophysica Acta (BBA) - Proteins and Proteomics* 1751**,** 119-139.

Linke, D., Frank, J., Pope, M.S., Soll, J., Ilkavets, I., Fromme, P., Burstein, E.A., Reshetnyak, Y.K., and Emelyanenko, V.I. (2004). Folding kinetics and structure of OEP16. *Biophys J* 86**,** 1479-1487.

Louis-Jeune, C., Andrade-Navarro, M.A., and Perez-Iratxeta, C. (2012). Prediction of protein secondary structure from circular dichroism using theoretically derived spectra. *Proteins: Structure, Function, and Bioinformatics* 80**,** 374-381.

Machettira, A.B., Groß, L.E., Tillmann, B., Weis, B.L., Englich, G., Sommer, M.S., Königer, M., and Schleiff, E. (2012). Protein induced modulation of chloroplast membrane morphology. *Frontiers in Plant Science* 2.

Pohlmeyer, K., Soll, J., Grimm, R., Hill, K., and Wagner, R. (1998). A high-conductance solute channel in the chloroplastic outer envelope from pea. *Plant Cell* 10**,** 1207-1216.

Pohlmeyer, K., Soll, J., Steinkamp, T., Hinnah, S., and Wagner, R. (1997). Isolation and characterization of an amino acid-selective channel protein present in the chloroplastic outer envelope membrane. *Proc. Natl. Acad. Sci. U. S. A.* 94**,** 9504-9509.

Röhl, T., Motzkus, M., and Soll, J.R. (1999). The outer envelope protein OEP24 from pea chloroplasts can functionally replace the mitochondrial VDAC in yeast. *FEBS Lett.* 460**,** 491-494.

Schleiff, E., Eichacker, L.A., Eckart, K., Becker, T., Mirus, O., Stahl, T., and Soll, J. (2003). Prediction of the plant beta-barrel proteome: A case study of the chloroplast outer envelope. *Protein Science* 12**,** 748-759.

Soll, J., Bolter, B., Wagner, R., and Hinnah, S.C. (2000). . . . response: the chloroplast outer envelope: a molecular sieve? *Trends Plant Sci* 5**,** 137-138.

Steinkamp, T., Hill, K., Hinnah, S.C., Wagner, R., Rohl, T., Pohlmeyer, K., and Soll, J. (2000). Identification of the pore-forming region of the outer chloroplast envelope protein OEP16. *J Biol Chem* 275**,** 11758-11764.

Tolleter, D., Hincha, D.K., and Macherel, D. (2010). A mitochondrial late embryogenesis abundant protein stabilizes model membranes in the dry state. *Biochimica et Biophysica Acta (BBA) - Biomembranes* 1798**,** 1926-1933.

Winter, D., Vinegar, B., Nahal, H., Ammar, R., Wilson, G.V., and Provart, N.J. (2007). An "Electronic Fluorescent Pictograph" Browser for Exploring and Analyzing Large-Scale Biological Data Sets. *PLoS ONE* 2**,** e718.

Zdobnov, E.M., and Apweiler, R. (2001). InterProScan – an integration platform for the signature-recognition methods in InterPro. *Bioinformatics* 17**,** 847-848.

Supplemental Figures

Supplemental Figure 1: Sequence blast for homologs of SoOMP24

Homologs of SoOMP24 can be found in several sequenced plants like Vitus vivifera (Vv), Populus trichocerpa (Pt), Arabidopsis lyrata and thaliana (Al/At), Oryza sativa (Os),Glycine max (Gm), Brachypodium distachya (Bd), Hordeum vulgare (Hv), and Zea mays (Zm).

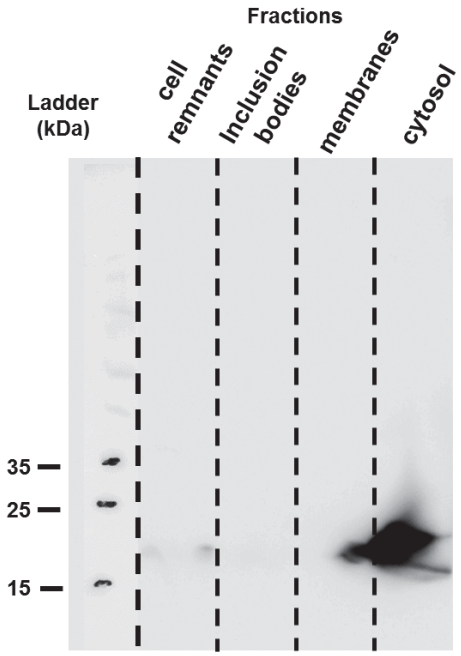

Supplemental Figure 2: Immuno blot of the fractionation of heterologous expressed HIS-AtOMP24 protein

Usage of His-antibody on fractionated Cell lysate resulted in the detection of His-tagged AtOMP24 in the cytosolic fraction.

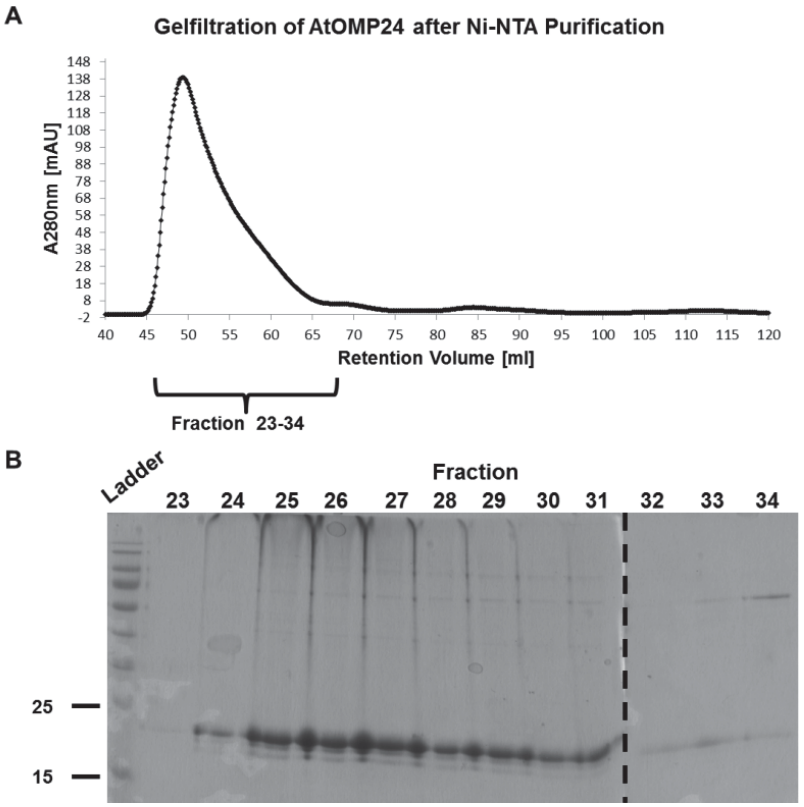

Supplemental Figure 3: Fractionation of Ni-NTA purified HIS-AtOMP24 through gelfiltration

A) Graphical output of ÄKTA based gelfiltration reveal highest protein concentration in early fractions 23 to 34. **B)** SDS page of ÄKTA fraction 23 to 34 result in purified 22 kDa sized protein.

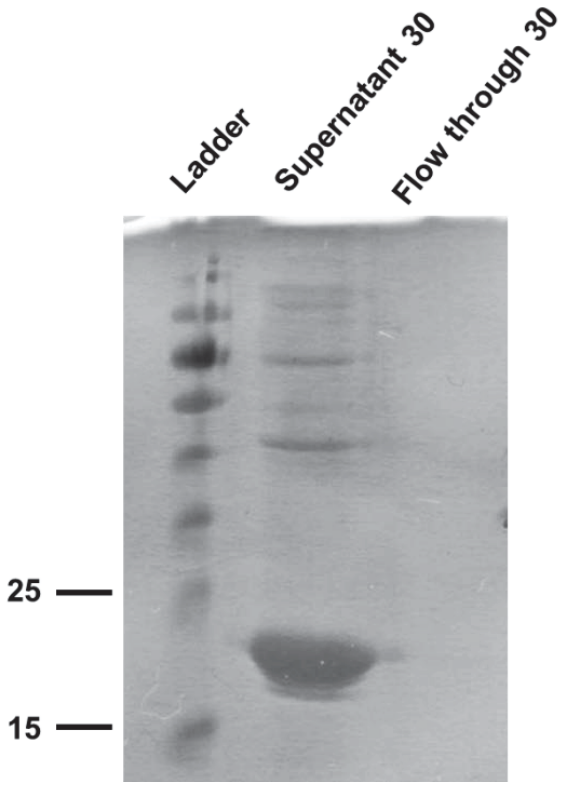

Supplemental Figure 4: SDS page of Centricon30 fractions

The supernatant fraction in the 30 kDa cutoff Centricon contains the 22 kDa sized HIS-SoOMP24 protein. The flow through did not contain any detectable protein.

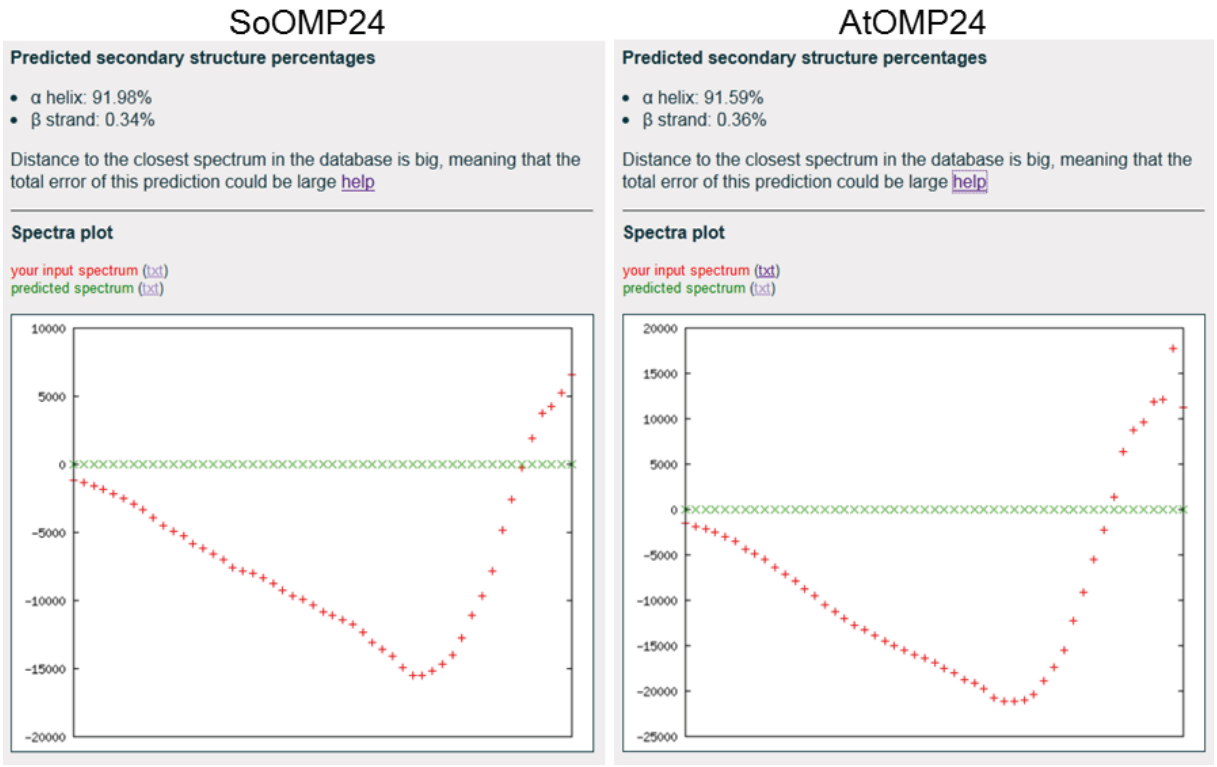

Supplemental Figure 5: Output of the K2D3 bioinformatics analysis of CD spectral data for SoOMP24 and AtOMP24

Analyses point on α-helical structure for both proteins.

IV. Material and Methods

Material

Chemicals

Common used chemicals were ordered from Sigma-Aldrich (Munich, D), Carl Roth (Karlsruhe, D), VWR Prolab (Darmstadt, D), Bacto™ (LePont de Claix, F), Invitrogen (Karlsruhe, D), Biorad (Munich, D), Fluka (Steinheim, D), Riedel de Häen (Seelze, D), Applichem (Darmstad, D), and Merck (Darmstadt, D). The brands of more specific chemicals are indicated at the appropriate position.

Enzymes

Enzymes were ordered from Fermentas (St. Leon-Rot, D), New England Biolabs (NEB; Frankfurt am Main, D), and Promega (Mannheim, D).

Antibiotics

Antibiotics were prepared in stock solutions using ddH2O (when not indicated differently) and sterile filtrated.

Antibiotic	**Stock concentration**	**Final concentration in media**
Ampicilin (Amp)	100 mg / ml (in 50 % ethanol)	100 µg / ml
Chloramphenicol (Clm)	12,5 mg / ml (in 100% ethanol)	25 µg / ml
Gentamycin (Gent)	50 mg / ml 12.5 mg / ml	50 µg / ml (Agrobacteria) 25 µg / ml (*E. coli*)

Antibiotic	Stock concentration	Final concentration in media
Hygromycin (Hyg)	50 mg / ml	30 μg / ml (plants)
Kanamycin (Kan)	50 mg / ml 15 mg / ml	50 μg / ml (Agrobacteria) 30 μg / ml (*E. coli* and plants)
Rifampicin (Rif)	30 mg / ml (in DMSO)	150 μg / ml

Microorganisms

Bacterial strainst

DH5α™ — *E. coli* F$^-$ Φ80*lac*ZΔM15 Δ(*lac*ZYA-*arg*F) U169 *rec*A1 *end*A1 *hsd*R17 (rK$^-$, mK$^+$) *pho*A *sup*E44 λ^- *thi*-1 *gyr*A96 *rel*A1

ccdB survival™ 2T1 — *E. coli* F$^-$ *mcr*A Δ(*mrr-hsd*RMS-*mcr*BC) Φ80*lac*ZΔM15 Δ*lac*X74 *rec*A1 *ara*Δ139 Δ(*ara-leu*)7697 *gal*U *gal*K *rps*L (Str^R) *end*A1 *nup*G *fhu*A::*IS2*

DB3.1 — *E. coli* F$^-$ *gyr*A462 *end*A1 *gln*V44 Δ(sr1-recA) *mcr*B *mrr hsd*S20(r$_B^-$, m$_B^-$) *ara*14 *gal*K2 *lac*Y1 *pro*A2 *rps*L20(Sm^r) *xyl*5 Δ*leu mtl*1

Mach 1-T1^R — *E. coli* F$^-$ delta *lac*X74 *hsdR*(r$_K^-$ m$_K^+$) delta *rec*1398 *end*A1 *tonA*

BL21(DE3) — *E. coli* B F$^-$ *dcm ompT hsdS*(rB$^-$ mB$^-$) *gal* λ(DE3)

BL21(DE3) gold	*E. coli* B F- *ompT hsdS*(rB– mB–) *dcm*+ Tetr *gal* λ(DE3) *endA*
GV3101/pMP90	*A. tumefaciens* C58C1 Rif^r Gm^r, (Van Larebeke et al., 1974; Koncz and Schell, 1986)

Yeast strains

Δpor1 / Y07374 - BY4741; YNL055c::kanMX4; Mat a; his3D1; leu2D0; met15D0; ura3D0

Δpor1 / Y17374 - BY4742; YNL055c::kanMX4; Mat a; his3D1; leu2D0; lys2D0; ura3D0

Δpor2 / Y02273 - BY4741; YIL114c::kanMX4; Mat a; his3D1; leu2D0; met15D0; ura3D0

Δpor2 / Y12273 - BY4742; YIL114c::kanMX4; Mat a; his3D1; leu2D0; lys2D0; ura3D0

Plant material

Col-0	Arabidopsis thaliana; Ecotype Columbia
WiscDsLoxHs044 At1g64850	Arabidopsis thaliana; Ecotype Columbia, T-DNA insertion in
GABI_226C05 At3g52230	Arabidopsis thaliana; Ecotype Columbia, T-DNA insertion in

Used Vectors

Vectors for Gateway® cloning

pDONR207	Gentamycin resistance containing entry vector by Invitrogen used to prepare entry clones via the Gateway® system
pAB-Vectors	Marc Curtis vector' based, ß-estradiol inducible binary plant expression vectors for C-terminal fluorophore fusion prepared by Dr. Andrea Bleckmann (AG Simon, Genetics Institute,

	Heinrich Heine University Düsseldorf) - used for stable and transient expression of target proteins in *Arabidopsis thaliana* and tobacco leaves. Separately: pAB114 – Venus fluorophore; pAB116 – Cerulean fluorophore; pAB117 – GFP fluorophore; pAB118 – mCherry fluorophore.
pGWB-Vectors	Cauliflower mosaic virus (CaMV) 35S promoter driven binary plant expression vector for C-terminal fluorophore fusion – used for stable and transient expression of target proteins in *Arabidopsis thaliana* and tobacco leaves. (Nakagawa et al., 2007) Separately: pGWB41 – EYFP fluorophore; pGWB44 – ECFP fluorophore;
pMDC-Vectors	Vector collection of Marc Curtis - binary plant expression vectors containing diverse promoters, resistances and fluorophore fusion options (Curtis and Grossniklaus, 2003) – used for transient expression of proteins in tobacco leaves Separately: pMDC7 – ß-estradiol inducible promoter; no fluorophore pMDC32 – 2xCaMV35S promoter; no fluorophore fusion pMDC83 - 2xCaMV35S promoter; C-terminal GFP fusion
pUB-Vectors	Vector collection of Christopher Grefen – binary plant

	expression vectors using the plant derived ubiquitin10 promoter to constitutive express proteins *in planta* (Grefen et al., 2010) – used for stable and transient expression of proteins in *Arabidobsis thaliana* and tobacco leaves. Separately: pUBC-YFP – C-terminal YFP fusion pUBC-GFP – C-terminal GFP fusion pUB – no fluorophore fusion
Lindquist Vectors	Vector collection of yeast expression vectors for constitutive and inducible production of protein (Alberti et al., 2007) – used for Yeast complementation assay. Separately: pAG426GPD-ccdB – constitutive Glyceraldehyde-3-phosphate dehydrogenase (GPD) promoter without tag; containing URA3 gene, providing auxotrophy to orotidine 5-phosphate decarboxylase (ODCase) deficient yeast strains. pAG426GPD-ccdB-HA – constitutive Glyceraldehyde-3-phosphate dehydrogenase (GPD) promoter with C-terminal HA- tag; containing URA3 gene, providing auxotrophy to orotidine 5-phosphate decarboxylase (ODCase) deficient yeast strains

Vectors for conventional cloning

pET-Vectors	Novagen® vector collection for Escherichia coli based protein expression. Separately:

pET15b – N-terminal 6xHIS fusion

pET28b – N- or C-terminal 6xHIS fusion

Media

Media were produced with ddH_2O (double distilled water) and autoclaved for 20 minutes on 120°C (when not indicated differently).

Lysogyeny Broth (LB) medium

To produce 1 liter of liquid LB medium, 10 g tryptone, 5 g yeast extract and 5 g sodium chloride (NaCl) were weighted out. A volume of 5 ml of 1M sodium hydroxide (NaOH) was added and medium was brought to a final volume of 1 liter with ddH_2O. For plate medium, 15 g/l bacto-agar was added. For selection media, medium was chilled after autoclaving to approximately 50°C ("hand-warm") and the appropriate amount of antibiotics were added (compare Antibiotics).

Yeast extract beef (YEB) medium

To produce 1 liter of liquid YEB medium, 1 g yeast extract, 5 g beef extract, 5 g peptone, 5 g sucrose and 0.5 g of magnesium sulfate hexahydrate ($MgSO_4$ x $6H_2O$) were weighted outand solved in ddH_2O. For plate medium, 15 g/l bacto-agar was added. For selection media, medium were chilled after autoclaving to approximately 50°C and the appropriate amount of antibiotics (compare Antibiotics) were added.

Yeast extract peef (YEP) medium

To produce 1 liter of liquid YEP medium, 10 g yeast extract, 10 g peptone and 5 g NaCl were weighted out and solved in ddH_2O. For plate medium, 15 g/l bacto-agar was added. For selection media, medium was chilled after autoclaving to approximately 50°C ("hand-hot") and the appropriate amount of antibiotics (compare Antibiotics) were added.

Synthetic complete (SC) and synthetic uracil drop-out (SD-uracil) medium

To produce synthetic yeast media, 6.7 g of yeast nitrogen base (YNB) without amino acids were solved in 850 ml ddH_2O. Medium were autoclaved prior to the adding of amino acid drop out solution and glucose. For plate medium, 20 g/l bacto-agar was added.. A volume of 100 ml of 20% glucose and a volume of 50 ml 20x amino acid stock solution (see alongside table) were prepared either with uracil (for SC) or without uracil (for SD-uracil). Both, glucose (final concentration of 2%) and amino acid mix were added to chilled medium.

Amino acids	mg / 50 ml 20x stock	Amino acids	mg / 50 ml 20x stock
Arginine	50	Histidine	20
Isoleucine	50	Leucine	100
Lysine	50	Tryptophan	50
Methionine	20	Tyrosine	50
Phenylalanine	50	Adenine	10
Threonine	100	(Uracil)	(20)
Valine	140	Total	770 (790)
Aspartate	80		

Yeast peptone dextrose (YPD) medium

To produce 1 liter of liquid YPD medium, 20 g pepton and 10 g yeast extract were solved in 900 ml of ddH_2O. For plate medium, 20 g/l bacto-agar was added.. Medium were autoclaved prior to the adding of glucose. A stock of 100 ml of 20% glucose was prepared and sterile filtrated. Glucose was added to the autoclaved medium to reach a final concentration of 2% glucose in the YPD medium.

½ Murashige Skoog (MS) medium

For 1 liter of liquid MS medium, 2.2 g MS powder (Duchefa) and 5 g sucrose were solved in 800 ml of ddH_2O. (For '-sucrose' medium sucrose was omitted.) Medium were adjusted to pH 5.8 via 0.1M potassium hydroxide (KOH) and medium was filled to a final volume of 1 liter. For plate medium, 7 g/l plant agar was added. For selection media, an appropriate amount of antibiotics were added to chilled media.

Methods

DNA methods

Total RNA extraction from plant material

Leaves of spinach, pea, or *Arabidopsis* (100 - 150 mg) were frozen on liquid nitrogen in a 2 ml round bottom reaction tube containing one glass bead (6 mm diameter). The material was ground for 3x 30 sec in a bead mill. 1 ml of RNAse-All working solution (2M guanidine isothiocyanate; 12.5mM sodium acetate; 0.5% (w/v) N-laurosyl sarcosine; 0.7% (v/v) β-mercapto ethanol; 50% water-saturated phenol) was added to the tissue powder. After a vortexing for 10 sec, 300 µl chloroform : isoamyl alcohol (CI; 24:1) were added to the tubes. Tubes were vortexed again and centrifuged for 10 min at 12000 rcf on 10°C. After centrifugation, the two phases separated. The top phase (aqueous; RNA containing; approx. 600 µl) was transferred to a new 1.5 ml reaction tube and an equal volume of water saturated phenol was added. After vortexing 10 sec, an additional 300 µl of CI was added. Again, tubes were vortexed and centrifuged for 10 min at 12000 rcf on 10°C and the top phase was again transferred to a new 1.5 ml reaction tube (approx. 600 µl). Next, 30 µl of 1M acetic acid and 600 µl pre-chilled 100% ethanol were added to the RNA containing solution. After inverting the mix, it was centrifuged for 20 min at 12000 rcf and 10°C. The supernatant was carefully removed and the resulting RNA pellet was re-suspended in 1 ml 3M sodium acetate. After centrifugation (10 min at 12000 rcf and 10°C),

supernatant was removed and the RNA pellet was re-suspended in 500 µl RNAase-free water. For complete re-suspension, pellet was heated on 60°C for 5 min. The RNA solution was mixed with an equal amount of 5M lithium chloride (LiCl) and incubated overnight on -20 °C. The next day, the tubes were centrifuged for 20 min at 12000 rcf and 10°C. The supernatant was removed and the pellet, containing RNA, was washed twice with 80% ethanol and centrifuged for 10 min at 12000 rcf and 10°C. Afterwards, pellet was dried on room temperature, re-suspended in 50 µl RNAse-free water and dissolved by shaking at room temperature for 30 min. RNA was stored on -80°C.

cDNA synthesis

First strand cDNA synthesis was performed on total RNA using reverse transcriptase SuperScript™ III (Invitrogen) according to the manufacturer's protocol. Incubation steps were processed in a PCR thermo cycler (BIORAD).

Polymerase chain reaction (PCR)

PCR was used for the cloning of genes and for analytical purposes such as colony-PCRs, test-PCR or gDNA analysis on plant or yeast material. The analytical procedures were performed via GoTaq DNA polymerase (Promega, #M300) or via home-made Taq. In both cases, PCR were run according to the GoTaq manufacturer's protocol. The proofreading DNA polymerase Phusion (Finnzymes, #F530) was used for all cloning associated amplifications according to manufacturer's protocol.

Colony PCR

Colony PCRs on bacterial cultures were performed on a small amount of culture (fitting on a pipet tip) directly transferred from plate into the PCR mix or by adding 1 µl of liquid culture to the PCR mix. Yeast Colony PCRs were performed on 3 µl of rehashed yeast, prepared like described in 'Yeast preparation for colony PCR'. PCR were performed using homemade Taq or GoTaq.

gDNA test

Analysis of plant genomic DNA were performed on 2 to 4 µl of gDNA, isolated like described in 'Genomic DNA (gDNA) extraction from *Arabidopsis* leaves' using homemade Taq or GoTaq.

Plasmid isolation from E. coli liquid cultures (Mini-prep)

Plasmid containing *E. coli* bacteria were grown on selection plates (containing appropriate selection markers) overnight on 37°C. When colonies were checked via colony-PCR, the first correct colony was used to inoculate 5 ml of a LB overnight culture. The plasmid of this culture was isolated via Wizard® Plus SV minipreps DNA purification system (Promega, #A1460) and used for sequencing (GATC; gatc-biotech.com).

For manual mini-preps, single colonies were used to inoculate 5 ml of LB overnight cultures, containing appropriate selection markers. The next day, 3 to 5 ml of the cultures were successively transferred to 1.5 ml reaction tubes and centrifuged for 1 min at max. speed (Eppendorf micro centrifuge) at room temperature (RT). The supernatant was removed and 150 µl Solution I (50 mM Tris-HCl pH7.5, 10 mM EDTA, 100 µg/ml DNAse-free water) was used to re-suspend the pellet. To perform the alkaline lysis of the bacterial cells, 150 µl Solution II (0.2 M sodium hydroxide, 1% (w/v) SDS) was added and the tubes were inverted and incubated for 5 min on RT. To neutralize the solution, 150 µl Solution III (3 M potassium acetate pH 5.2) was added and tubes were inverted again. Tubes were incubated on ice for 5 min and subsequently centrifuged for 15 min at max. speed at RT. To precipitate the plasmid, supernatants were transferred to fresh 1.5 ml reaction tubes containing 1 ml 100% ethanol. Tubes were vortexed and centrifuged (10 min, max. speed, RT). Supernatants were discarded and pellets were washed twice with 70% ethanol. Any remaining liquid was removed by drying the pellet at RT in a clean bench. Dry pellets were re-suspended in 50 µl ddH_2O by pipetting and stored at -20°C.

Restriction digests

Restriction digests of DNA were performed during cloning and for analytical reasons. Large setups for digestion of vectors were performed in 20 to 100 µl reactions containing up to 200 µg of the plasmid and an appropriate concentration of restriction enzymes according to the manufacturer's protocol. Large setups were incubated for at least three hours or overnight at 37°C. Standard digests for analytical reasons were performed in 20 µl reactions containing 0.5 µl restriction enzyme, 0.5 to 1 µg DNA, and 2 µl of 10 x reaction buffers. Digests were incubated for 1 hour at 37°C and used in agarose gel electrophoresis.

Cloning

Two different cloning strategies were processed: conventional cloning based on restriction enzymes and T4 DNA ligase and the homologous recombination based system of Gateway® cloning (Invitrogen).

Conventional cloning

Conventional cloning was performed using the restriction enzymes BamHI-HF (NEB; #R3136) and NdeI (NEB; #R0111). Restriction sites were introduced into the DNA-products by the oligos (see TABLEXXX), used in PCR. Sub-cloning of the blund-end DNA-products were performed using CloneJET PCR Cloning Kit (pJET1.2; Fermentas; #K1232) according to the manufacturer's protocol. After amplification of the resulting plasmids in an *E. coli* (DH5α or Mach1) based manner, gene-products were cut out via restriction enzymes, isolated via agarose gel electrophoresis and Wizard® SV gel and PCR clean-up system (Promega; #A9282), and ligated into the, similarly prepared, final vector (mainly pET15b and pET28b), using T4 DNA ligase (NEB; #M0202). Ligation mixes were transformed into *E. coli* (DH5α or Mach1), colonies were screened by colony-PCR, and positive plasmids were sequenced (GATC).

Gateway® cloning

Based on the λ-phage recombination system, the Gateway® cloning requires specific recombination sites (*att*-sites) at DNA-products and inside entry and final vectors. A specialty of this system is a positive and negative selection system for correct vectors. The positive selection is based on the antibiotic resistance gene in the vector. An additional negative selection happens via the *ccdB* gene. This gene is located between the *att*-sites of unprocessed Gateway® vectors and can be removed during the clonase reaction. When an unprocessed Gateway® vector enters an *E. coli* cell, the *ccdB* gene product is expressed and inhibits the bacterial gyrase, resulting in cell death and a lack of negative colonies.

The *att*B sites were introduced during the PCR amplification process using appropriate oligos. Sub-cloning was performed using the entry vector pDONR207 (Invitrogen; Gentamycin resistance) and BP clonase® enzyme mix II (Invitrogen; #11789-020). According to the manufacturer's protocol, 75 µg of the PCR amplification and 75 µg of pDONR207 were mixed in a 4 µl reaction and started by the adding of 1 µl of the clonase mix (½ reactions). Reactions were incubated for 1 h at room temperature. In the case of large (>2 kb) products, incubation time was lengthened to overnight. Afterwards, the complete reactions were transformed into *E. coli* (DH5α or Mach1). Positive selected colonies were screened by colony-PCR or restriction digests of the plasmid after isolation. Positive vectors were cleaned by Wizard® kits (see above) and used in LR reactions. LR reactions and their follow up were performed similarly to the described BP reactions, except that the ½ reactions were started by adding LR clonase® enzyme mix II (Invitrogen; #11791-020). A list of the used final vectors can be found in passage 'used vectors'.

Agarose gel electrophoresis

Agarose gel electrophoresis was used to separate PCR products and restriction digests (test and cloning). According to their expected size, DNA-products were

separated on 0.7 % to 2 % agarose gels (0.7g - 2g agarose per 100ml 1x TAE buffer) containing 10 µg/ml ethidium bromide. Aliquots of DNA containing solutions were mixed with an appropriate amount of 10x DNA loading dye and loaded on the gel. Gels were run at a constant voltage of 80 to 120 mV in a horizontal gel aperture (BIORAD) using 1 x TAE buffer. A 1 kb DNA ladder was used for size reference (Fermentas GeneRuler 1kb DNA ladder; #SM0311 or NEB 1 kb DNA ladder; #N3232S).

For extraction, DNA containing slices were cut out of the gel and were processed via Wizard® SV gel and PDR clean-up system (Promega; #A9282) according to manufacturer's protocol.

50x TAE buffer

2	M	Tris base (242 g/L)
0.05	M	EDTA pH 8.0
1	M	glacial acetic acid (57.1 ml/L)

10x DNA Loading dye

200	mM	Tris-HCl pH 7.6
50	%	Glycerol
0.25	%	Bromphenolblue

Genomic DNA (gDNA) extraction from Arabidopsis leaves

This protocol was adapted from the high throughput gDNA isolation protocol of Starla Zemelis, Brandizzi Laboratory, Plant research laboratories, Michigan State University, East Lansing, Michigan (Pepper and Chory, 1996)

A single leaf of *A. thaliana* (approx.. 30 mg) was transferred into each reaction tube (2 ml; round bottomed) containing 5 metal beads (2 mm diameter), and frozen in liquid nitrogen. The material was ground for 30 sec on a speed of 30 Hz in a bead mill to a

green powder. Afterward, 150 µl of extraction buffer 1 (EB1; 200 mM Tris/HCl pH 7.5; 250mM NaCl; 25mM EDTA pH 8.0) was added, tubes were closed and again milled for 5 min. Tubes were carefully opened and 150 µl of extraction buffer 2 (EB2; 200 mM Tris/HCl pH 7.5; 250 mM NaCl; 25 mM EDTA pH 8.0; 1% SDS) was added. Tubes were closed, inverted and centrifuged (12000 rcf; 10 min; room temperature). An aliquot (approx.. 200 µl) of each supernatant was transferred to a fresh 1.5 ml tube already containing 200 µl 100% isopropanol. Samples were inverted and chilled on ice for 10 min. After centrifugation (12000 rcf; 15min; RT), supernatant was removed and pellets were washed twice with 70% ethanol. The supernatant was removed via pipetting and pellets were air dried using the sterile bench. Dry pellets were dissolved in 50 µl ddH_2O and stored in -20°C.

Protein methods

Expression of recombinant protein

To express recombinant protein, genes of interest were cloned into the *E. coli* expression vector pET15b (Novagen) and transformed into cells of the *E. coli* strain BL21DE. A main culture of 1 liter LB-Amp was inoculated with an overnight culture to an OD_{600} of 0.1. Main culture was grown at 37°C in an incubation shaker to an OD_{600} of 0.7. Protein expression was induced by adding IPTG (isopropyl –β-D-1-thiogalactopyranoside) to a final concentration of 1 mM. Cells were harvested after 5 hours (in respect to the results of a previous pilot expression) by centrifugation on 3000 rcf and 4°C for 20 min. Supernatant was removed, pellet was balanced, and stored on -20°C.

Isolation of recombinant protein

The cell pellet containing recombinant protein was re-suspended in 4 ml/g pellet lysis buffer (20 mM sodium phosphate buffer, pH 7.4; cOmplete EDTA-free protease inhibitor (1 tablet per 50 ml; Roche); 1% Triton X-100; 1 mg/ml Lysozym (Sigma-

Aldrich; #L7651); 0.1 mg/ml DNAse I (AppliChem; #A3778)). Lysis reaction was incubated for 30 min at RT under constant shaking. Suspension was sonicated 3x 45 sec on ice and afterwards processed 2 to 3 times through a FrenchPress® system (Thermo Fischer; Pressure: 1500 bar). The resulting cell lysate was used for fractionation and afterwards for further purification steps.

Cell fractionation

To analyze the expression, cell lysate was fractionated by differential centrifugation. Therefore, 1 ml cell lysate was centrifuged for 10 min on 10000 rcf. The supernatant was further centrifuged (20 min; 100000 rcf) using a Beckmann-Coulter Ultra centrifuge. This procedure resulted in the pellet fraction containing the bacterial membranes and the supernatant, which contained the cytosolic components. The pellet from the first centrifugation was re-suspended in 1 ml lysis buffer and centrifuged for 5 min on 1100 rcf. This procedure resulted in the liquid fraction contained lighter cell components like inclusion bodies and in the pellet fraction containing heavy cell components (e.g. crushed cell walls). The pellet fraction was re-suspended in 1 ml lysis buffer. Each fraction was separately analyzed via SDS-PAGE.

Purification of recombinant protein via Ni-NTA (Nickel nitrilotriacedic acid)

A Ni-NTA column was packed with 10 ml Ni-NTA agarose (Qiagen; #30210) in a gravity-flow column (ThermoFisher; #29920) with a frit resulting in a final column volume (CV) of 5 ml. Column was equilibrated by gravity flow with 15 ml of Buffer 0 (B0; 40mM Tris-HCl, pH 8.0; 300mM NaCl).

Cell lysate was centrifuged for 30 min (40000g, 4°C) and supernatant was transferred on the Ni-NTA column. Afterwards, column was washed subsequently with 5 ml B1 (B0 + 1% Triton X-100); 5 ml B2 (B0 + 50mM NaCholate), and 10 ml CV B3 (B2 + 10mM Imidazol). To elute the histidine tagged protein from the Ni-NTA column, the column was washed four times with 5 ml elution buffer 1 (EB1; B2 + 300mM Imidazol). Two additional elution steps were done with 5 ml EB2 (B2 + 750mM

Imidazol) each. All flow through were collected and stored on 4°C. An aliquot of each sample was analyzed via SDS-PAGE, evaluating the localization of the protein.

Protein extraction form A. thaliana leaf material

Proteins were extracted from leaves of *Arabidopsis* overexpresser lines (Tab. 2.3) using phenol extraction and methanolic ammonium acetate precipitation adapted by Hurkman and Tanaka (1986). 150 mg leaf tissue was harvested, transferred to a 2 ml reaction tube containing 5 metal beads (diameter 2 mm) and immediately frozen in liquid nitrogen. The material was grinded via the bead mill to a fine powder (3 x 30 sec; 30 hertz). Afterwards 0.75 ml extraction medium (0.1 M Tris-HCL, pH 8.8; 0.01 M EDTA, pH 8.0; 0.4 % (v/v) β-mercapto ethanol; 0.9 M Sucrose) and 0.75 ml phenol were added and the mixture was agitated for 30 min on ice. After centrifugation at 16000 rcf for 10 min at 4°C the green upper phenolic phase (~0.7 ml) containing the proteins was transferred to a 15 ml tube. The remaining aqueous phase was back-extracted by adding 0.75 ml phenol. After another agitation and centrifugation step both phenolic phases were combined. For the precipitation 5 to10 volumes (approximately 9 ml) of methanolic 0.1 M ammonium acetate was added, the sample thoroughly mixed and incubated at -20°C overnight. The precipitated proteins were collected at 3500 rcf for 20 min at 4°C The remaining pellet was dissolved in 4.5 ml 0.1 M ammonium acetate and incubated at -20°C for 15 min. After centrifugation (3500 g for 20 min at 4°C) the pellet was washed in 4.5 ml ice-cold 80 % (v/v) acetone and 80 % (v/v) ethanol. After the last washing step the pellet was dried at room temperature for 2 h and re-suspended in 400 µl 3x SDS loading buffer containing 100 mM DTT for the subsequent gel SDS-Page.

SDS-Page (Sodium Dodecyl Sulfate Polyacrylamide gel electrophoresis)

SDS pages were performed using 12.5% SDS gels (compare below) and Mini-Vertical SE250 gel electrophoresis units (GE Healthcare Life Science, Freiburg). Electrophoresis was cassied out at 15 mV per gel in a 1x Tris-glycin running buffer

(25 mM Tris-HCl pH 8.3, 200 mM Glycine, 0.1 % (w/v) Sodium dodecyl sulfate (SDS)). Proteins were loaded using 5x protein sampling buffer.

Separating Gel (12.5%)

15	ml	30 % (w/v) Acrylamid / 0.8 % (w/v) Bis-acrylamid (Rothiphorese® Gel 30)
13.1	ml	ddH_2O
9.4	ml	1.5 M Tris-HCl pH 8.8
0.15	ml	20 % (w/v) Sodium dodecyl sulfate (SDS)
0.125	ml	10 % (w/v) Ammonium persulfate (APS)
0.025	ml	Tetramethylethylendiamine (TEMED)

Stacking Gel (20 ml)

12.2	ml	ddH_2O
5	ml	1.5 M Tris-HCl pH 6.8
2.6	ml	30 % (w/v) Acrylamid / 0.8 % (w/v) Bis-acrylamid (Rothiphorese® Gel 30)
0.15	ml	20 % (w/v) Sodium dodecyl sulfate (SDS)
0.125	ml	10 % (w/v) Ammonium persulfate (APS)
0.025	ml	Tetramethylethylendiamine (TEMED)

5x Protein-Sampling Buffer

200 mM		Tris-HCl pH 6.8
10 mM		β-mercapto ethanol
20 %	(v/v)	Glycerol
10 %	(w/v)	Sodium dodecyl sulfate (SDS)
0.05 %	(w/v)	Bromphenolblue

Western Blot / Immuno blotting

Western Blotting (Sambrook et al., 2001) were used to transfer proteins from a SDS gel to a PVDF membrane for further immune detection analysis.

Blotting

The polyacrylamide gel was placed on a polyvinylidenfluorid (PVDF) membrane pre-wetted in 100 % (v/v) methanol. This sandwich was positioned between two pieces of Whatman-paper of the same size that were soaked in 1x anode buffer (10 % (v/v) 10x Anode buffer (Roth); 5% (v/v) Methanol) or 1x cathode buffer(10% (v/v) 10x Cathode buffer (Roth); 20% (v/v) Methanol), respectively. The resulted package was then placed on the blotting apparatus (Biometra). The transfer was achieved by amperage of 1 mA/cm² and a transfer time average of 2 h.

Immuno-detection

Immuno-detection of HIS-tagged proteins was performed on PVDF membranes after the blotting procedure. The membrane was incubated for 30 min in blocking Buffer composed of 5% (w/v) milk powder in1x TBS buffer (20 mM Tris-HCl; pH 7.5; 150 mM sodium chloride) to avoid unspecific binding of antibodies on the membrane surface. Blocking buffer was discarded and membrane was washed once with 1x TBS and twice with 1xTBS-T buffer (1x TBS; 0.1% (v/v) Tween-20) for 10 min each. In case of HIS-tagged proteins, mouse penta-HIS antibody (Qiagen; #34660) was used as primary antibody in a dilution of 1:2500 in TBS buffered 5% (w/v) milk powder. The PVDF membrane was incubated for 1.5 hours and washed similar as described before. As second antibody, alkaline phosphatase (AP-) conjugated anti-mouse IgG (Promega;#S3721) was used to incubate the membrane for one additional hour.

Coomassie Staining

To visualize proteins in a polyacrylamide gel, Coomassie Brilliant Blue R-250 (Sambrook and David, 2001) was used. For rapid protein staining, SDS gel was

cooked for 1 min in coomassie staining solution (RCS; 40 % (v/v) ethanol; 10 % (v/v) Acetic acid; 2.5 g/L Coomassie Brilliant Blue R-250) using a microwave. Afterwards, CS was exchanged by water and the gel was de-stained by microwaving up to 10 min. For a more decent result, gels were stained for 1 h in CS and de-stained overnight in de-staining solution (DS; 40 % (v/v) Ethanol; 10 % (v/v) Acetic acid) to remove the excess of Coomassie. The stained gels were dried using the drying solution (20% (v/v) ethanol; 10% (v/v) glycerol) and laminated.

Bacteria Methods

Preparation of competent cells

For all competent cell preparations, autoclaved media and sterile filtrated solutions were used. Single bacterial colonies were obtained by streaking out frozen glycerol stocks on media plates containing appropriate selection markers.

Chemical competent Escherichia coli (Mach1; DH5α)

A 5 ml liquid LB overnight pre-culture was inoculated using a single colony of the bacterial strain. A 1 ml aliquot of the pre-culture was used to inoculate 250 ml main culture in a 500 ml Erlenmeyer flask. Culture was grown to an OD_{600} of 0.3 to 0.5 and chilled on ice. Every further step was performed in a 4°C cold room.

Culture was distributed into 50 ml reaction tubes and centrifuged (2000 rcf, 4°C). Supernatant was discarded and pellet of 100 ml culture was re-suspended in 20 ml sterile filtrated SEM buffer (Simple and efficient method buffer; 30 mM Potassium acetate, pH 5.8; 10 mM HEPES, pH 6.7; 15 mM $CaCl_2$; 250 mM KCl; 55 mM $MnCl_2$; Inoue et al., 1990). The Solution was incubated 10 minutes on ice and centrifuged (2000 rcf, 4°C). Supernatant was discarded and pellet re-suspended by shaking in 15 ml SEM buffer containing 1 ml 100% (v/v) DMSO. After 15 min incubation on ice, competent cells were dispend in 100 µl aliquots in 1.5 ml reaction tubes and frozen in liquid nitrogen. Aliquots were stored at -80°C.

Chemical competent Agrobacteria tumefacience (GV3101/pMP90; GV2210)

A 5 ml liquid YEB (+antibiotics) overnight pre-culture was inoculated using a single colony of the bacterial strain. A 2 ml aliquot of an overnight pre-culture was used to inoculate a 50 ml YEB (+ antibiotics) culture in a 250 ml Erlenmeyer flask with chicanes. Cells were grown to an OD600 of 0.5 to 1.0 at 28°C. After chilling the culture on ice, bacteria were pelleted by centrifugation (3000 rcf, 4°C). Supernatant was discarded and bacteria were re-suspended in 1 ml of 20 mM calcium chloride. Bacteria suspension was distributed in 50 to 100 µl aliquots in 1.5 ml reaction tubes and frozen in liquid nitrogen. Aliquots were stored at -80°C.

Electro competent bacterial cells

A 5 ml liquid LB (*E. coli*) or YEB (+antibiotics; *A. tumefacience*) overnight pre-culture was inoculated using a single colony of the bacterial strain. A 1 ml aliquot of the pre-culture was used to inoculate 250 ml main culture in a 500 ml Erlenmeyer flask. Culture was grown to an OD_{600} of 0.3 to 0.4 and chilled on ice. Every further step was performed in a 4°C cold room.

Culture was distributed into 50 ml reaction tubes and centrifuged (2000 rcf, 4°C). Supernatant was discarded and pellet of 100 ml culture was washed four times with 50 ml ice-cold 1 mM HEPES buffer (pH 7.0) by re-suspension and centrifugation (2000 rcf, 4°C). For each 500 ml culture, pellet was re-suspended in 20 ml chilled 10% glycerol and distributed in 40 µl aliquots into 1.5 ml reaction tubes. Cells were frozen in liquid nitrogen and stored at -80°C.

Transformation of plasmids into bacterial cells

Heat shock transformation (E. coli)

An amount of 20 to 100 ng vector DNA or a 6 ml clonase reaction was combined with a 50 to 100 µl aliquot of thawed competent *E. coli* cells. Cells were incubated with the DNA for 15 min on ice and heat-shocked for 90 sec at 42°C. Cells were chilled on ice for 1 min and 500 µl LB were added. Transformed cells were shaking for 1 or 2 hours

at 37°C in order to regenerate. Transformed cells were selected on LB plates containing appropriate antibiotics.

Freeze-thaw method for transformations into A. tumefaciens

An amount of 1 to 3 μg DNA of destination vectors was added to a frozen aliquot of competent Agrobacteria. The cells were thawed on ice and afterward 5 min frozen in liquid nitrogen. The frozen cells were thawed again in a heating block at 37°C. Regeneration of the cells was performed by adding 1 ml of YEB and shaking for two to four hours at 30°C. Transformed cells were selected on YEP, YEB, or LB plates containing appropriate antibiotics (compare Weigel and Glazebrook, 2002)

Transformation by electroporation

Electro competent bacterial cells were combined with 1 μg of plasmid and thawed on ice. For electroporation, the transformation mix was transferred to electroporation cuvettes (Eppendorf; 1 mm split) and chilled on ice for 2 min. Cuvette was cleaned with tissue paper and transferred into the electroporator (Eppendorf Electroporator 2510). Electroporation was performed with a voltage of 2400 V, a resistance of 600 Ohms and a capacity of 10 μF for 5 ms. Immediately, 1 ml LB medium was added to the cuvette, cell suspension was back transferred to the reaction tube and cells were shortly chilled on ice. Regeneration of the transformed cells was performed for 2 hours at 30°C (Agrobacteria) or 37°C (E. coli). Transformed cells were selected on LB plates containing appropriate antibiotics.

Yeast Methods

Yeast preparation for colony PCR

To gain access to yeast DNA, Lyticase (Sigma-Aldrich; #L4025) was used to disrupt yeast cell walls. Lyticase was solubilized in 100 mM sodium phosphate buffer (NaPi; pH 7.4) in a concentration of 3 units / μl. For each yeast sample, a 1.5 ml reaction tube was pre-filled with 50 μl of the lyticase buffer. Yeast was scraped off a culture plate

with a pipet tip, transferred into the buffer, and incubated at 30°C for 30 min. Lyticase was inactivated by cooking at 95°C for 10 min. An aliquot of 3 µl was used for yeast colony-PCR.

Yeast complementation

To transform yeast for the purpose of complementation, the lithium acetate method was used (compare Schiestl and Gietz, 1989). Therefore, a 50 ml YPD culture was inoculated with an overnight yeast culture to an OD_{600} of 0.4 and grown for 4 hours at 30°C. Culture was pelleted on 2.500 rcf for 10 min at room temperature, washed with 40 ml TE buffer (10 mM Tris-HCl pH 7.4; 1 mM EDTA pH 8.0), and centrifuged again. Washed pellet was re-suspended in 2 ml lithium acetate/TE buffer (0.1 M lithium acetate in TE buffer) to use for transformation. For transformation, 100 µl yeast suspension was mixed with 2 µg of plasmid (carrying the construct for complementation) and 50 µl of denaturized carrier DNA (2 mg/ml). To this mix, 700 µl of litium acetate/PEG 3350 Buffer (0.1 M lithium acetate, 40% PEG 3350, in TE buffer) was added, vortexed, and reaction was incubated for 30 min at 30°C. Transformation was processed by adding 88 µl DMSO to the reaction. Transformation was mixed and heat-shocked for 7 min on 42°C. Cells were washed twice in TE buffer and transferred to drop out plates (SD –uracil) and grown for 3-4 days at 30°C.

Plant methods

Seed harvesting

To obtain seeds from A. thaliana, seeds were dried at the plant. Dried siliques were transferred to a metal sieve of 450 µm mesh size. Repeated sieving resulted in a collection of clean round brown seeds, which were stored in cryo tubes.

Chlorine gas sterilization of seeds (Clough and Bent, 1998)

Reaction tubes of 1.5 ml were filled to a high of 0.5 mm with seeds of *A. thaliana* or tobacco (*N. benthamiana, N. tabaccum, N. sylvestris*). Tubes were openly transferred to a glass desiccator. A beaker containing 100 ml 5 % sodium hypochlorite solution was placed next to the samples. By adding 3 ml of concentrated hydrochloric acid, chlorine gas production was induced and the desiccator was fast closed. Seeds were incubated in gas for 2 to 3 hours. Tubes were closed and transferred to a sterile bench, opened, and rested for 10 min to evacuate remaining gas. Seeds were transferred on ½ MS plates by spreading or spotting with toothpicks.

Microscopy

Confocal microscopic analysis

Confocal microscopy was performed on leave slices and protoplasts of Arabidopsis and tobacco using an inverted or an upright Zeiss LSM 510 META confocal laser-scanning microscope. GFP and chlorophyll were excited by the 488 nm laser line of an Argon laser and the emission was collected at 505-550 nm and at > 650 nm, respectively. DIC (Differential interference contrast) microscopic analysis was done via a Nikon Eclipse T inverse microscope. Pictures were taken via a b / w-ProgResMF™-camera by Jenoptik.

References

Alberti, S., Gitler, A.D., and Lindquist, S. (2007). A suite of Gateway® cloning vectors for high-throughput genetic analysis in Saccharomyces cerevisiae. *Yeast* 24**,** 913-919.

Curtis, M.D., and Grossniklaus, U. (2003). A gateway cloning vector set for high-throughput functional analysis of genes in planta. *Plant Physiol.* 133**,** 462-469.

Grefen, C., Donald, N., Hashimoto, K., Kudla, J., Schumacher, K., and Blatt, M.R. (2010). A ubiquitin-10 promoter-based vector set for fluorescent protein tagging facilitates temporal stability and native protein distribution in transient and stable expression studies. *Plant J* 64**,** 355-365.

Hurkman, W.J., and Tanaka, C.K. (1986). Solubilization of Plant Membrane Proteins for Analysis by Two-Dimensional Gel Electrophoresis. *Plant Physiol.* 81**,** 802-806.

Nakagawa, T., Kurose, T., Hino, T., Tanaka, K., Kawamukai, M., Niwa, Y., Toyooka, K., Matsuoka, K., Jinbo, T., and Kimura, T. (2007). Development of series of gateway binary vectors, pGWBs, for realizing efficient construction of fusion genes for plant transformation. *J. Biosci. Bioeng.* 104**,** 34-41.

Sambrook, J., Russell, D., Irwin, N., and Janssen, K. (2001). Molecular cloning: a laboratora manual. *Cold Spring Harbor Laboratory Press, Cold Spring Harbor, New York* third edition.

Schiestl, R.H., and Gietz, R.D. (1989). High efficiency transformation of intact yeast cells using single stranded nucleic acids as a carrier. *Curr Genet* 16**,** 339-346.

Weigel, D., and Glazebrook, J. (2002). The Arabidopsis Book. *Kalte-Frühlings-Hafen-Laborpresse*.

Eidesstattliche Erklärung

Hiermit versichere ich an Eides Statt, dass die Dissertation von mir selbständig und ohne unzulässige Hilfe unter Beachtung der „Grundsätze zur Sicherung guter wissenschaftlicher Praxis an der Heinrich-Heine-Universität Düsseldorf“ erstellt worden ist. Diese Dissertation habe ich in dieser oder ähnlicher Form noch bei keiner anderen Fakultät vorgelegt. Ich habe bisher keine erfolglosen Promotionsversuche unternommen.

Düsseldorf, den 31. April 2013

Frederique K.H. Breuers